

Machining Science and Technology



An International Journal

ISSN: (Print) (Online) Journal homepage: www.tandfonline.com/journals/lmst20

Comprehensive review of drilling strategies for CFRP/Ti stacks in aircraft manufacturing

Joy Mathavan Jebaratnam & Muhammad Hafiz Hassan

To cite this article: Joy Mathavan Jebaratnam & Muhammad Hafiz Hassan (21 Apr 2025): Comprehensive review of drilling strategies for CFRP/Ti stacks in aircraft manufacturing, Machining Science and Technology, DOI: 10.1080/10910344.2025.2475484

To link to this article: https://doi.org/10.1080/10910344.2025.2475484

	Published online: 21 Apr 2025.
	Submit your article to this journal 🗷
a Q	View related articles ☑
CrossMark	View Crossmark data 🗹



REVIEW ARTICLE



Comprehensive review of drilling strategies for CFRP/Ti stacks in aircraft manufacturing

Joy Mathavan Jebaratnam^a 🕟 and Muhammad Hafiz Hassan^{b,c} 🕞

^aDepartment of Engineering Technology, Faculty of Technology, University of Jaffna, Kilinochchi, Sri Lanka; ^bSchool of Mechanical Engineering, Engineering Campus, Universiti Sains Malaysia, Pulau Pinang, Malaysia; ^cAdvanced Machining Lab, Melaka, Malaysia

ABSTRACT

Single-shot drilling of carbon fiber-reinforced polymer/titanium alloy stacks in aerospace applications poses unique challenges. The interaction between the cutting tool and the compositemetal contact often leads to poor hole quality and increased tool wear. The review extensively examines research achievements and developments in drilling CFRP/Ti stacks to comprehensively assess the impact of various machining settings on hole quality. Contributing factors such as stack-up machining thrust force, temperature, chip form and tool wear characteristics are thoroughly investigated. Moreover, this article highlights manufacturing defects in metallic and composite panels during drilling operations, contributing to a higher rejection rate in the assembly process. Usually, the maximum delamination of 1 mm, diameter deviation of ±30 µm, burr height of 150 μm, metal part's surface roughness of 1.6 μm and CFRP part's surface roughness of 3.2 µm are allowed in the aerospace industry. Additionally, the research explores strategies to mitigate manufacturing defects, including measures to limit hole and tool damage. These tactics encompass tool structure, machining environment, machining parameters and machining technology. On the whole, this review study aims to fill the research gap regarding process enhancement and performance evaluation of single-shot drilling of CFRP/Ti stacks in aerospace applications.

KEYWORDS

CFRP/Ti stack; delamination; machining; surface analysis

Introduction

The aerospace sector is increasingly using composite/metal stacked materials in structural components and aiming to lower production and assembly expenses (Cheng et al., 2017). Composite materials account for about 50% of the weight of the structure of some commercial aircraft, like Boeing 787 and Airbus 350. The majority of these are built up of carbon fiber- reinforced

polymer (CFRP), with roughly 15% made of Ti alloys (Kuo et al., 2018). There are primarily three stack panels used in big passenger aircraft (Boeing 787 and COMAC C919) such as CFRP/Al, CFRP/Ti and CFRP/CFRP. The CFRP/Ti stack is the most complex to machine among these three (Isbilir and Ghassemieh, 2013).

Fiber metal laminates (FMLs) were developed because standard materials, such as aluminum, do not have the fatigue crack resistance required to withstand huge strain in aeroplane sections such as the fuselage. The ability to improve some noticeable characteristics without considerably raising the total weight is the advantage of FML setups (Ramulu et al., 2001; Brinksmeier and Janssen, 2002; Kim and Ramulu, 2007; Xu et al., 2016). Combining metals and composites in FMLs addresses the limitations of metals in corrosion resistance and fatigue strength, and composites in impact strength, bearing strength and reparability (Sinmazçelik et al., 2011; Pawar et al., 2015). FMLs can be made by using adhesives like epoxy to join thin sheets of metallic alloy and composite materials (Ad Vlot, 2001; Giasin et al., 2020). The fuselage, skin and wing parts of an aeroplane are currently made of CFRP-metal layers, and the composite is usually placed on top of the metal (Zitoune et al., 2010). Since CFRP/Ti stacks have a density of roughly 4 g/cm³ and yield strength up to 830 MPa, they offer a high strength-to-weight ratio (Park et al., 2014). Sinmazcelik et al. grouped FMLs into categories based on the metal utilized, such as titanium-based, aluminum-based and magnesium-based (Sinmazçelik et al., 2011). Because of their excellent performance under impact and at high temperatures, CFRP/Ti stacked laminates are the most preferred choice among the available FMLs (Isbilir and Ghassemieh, 2012).

Titanium (Ti) alloys are lightweight metallic materials with high specific strength, great corrosion resistance, great biocompatibility and extraordinary characteristics at high temperatures (Ezugwu and Wang, 1997; Hong et al., 2001). They are used in many sectors, such as surgical implantation (Hatamleh et al., 2018), the aerospace sector (López De Lacalle et al., 2000) and marine applications (Gorynin, 1999). The aerospace industry uses the Ti alloy called as duplex alpha-beta alloy (Ti6Al4V). Over half of all titanium alloy manufactured worldwide is Ti6Al4V (Arrazola et al., 2009), because of its ability to build lightweight structures at elevated temperatures above 600 °C (López De Lacalle et al., 2000). Ti6A14V titanium alloy is prepared by solution treatment and age hardening, after which it will have a Rockwell C hardness value of 39 (HRC = 39) (Budinski, 1991). But its low thermal conductivity and low thermal plastic instability result in extreme temperatures while drilling. The temperature can easily surpass 1000 °C at the cutting edge because of its low thermal conductivity (Hartung et al., 1982; Zhang et al., 2008), which can significantly decrease

the mechanical integrity (stiffness, strength and hardness) of the cutting tool. The elevated temperature also leads to the welding of workpiece, with cutting edges of the tool material due to its high adhesion tendency, which generates built-up edge (BUE) (Li et al., 2007; Rahim and Sharif, 2007). It is also regarded as a tough-to-cut material because of its poor processability and machining quality (Li and Shih, 2007; Çalışkan and Küçükköse, 2015; Liang et al., 2015). (Hartung et al., 1982; Narutaki et al., 1983; Machado and Wallbank, 1990; Berger et al., 1998; Klocke and Krieg, 1999; Park et al., 2014). Adhesion (or attrition) wear (Trent and Wright, 2000) occurs when Ti-adhesion occasionally detaches from the tool, peeling off the tool material pieces (Yang and Richard Liu, 1999; Sharif and Rahim, 2007), which causes tool failure due to chipping and premature failure (Sharif and Rahim, 2007; Zhang et al., 2008).

CFRPs are intended to replace traditional metallic materials gradually because metals cannot be completely replaced at the moment (Tyczyński et al., 2014). Though there are many special CFRP-metal stacks that have appeared in a variety of products (Zhang et al., 2015), the useful ones for structures are CFRP/Ti and CFRP/Al stacks (Cheng et al., 2017). Some salient mechanical and physical properties of CFRP are its light weight (Singh et al., 2013; Stocchi et al., 2013), better modulus of elasticity than steel, excellent strength-to-weight ratio, low density, high fatigue strength (Altin Karatas and Gökkaya, 2018; Sorrentino et al., 2018; Xu and Zhang, 2018; Aamir et al., 2019; Xu et al., 2022), low coefficient of thermal expansion, low impact resistance, excellent corrosion resistanceand strong electrical conductivity (Uhlmann et al., 2016; Aamir et al., 2019). Principally, fibers govern the strength of the composite material (Mathavan and Patnaik, 2020; Saracoglu and Yapici, 2020). Metals are generally used in aircraft structures to construct multi-material composite parts with outstanding chemical and physical qualities such as high hardness, low density and superior strength-to-weight ratio (Impero et al., 2018; Prisco et al., 2019; Yaşar et al., 2021). However, due to the heterogeneous architecture and anisotropic behavior of CFRP composites, machining is likely to result in significant geometrical flaws and subsurface damage (Gaugel et al., 2016; Che et al., 2014). Furthermore, because the reinforcing fibers are abrasive and hard, the drill edge-composite interface experiences high friction, which leads to stress accumulation at the drill edges and causes edge rounding or microchipping (Rawat and Attia, 2009; Wang et al., 2013). Anisotropy, abrasion resistance and heterogeneity increase the difficulty of cutting mechanisms in CFRP composites, resulting in fiber pull-out, delamination, fuzzing, spalling and thermal degradation (Abhishek et al., 2015). Despite much research conducted on CFRP cutting mechanisms (Calzada et al., 2012; Qi et al., 2015; Anand and Patra, 2017; Li et al., 2019; Liu et al., 2018), burr formation mechanisms, delamination (i et al., 2018; Geier et al., 2019; Geng et al., 2019), drilling environment and influences of cutting parameters (Campos Rubio et al., 2008; Wang et al., 2017; Anand and Patra, 2018; Qiu et al., 2018), CFRP machining remains an expensive, difficult-to-plan and time-consuming technology (Wang et al., 2013).

Stacking metal and fiber sheets together using bolts is the most convenient manner of mounting/dismounting them during repair or maintenance activities (Shyha et al., 2011), which makes drilling holes an important machining process for stack-up material. Drilling is a conventional machining procedure used in aerospace constructions to create round holes of varying sizes and depths, and the most common shape of holes in the aviation sector is drilled with countersinking (Falconieri and Franco, 2015). CFRP/Ti6Al4V stack holes are typically made in a single-shot drilling operation (Li et al., 2022) in order to reduce processing time and positioning error (Soo et al., 2019; Mahdi et al., 2020). To produce high-quality drilling results, the machining parameters must be carefully chosen. This is a difficult task in CFRP/Ti6Al4V stacks drilling since the optimal conditions for CFRP are not beneficial for Ti6Al4V and vice versa. Cutting conditions that include modest feed rates (0.05 mm/rev) and lower cutting speeds can produce better results in both metal and composite panels (Park et al., 2014; Xu et al., 2016). Because of the varied characteristics of CFRP/ Ti6Al4V stacks, many processing errors could emerge from the stack up drilling process than from single-material drilling (Rodríguez et al., 2021). It has been found that four different cutting mechanisms are engaged in removing material from CFRP composites while drilling: (i) for the parallel fiber cutting relation (i.e., $=0^{\circ}$), the buckling-dominated mode, (ii) for the forward fiber cutting relations (i.e., $0^{\circ} \ll 90^{\circ}$), the shear-dominated mode, (iii) for the vertical fiber cutting relation (i.e., = 90°), the crushing-dominated mode and (iv) against fiber cutting relations (i.e., 90°<.<180°) the bending-dominated mode (Wang et al., 1995; Iliescu et al., 2010; Ben Soussia et al., 2014; Xu et al., 2019). Besides the effect of fiber orientation, the radius of the cutting-edge also has a substantial impact on composite drilling mechanisms because the size impacts their performance when the radius of the cutting-edge exceeds the nominal depth of cut (Shu et al., 2021). Figure 1 shows the overview of all the considerable factors while performing single-shot drilling of a CFRP/Ti panel.

The primary scope of this study is to provide a comprehensive analysis of single-shot drilling of carbon fiber-reinforced polymer/titanium (CFRP/Ti) stacks by addressing critical challenges in the industry and proposing potential solutions. The three major objectives of the article are as follows. First, analyzing the key characteristics of CFRP/Ti stacks used in the aerospace industry, emphasizing their influence on drilling performance and

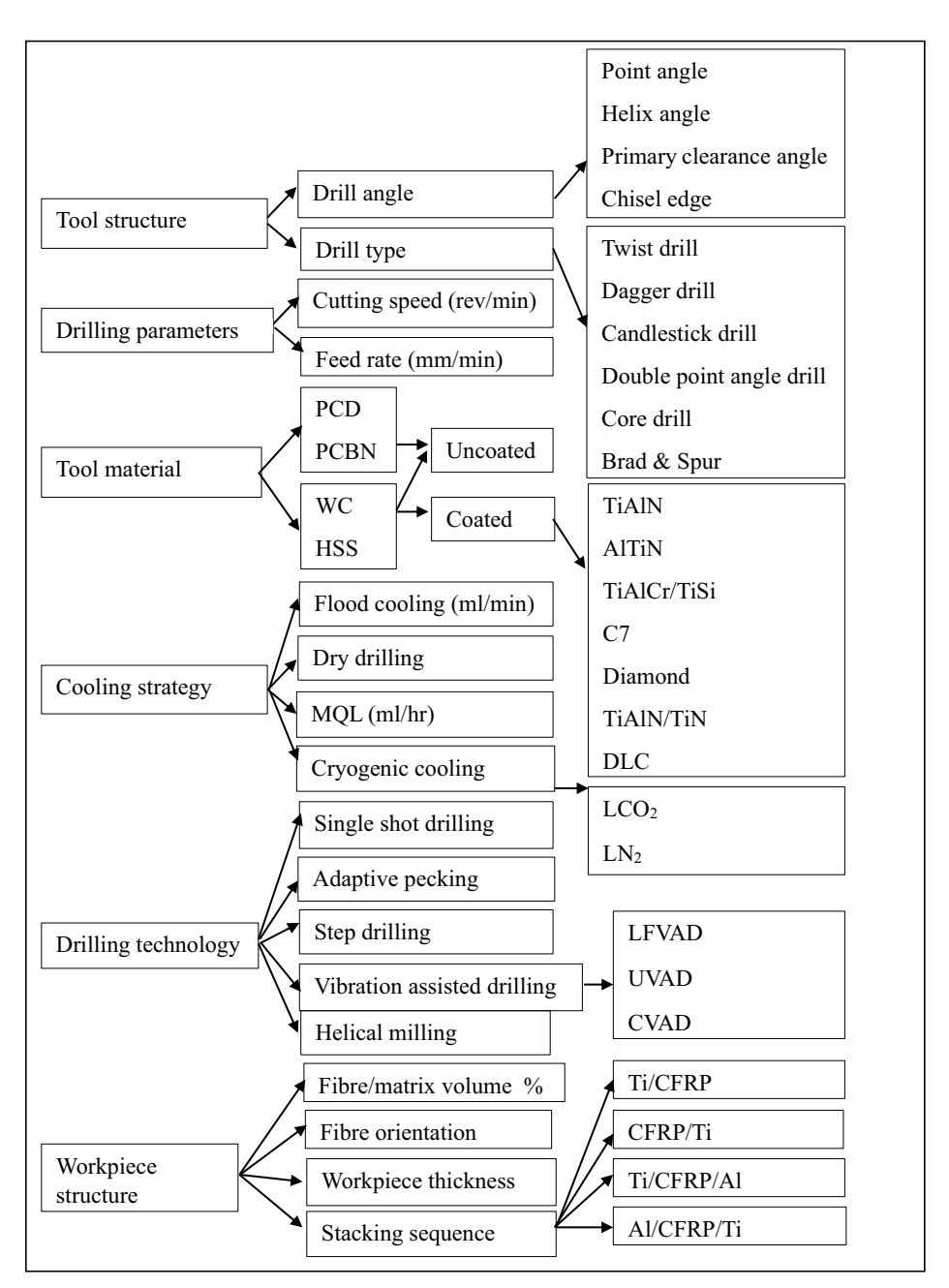


Figure 1. Overview of stack up drilling of CFRP/Ti panel.

evaluating common defects using performance indicators such as temperature generation, drilling forces, chip formation and tool wear. Second, reviewing key experimental findings to identify their impact on hole quality in single-shot drilling processes for CFRP/Ti stacks. Third, investigating advanced technologies and machining strategies aimed at mitigating defects, minimizing hole damage, improving surface finish and providing practical

recommendations for aerospace manufacturers and researchers to select optimal strategies for precision drilling of CFRP/Ti stacks. Accordingly, this review article is targeting to fill the research gap regarding process enhancement by mitigating damage formation using advanced techniques in single-shot drilling of CFRP/Ti stacks in aerospace applications through performance evaluation.

Performance indicators when drilling stack materials

Evaluation of drilled-hole quality in the aircraft industry encompasses various online and offline parameters to ensure optimal drilling performance and minimize drilling-induced damages. The mechanical forces and heat generated during CFRP/Ti drilling govern the material removal process, significantly influencing the quality of machined holes and the progression of tool wear. These thermo-mechanical effects often result in severe damage to the interface area and the machined CFRP surface, including interface delamination, titanium burr intrusion into the composite phase, scratches from sharp titanium chips on the CFRP holes and high-temperature ablation of the CFRP matrix (Jebaratnam and Hassan, 2024; 2025). Offline parameters include delamination, burr height formation, hole surface roughness, hole size deviation and hole circularity error. These parameters are evaluated post-drilling to assess the quality of the drilled holes (Franz et al., 2022). Additionally, monitoring and assessing methodologies for online parameters such as chip formation, tool wear, drilling forces and drilling temperatures are essential for real-time feedback during the drilling process (Panchagnula and Palaniyandi, 2018). These comprehensive evaluations and monitoring techniques are critical for maintaining high-quality standards in aerospace assemblies and minimizing structural integrity issues caused by drilling operations. In this section, the online parameters will be discussed in detail.

Cutting temperature

One of the main factors restricting the process parameters while drilling a CFRP/Ti stack is the high cutting temperature produced (Pecat and Brinksmeier, 2014; An et al., 2020). The low heat conductivity of the fiber/matrix makes it easy to attain excessive machining temperatures, which is also likely to cause the composite matrix to go through the glass transition, degrading the composites' qualities (Geier et al., 2021). Khashaba et al. (2010) and Lee et al. (2019) mentioned that FRP composites have a relatively low thermal conductivity (GFRP = 0.59 W/m°C and CFRP = 0.912 W/m°C) in comparison to aluminum (= 210 W/m°C), steel (= 53 W/m°C) and brass

(= 109 W/m°C). As a result, the heat produced during drilling cannot be efficiently transmitted to the outside and instead interferes with the drilling process. Drilling FRP composites causes the machined surface to soften and then re-solidify, increasing the buildup of stress that encourages localized crack development and propagation while reducing the capacity of the drilled holes to support loads (Khashaba and El-Keran, 2017). According to Rawat and Attia, low damage is caused by the workpiece's reduced rigidity and therefore reduced thrust force as drilling temperature rises (Rawat and Attia, 2009). Hocheng et al., however, presented that the polymers' static friction coefficient rises and they become more ductile when the temperature increase is significantly higher than their glass transition temperature (T_{σ}) (Hocheng et al., 1993). Cong et al. (2012) mentioned that thermal fracture and resin deterioration occur at temperatures exceeding the T_g of the resin matrix, which is around 180 °C. The cutting blades of the rotating drill spread the ductile material across the hole wall surface, which results in surface irregularity (Khashaba and El-Keran, 2017). Delamination, surface roughness and a decrease in fatigue strength in machined CFRP components are some unavoidable results of this (Geng et al., 2020). The hardness and elastic modulus of CFRP specimens drilled at temperatures above T_g were significantly lower than those drilled at temperatures near to T_g (Merino-Pérez, Royer, et al., 2015; Merino-Pérez, Hodzic, et al., 2015).

Moreover, it was observed that employing high feed rates and low cutting speeds when machining CFRP can help decrease cutting temperatures by preventing matrix burning at hole edges, resulting in a smoother surface produced by the fibers (Rawat and Attia, 2009; Boccarusso et al., 2019). It is also noted that the drilling temperature rises as the feed rate is increased when machining CFRP/Ti6Al4V stacks and when the speed grows, it increases rapidly (An et al., 2020). It shows that the drilling speed has a greater influence than the feed rate on drilling temperature. Heat generated during drilling of the titanium alloy transfers to the CFRP plate through the chips, causing a rise in the CFRP plate's temperature (Li et al., 2022). While drilling CFRP alone, however, the situation is reversed. Temperature tends to drop as feed rate increases (with the same spindle speed) because increasing feed rate reduces contact friction between the surface being machined and the tool that causes temperature reduction (Li et al., 2022). Also, broken CFRP chips are easily evacuated, and the heat that the chips absorb also rises as drilling thickness is increased, despite the fact that this may increase cutting energy and temperature (Li et al., 2022).

When drilling a CFRP/Ti stack in the CFRP \rightarrow Ti sequence, the hightemperature ribbon chips from Ti6Al4V drilling may scratch the CFRP hole wall during chip removal (An et al., 2021). As a result, serious scratches and resin burns are produced on the CFRP hole wall and the hole quality is reduced (Li et al., 2019). When machining CFRP/Ti from the Ti6Al4V side, the machining temperature surpasses the vitrification temperature of the resin, accelerating fiber-resin debonding and fiber pull-out and resulting in surface pits (An et al., 2021). An et al. mentioned that the maximum temperature generated when machining a CFRP panel is $133\,^{\circ}$ C which is below T_g of CFRP, and then it increased quickly to $347.2\,^{\circ}$ C when drilling the Ti6Al4V phase as shown in Figure 2 (An et al., 2020). A high quantity of heat is created in the Ti6Al4V drilling process when the drilling sequence is Ti \rightarrow CFRP (336 $\,^{\circ}$ C), and it reduces once the drill bit starts to enter the CFRP region as shown in Figure 2. But until halfway through the CFRP phase, the temperature was above the T_g of the

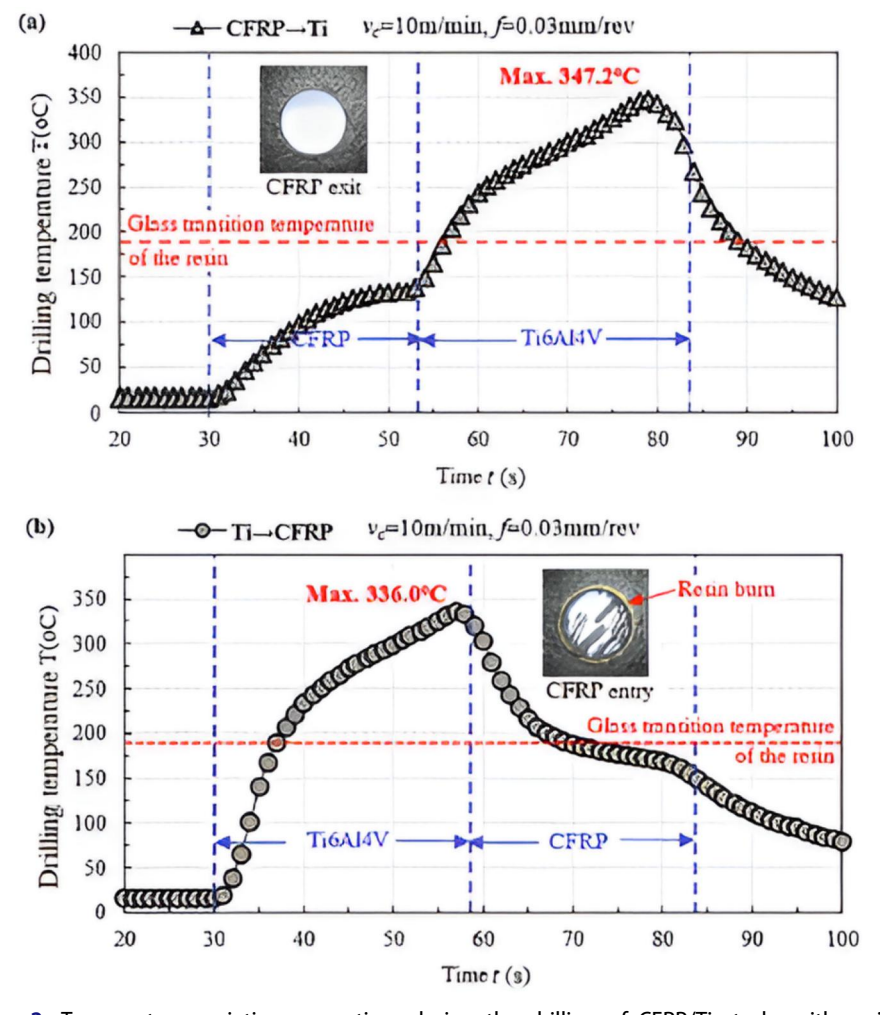


Figure 2. Temperature variations over time during the drilling of CFRP/Ti stacks with various drilling sequences: (a) CFRP \rightarrow Ti, (b) Ti \rightarrow CFRP (An et al., 2020).

resin (An et al., 2020). Therefore, the elevated cutting temperature would severely thermally damage the hole-wall, particularly at the metal composite interface (MCI) region (An et al., 2021). Furthermore, because of the absence of backing at the exit of the CFRP panel, cutting imperfections such as splitting and delamination are extremely common in this sequence (Faraz et al., 2009). Sato et al. discovered that when machining the Ti6Al4V panel, the temperature increased to 745 °C from an initial temperature of less than 95 °C for the CFRP layer in the CFRP \rightarrow Ti sequence. When drilling at the Ti→CFRP sequence, the temperature was less than 170 °C at first, rising to 695 °C after the drill reached the interface zone (Masahiko et al., 2016). Brinksmeier et al. observed while drilling Al/CFRP/ Ti stacks that, at a speed of 40 m/min and a feed rate of 5 mm/min, the drill bit's rake face registered temperatures of 90 °C when drilling the Al layer, 190 °C when drilling the CFRP layer, and 350 °C when drilling the Ti layer (Brinksmeier et al., 2011).

It can be said that high cutting temperatures during CFRP/Ti drilling significantly impact the process and machined surface quality. The low thermal conductivity of CFRP causes excessive heat buildup, leading to matrix degradation, delamination and surface damage, especially when temperatures exceed the glass transition temperature (T_{σ}) of the resin. Drilling sequences influence thermal effects in a way that Ti-CFRP generates high temperatures in the Ti phase, causing resin debonding and fiber pullout, while CFRP→Ti can lead to resin burns and scratches on CFRP walls. Feed rates and cutting speeds also affect temperature; higher feed rates increase the temperature in CFRP/Ti stacks. Elevated temperatures near the metalcomposite interface result in severe thermal damage, and the absence of backing exacerbates defects like delamination at CFRP exits. Using optimized parameters, such as low speeds and high feed rates, damage can be reduced and hole quality can be improved.

Thrust force

The cutting force is a function of the geometry of the tool and the friction between the tool and the workpiece (Luo et al., 2016; Khashaba, 2018). The importance of cutting CFRP/metal lies in the tool's distinct design, where multiple cutting edges can engage with the same material concurrently, and a single cutting edge may interact with both CFRP and metal simultaneously. Consequently, during combined machining, the forces acting on different cutting-edge components vary significantly and fluctuate continuously (Jayabal and Natarajan, 2010; Zitoune et al., 2010).

Thrust force is a key metric for assessing the machinability and power usage of different composite/metal stacks during drilling. It impacts hole

quality and tool wear, making it an important indicator in machining operations (Faraz et al., 2009; Montoya et al., 2013; Wang et al., 2013; D'Orazio et al., 2017). Experiments were conducted on hole quality to determine the impact of the drilling parameters and tool materials on CFRP/Ti stacks drilling (Ramulu et al., 2001; Kim and Ramulu, 2004, 2007; Sushinder et al., 2015) and on Ti/CFRP/Al stacks drilling (Shyha et al., 2011) by various researchers. Typically, the titanium phase's thrust forces are greater than those observed in the composite phase. The titanium alloy is machined with chips that are split due to elastoplastic deformation and have continuous, irregular shapes, which results in significant resistance for chip evacuation and consequently large force magnitudes (Xu, El Mansori, Chen, et al., 2019; Xu, El Mansori, Voisin, et al., 2019). On the other hand, the CFRP panel undergoes chip removal primarily through brittle fracture, which creates powdery chips and results in thrust forces that are much smaller (Xu et al., 2020).

When drilling composite/titanium stacks, a rise in tool feed causes a rise in thrust force as shown in Figure 3a and 3d (Xu, 2016). This is because, when feed rises, the volume of the discharged material increases, increasing the cutting forces (Boutrih et al., 2022). Cutting speed has minimal impact on thrust force in both phases, as shown in Figure 3b and 3c. Contrarily, Prabukarthi et al. claimed that achieving a lower thrust force at a greater feed rate was possible since drilling at high feeds causes the material's elasticity to diminish due to the rise in temperature in the cutting zone. Merino-Pérez et al. concurred that cutting at temperatures above T_{σ} of the matrix reduces the composite's elastic modulus, which in turn reduces the maximum thrust force (Merino-Pérez et al., 2016). Opposite results were also recorded that lower feed rate can result in higher thrust force (Mouleeswaran et al., 2011). Xu et al. said that the effect of cutting speed on thrust force in both CFRP and Ti phases is lower in either the CFRP \rightarrow Ti or Ti \rightarrow CFRP sequence (Xu, 2016). An et al. (2020) mentioned that the thrust forces increased up to 480 N in the CFRP \rightarrow Ti sequence due to chip blockage, while the thrust force in the Ti → CFRP sequence reached only up to 280 N. Xu and Mansori mentioned that the thrust forces increased up to $700 \,\mathrm{N} - 900 \,\mathrm{N}$ in CFRP \to Ti sequence, while in the Ti \to CFRP sequence it ranged between 600 N and 800 N (Xu and El Mansori, 2016). Sushinder et al. (2015) said that greater resistance to plastic deformation during Ti6Al4V drilling produced higher torque and thrust force at lower cutting speeds. Torque and thrust force decline when greater cutting speeds are used because of the thermal softening that takes place and is exacerbated by the extremely low thermal conductivity of titanium alloys (Sushinder et al., 2015).

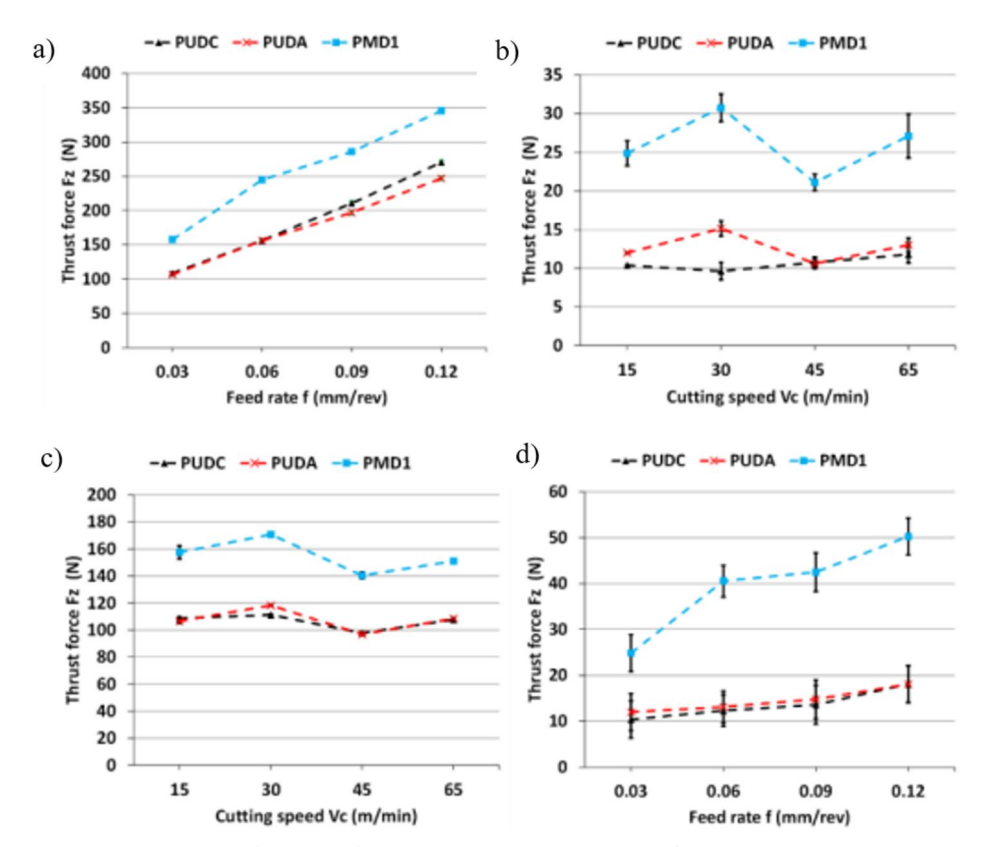


Figure 3. Evolution of thrust force versus cutting speed (f = 0.03 mm/rev, and CFRP-Ti sequence) (a) in Ti phase; (b) in CFRP phase and evolution of thrust force versus feed rate (Vc = 15 m/min and CFRP-Ti sequence) (c) in Ti phase; (d) in CFRP phase.

Compared to unidirectional CFRP (UD-CFRP), multidirectional CFRP (MD-CFRP) encourages stronger forces in both longitudinal and transverse directions because MD-CFRP, as opposed to UD-CFRP, has increased strength in both directions, which leads to cutting resistance for chip breakage (Boutrih et al., 2022). The majority of fiber fractures that occur when cutting along the fiber orientation produce a strong thrust force and need a lot of energy. The fiber is vulnerable to bending fracture when cut directly across its orientation, which causes the fiber to separate from the matrix (Bonnet et al., 2015; Li et al., 2022). The heat transmission effectiveness along the fiber direction is also higher for UD-CFRP (Liu et al., 2014), and the fracture propagation is quicker along the fiber orientation (Ke et al., 2005).

Ti6Al4V alloy sheet assembled with UD-CFRP using adhesive (PUDC), using autoclave joining method (PUDA) and using autoclave joining method with MD-CFRP (PMD1)

When it comes to the effect of tool geometry on thrust force, Wika et al. found that, because of its increased helix angle and ample flute volume for

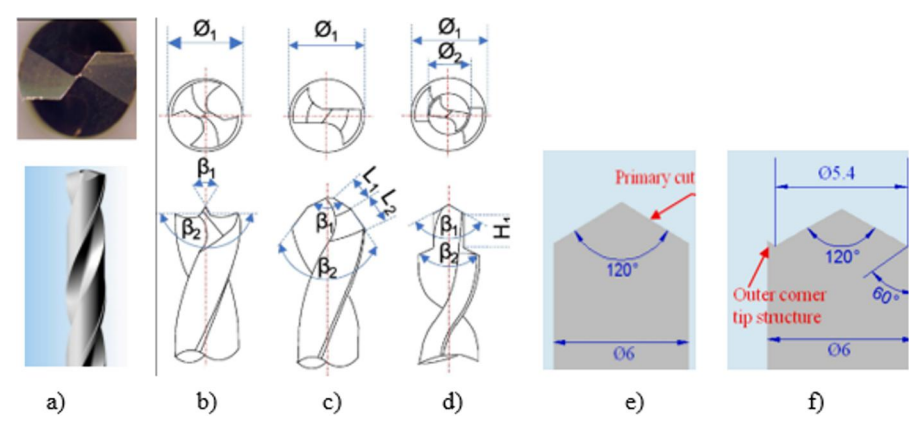


Figure 4. Geometrical features of different drill bits used to drill CFRP/Ti stacks (a) Two-flute drill (Wika et al., 2011). (b) Brad point drill (c) Double point drill (d) Step drill (Rodriguez et al., 2023) (e) Twist drill (f) Candle stick drill (Kim et al., 2015).

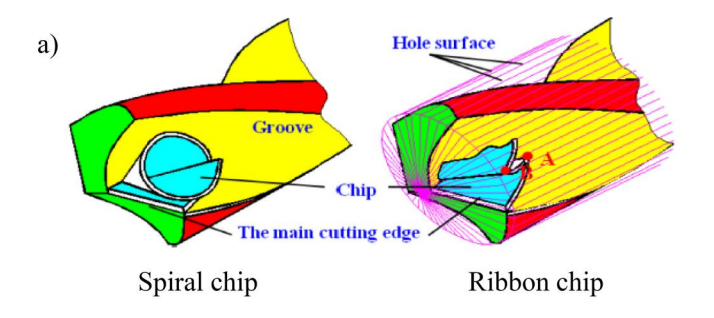
chip removal and heat dissipation, the two-flute drill bit is effective in (Figure 4a) offering the least cutting temperature and the lowest cutting force (Wika et al., 2011). Rodriguez et al. (2023) mentioned that brad point drill effectively cut CFRP/Ti6Al4V stacks. In this case, as shown in Figure 4b, the center point and two peripheral cutting edges produce a 180°-point angle. These side cutters drilled composites with less thrust force and delamination, thanks to the center 140°-point angle (Rodriguez et al., 2023). They further mentioned that double-point angle drilling also lessens the thrust force due to the smaller point angle in the initial stage of the tool, as can be seen in Figure 4c. This is because the enhanced chip breakability of twin cutting edges is achieved by altering the chip flow direction, which is promoted by having double cutting edges (Rodriguez et al., 2023). As a result, the broken chips can be efficiently removed from the drilling area without causing any obstruction to the process. Qiu et al. found that the maximum thrust force produced by the candlestick drill (Figure 4f) for drilling CFRP layers is 39.4% and 17.4% less and for drilling titanium alloy is 12.9% and 16.6% less compared to the twist drill (Figure 4e) and double-point angle drill, respectively. The outer edge tip configuration and the secondary cutting edge featuring a smaller point angle can both help reduce the thrust force in a candlestick drill (Qiu et al., 2021). When machining CFRP/Ti stacks, it was discovered that the point angle, helix angle and cutting-edge length all played significant roles in impacting thrust force (Kim et al., 2015). By using a smaller helix angle (30°), smaller point angle (135°) and a shorter chisel edge, the thrust force may be decreased (Ashrafi et al., 2013; Senthilkumar et al., 2018).

Thrust force during CFRP/Ti stack drilling is influenced by tool geometry, feed rate, cutting speed and material properties. Titanium phases produce higher thrust forces due to elastoplastic deformation, while CFRP phases experience lower forces from brittle fracture. Increasing feed rate generally raises thrust force by removing more material, though higher cutting speeds reduce thrust due to thermal softening, particularly in titanium alloys. Tool geometry significantly impacts thrust force; designs like twoflute, brad point and candlestick drills improve chip evacuation, reduce cutting forces and minimize delamination. Multidirectional CFRP generates stronger forces than unidirectional CFRP due to higher strength in multiple directions.

Chip formation

The most significant component for the quality of a drilling operation is chip form. If the chips are well broken, the drilling operation will be smooth. Because of their high abrasive properties, CFRP chips are fragmented into tiny dust particles during drilling CFRP/Ti stacks. As the drill moves from CFRP to Ti alloy, a continuous chip of titanium is produced because ductile materials typically generate continuous chips rather than breaking during drilling. Continuous chips are classified under spiral chips, string chips and ribbon chips depending on their chip formation methods, as shown in Figure 5. The primary cutting edge's varying cutting speeds cause the chip to bend and form a curl chip before rotating continuously, resulting in the spiral chip (Qiu et al., 2021). The structural design of a spiral chip allows it to rotate on its own axis as it ascends when the drilled hole is shallow (Ke et al., 2005). When the chip-holding groove and hole wall impede the chips, string chips are produced. These chips cannot be removed from the hole smoothly (Qiu et al., 2021). Ribbon chips are formed in the following way. Cutting temperature rises as drilling depth increases due to the accumulation of cutting heat. Friction between the hole wall and the drill groove at this point makes the entire chip longer and hinders chip discharge (Zhu et al., 2018). The chip deforms when it strikes the groove due to the large spiral radius that causes it to flow out of the rake surface. The chip then makes contact with the hole wall and is subjected to resistance, resulting in the formation of the ribbon chip. This is the chip that increases the roughness of the Ti surface. The most challenging of the three types of chips to discharge outside the hole is the compressed string chip (Qiu et al., 2021), and it has the highest temperature (Brinksmeier and Janssen, 2002). Senthilkumar et al. mentioned that the chip shape for the first 40 holes was spiral cone, which was simpler to expel. As wear increases from 40 to 70 holes, the spiral cone's length decreases and the bending action begins to work, producing ribbon chips of various lengths. The chips' inability to rotate around their own axis is the cause of this. After 70 holes, the wear turns serious, causing the thrust





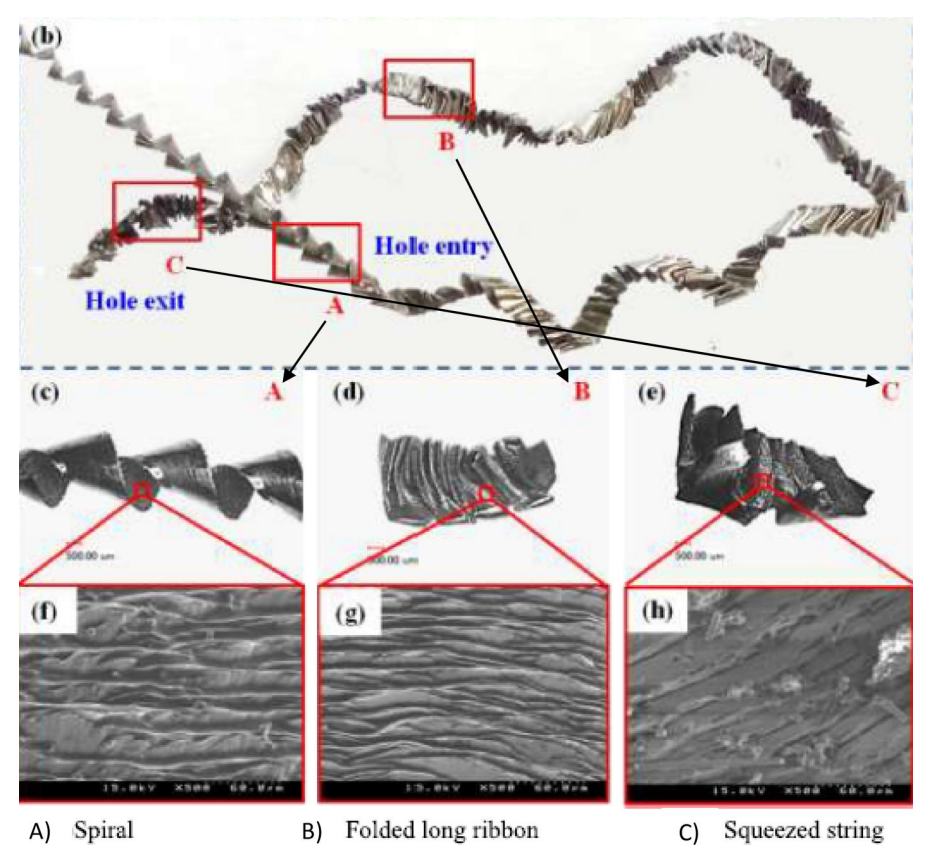


Figure 5. The micro and macro morphology of chips formed while drilling CFRP/Ti (Qiu et al., 2021).

force to quickly increase. As a result, the chip's thickness decreases and the pitch begins to increase, and therefore, lengthy ribbon chips are formed, which are detrimental in terms of chip removal and hole surface smoothness (Senthilkumar et al., 2013). In terms of feed rate, when drilling under low feed rate, long, ribbon-like titanium chips were generated and tended to tangle around the drill body. This phenomenon can have several negative effects. First, it leads to significant abrasion and erosion on the drilled hole surfaces, resulting in a deteriorated surface finish. Secondly, it increases the likelihood of premature tool failures, such as micro-chipping, edge fractures, or coating delamination (Xu and El Mansori, 2016). At low feed rates (0.02 mm/rev), the section modulus of the chip in bending is small. Consequently, the spiral continuous chips easily compress and bend against the friction of the hole wall, resulting in the formation of folded continuous chips (Zhu et al., 2018).

However, when the feed rate is increased (0.08 mm/rev), the Ti chips break into smaller segments by the friction of the hole wall, resulting in chip blockage. This is because the force imposed on the chip by the hole wall is larger than the force applied by the cutting edge and chip-removing groove (Pecat and Brinksmeier, 2014; Xu, El Mansori, Voisin, et al., 2019) as the surface of CFRP hole walls tends to be rougher compared to that of metals. There are axial and tangential friction stresses on the hole wall during chip removal (Mellinger et al., 2002). Fresh chips are regularly produced at the drilling area during drilling operations, which are distorted and crumpled due to the obstruction of hindering chips. The compressed chips will be pushed out of the hole when the friction on the hole wall is no longer able to further compress the chips (Li et al., 2022). In contrast, the impact of cutting speed on chip breakability is minimal, with the Ti chips generally maintaining the same length and type regardless of changes in cutting speed and therefore not having any impact on hole quality (Xu and El Mansori, 2016). Additionally, at higher cutting speeds, chips were wound more tightly with greater kinetic energy, which facilitated chip breaking (Wei et al., 2016).

Tool geometry is also important in chip morphology, and the length of a spiral cone chip can serve as a measure to evaluate the difficulty of chip removal. Shorter chips are desirable, with tighter helix chips providing a better surface finish. Senthilkumaran et al.'s studies show that chip creation is the same for 130° and 118° point angle drills (Senthilkumar et al., 2013). Qiu et al mentioned that in a candlestick drill, the chip created by the main cutting edge and the point structure splits into two separate parts. As a result, the chip width from the main cutting edge of the candlestick drill is narrower than that of twist drills and double-point angle drills. This narrower chip width facilitates efficient chip removal, minimizing damage to the hole wall and reducing the likelihood of entry into the CFRP layer (Qiu et al., 2021). Further, when using a twist drill for the drilling process, the primary chip produced from the titanium alloy is a string chip. For feed rates below 0.08 mm/rev, both the double-point angle drill and the candlestick drill generate ribbon chips. However, at a feed rate of 0.12 mm/ rev, string chips are formed for both the double-point angle drill and the candlestick drill as shown in Figure 6 (Qiu et al., 2021). Additionally, chips generated by the multi-facet drill tended to be straighter due to its smaller

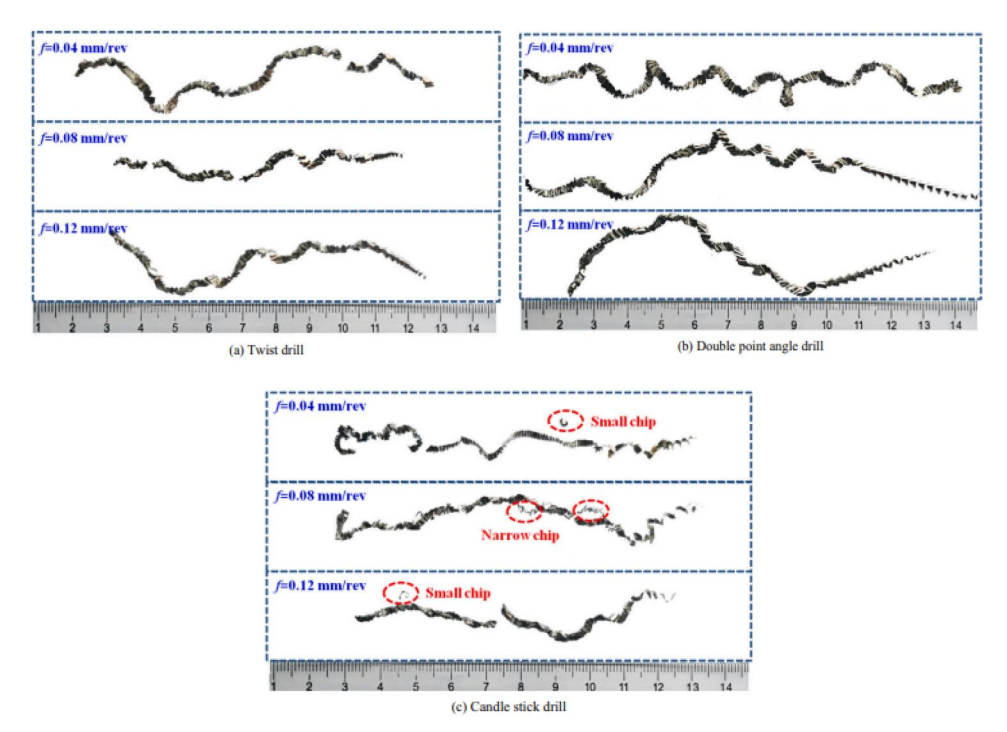


Figure 6. Different chip morphologies obtained using various tools in CFRP/Ti stack drilling (Qiu et al., 2021).

secondary point angle. As the feed rate increased, the chips from this drill formed a spiral tower, increasing their stiffness and making them easier to break. In contrast, the brad spur drill, which features three drill tips, was less effective at winding chips. As a result, the chips produced were relatively flat and more difficult to break (Wei et al., 2016).

Regardless of whether the drilling sequence is CFRP to Ti or Ti to CFRP, the chip-breaking performance improves as the feed rate rises; however, cutting speed has no effect on chip shape (An et al., 2020). On the other hand, regular spiral-shaped chips are obtained when drilling the Ti → CFRP sequence, but irregular, shorter and compressed -shaped chips are obtained when drilling the CFRP \rightarrow Ti sequence (An et al., 2021) as shown in Figure 7. Moreover, the rubbing between the Ti6Al4V chips and the CFRP hole surface not only complicates chip removal but also leads to blockages in the spiral groove (An et al., 2020).

The quality of drilling operations in CFRP/Ti stacks heavily depends on chip morphology, as well-broken chips ensure smoother operations. CFRP generates fragmented, dust-like chips due to its abrasive nature, while titanium produces continuous chips (spiral, string, or ribbon) influenced by cutting conditions and heat. Spiral chips are easier to expel, while ribbon and string chips, particularly compressed string chips, are more challenging to remove and result in higher temperatures and surface roughness. Tool

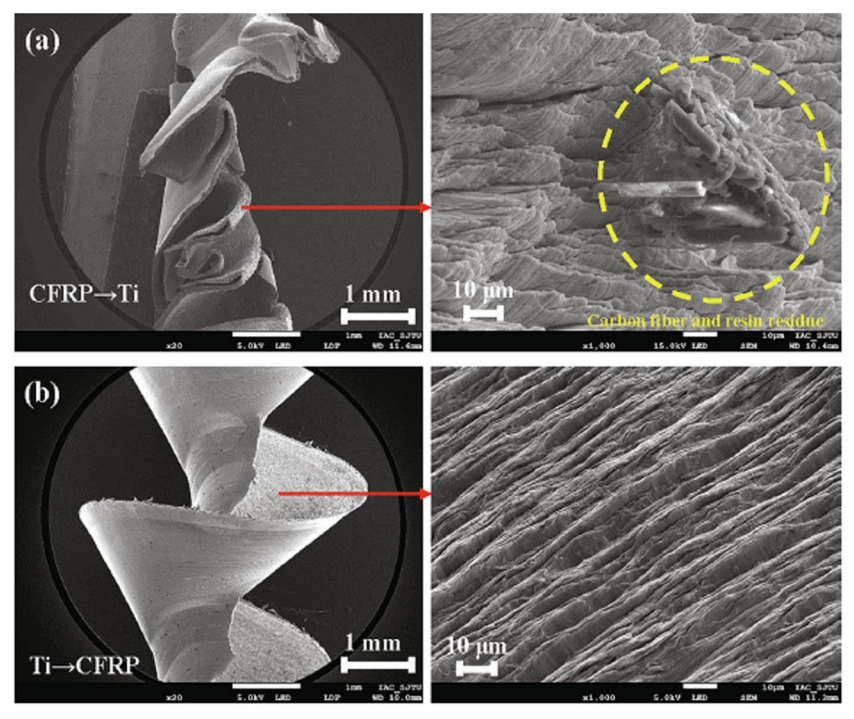


Figure 7. Various chip morphologies produced at a cutting speed of 10 m/min and a feed rate of 0.06 mm/rev under different drilling sequences: (a) CFRP \rightarrow Ti, (b) Ti \rightarrow CFRP (An et al., 2020).

wear increases chip length and alters chip formation, with ribbon chips dominating as wear progresses. Tool geometry significantly impacts chip morphology in a way that candlestick drills create narrower, more manageable chips than twist drills. While higher feed rates improve chip-breaking performance, cutting speed has little impact. Further, challenges in chip removal occur especially in CFRP \rightarrow Ti drilling due to friction-induced blockages in the hole.

Tool wear

Wear refers to the erosion of material from a solid object's surface due to the mechanical action of another object. Wear can associate the impacts of many chemical and physical processes, such as plastic deformation, microplowing, micro-cutting, fracture, melting, welding, cracking and chemical contact, during friction between two materials. Tool wear typically occurs rapidly when tools are new, but it slows down as more holes are drilled (Unai et al., 2019). This is because there is an increase in the contact area between the tool and the work material in the thrust direction, and the cutting edge gradually becomes rounded (Park et al., 2011; Pramanik and Littlefair, 2014).

Tool wear on drills includes crater wear, flank wear, chisel edge wear and chipping (Park et al., 2011). When the rake face is worn down by chip contact, this is known as crater wear. Till it develops severe enough to result in a cutting-edge failure, the utility of a tool is not significantly diminished. It can be caused by a high feed rate or a low spindle speed, and in orthogonal cutting, this often happens when the temperature of the tool is high. At about the same height as the material's cutting depth, crater wear starts to appear (Senthilkumar et al., 2013). Flank wear is commonly unaffected by spindle speed due to abrasion, which is the friction between the freshly drilled workpiece surface and the contact region on the tool flank (Senthilkumar et al., 2013). In other words, the portion of the tool in contact with the finished part erodes. Wear progression occurs largely on the flank face while drilling CFRP-Ti stacks, with a rate roughly twice that of edge wear because of abrasion on the flank surface (Park et al., 2014). When the flank wear reaches a maximum value of 200 µm, the tool life ends (Dahnel et al., 2020). Local wear quantity (LWQ) is a more pertinent measure for characterizing tool wear when flank wear and edge rounding coexist (Wika et al., 2011; Montoya et al., 2013). Chisel edge wear in a drill is the term used to describe wear to a drill bit's outside edge surrounding the cutting face due to the cutting speed. It goes down the drill flutes and must be addressed by removing a significant amount of material from the drill bit. The relief angle and feed rate also influence chisel edge wear. Lower relief angles are not suggested since they contribute significantly to chisel edge wear, and higher feed rates cause the wear to increase (Senthilkumar et al., 2013). Chipping wear causes an unprecedented breakdown early in the tool's life, resulting in the failure mode. Chipping wear is exacerbated by mechanical difficulties such as machine spindle or component fixture vibration. Harmonic vibrations at the cutting edge are enhanced by a tool holder having a large cantilever condition. High loads on the tool also induce chipping (Faraz et al., 2009; Senthilkumar et al., 2013). A build-up edge (BUE) is a buildup of workpiece material on the cutting edges, which may result from the adhesion because some substances have a propensity to weld to the cutting edge of the tool. It commonly occurs on softer metals with lower melting points but can be prevented by increasing cutting speeds and using lubricants.

Theoretically, multi-material drilling requires various tools, one that is suited to composite and another that is suited to aluminum or titanium (Rawat and Attia, 2009). For instance, PCD is preferable when drilling CFRP, while carbide tools are used to machine Ti6Al4V (Pan et al., 2014). Kim et al. (2015) examined the quality of holes and the wear of tools when drilling CFRP/Ti samples with PCD and tungsten carbide (WC) drills. Since CFRP is anisotropic and will have confined responses to the same loads while metals are isotropic and will respond uniformly to all loads, this can result in imperfections in the interior of the work-piece (Lazar and Xirouchakis, 2011; Che et al., 2014). Solving the issue of tool wear during single-shot drilling of stacked-up materials is therefore incredibly difficult (Wang et al., 2017). At low speeds, drills made of PCD wear down onethird less than drills made of WC; however, PCD drills are not usable on CFRP/Ti stacks at increased speeds due to chipping (Park et al., 2011). This rationale is grounded in cutting temperatures; when temperatures rise, PCD undergoes graphitization and interacts with Ti6Al4V, creating a diffusion effect on the edge, making it unsuitable for further machining (Kerrigan and Scaife, 2018). When drilling CFRP/Ti stacks, drills with diamond coating suffer from serious edge chipping at the chisel edge's end. This is due to the fact that, on the one hand, the coating's addition increases the chisel edges' radius, aggravating the plowing action of chips at the drill's chisel edge zone and, on the other hand, the diamond coating's intrinsic brittleness causes an elevated susceptibility to fracture when cutting the titanium alloy (Xu et al., 2020). The intrinsic brittleness of PCD drills, along with the abrasive operations by the carbon fibers and inhomogeneity in the Ti microstructure, led to a large amount of cutting-edge chipping (Xu et al., 2020). The primary problem with the carbide drills was adherence, which completely covered the cutting edges (Wang et al., 2014). But Ramulu et al. (2001) and Kim and Ramulu (2004) found that compared to HSS-Co and HSS drills, the tool life of carbide drills is four times greater. Despite the fact that serious tool wear problems specific to the machining of CFRP/Ti6Al4V stacks exist, drilling CFRP and Ti materials in a single shot is advantageous from an industrial perspective (Ramulu et al., 2001; Brinksmeier and Janssen, 2002; Kim and Ramulu, 2004, 2007; Vijayan et al., 2010; Zitoune et al., 2010; Park et al., 2011; Shyha et al., 2011) in order to achieve tight tolerance for the post-mechanical assembly and reduce positional mistakes (Xu, 2016).

Drilling parameters have an impact on the composite material's mechanical strength, as demonstrated by Krishnaraj et al. (2007). Higher cutting speeds along with low feed rates are needed to drill brittle, hard materials like CFRP, but low cutting speeds are preferable to minimize tool wear when drilling titanium alloys like Ti6Al4V (M'Saoubi et al., 2015). The main wear processes on the WC drill at high drilling speeds are abrasive wear brought on by the hard, broken fibers and carbide grains and edge micro-chipping. When drilling CFRP, the WC drill's flank wear was greatly impacted by cutting speed (Park et al., 2011). The right choice of (i) enhanced and controlled process parameters (Geier et al., 2021), (ii) tool coating (a thin diamond coating), (iii) cutting tool material (preferably solid carbide with a smaller grain size and a higher cobalt concentration)

(Wang et al., 2013) and (iv) the use of self-sharpening cutting tools (Byrne et al., 2021) would allow tool wear to be reduced.

The overall wear volume post drilling of the CFRP/Ti stack almost matches the combined wear volumes from flank wear during drilling of Tionly and edge rounding wear during drilling of CFRP-only, excluding severe edge chipping in drilling Ti-only as shown in Figure 8. This is due to the fact that while drilling CFRP only, edge rounding wear predominates, whereas when drilling Ti only, flank wear and edge chipping occur (Wang et al., 2014). Dahnel et al. (2020) demonstrated that when drilling CFRP/Ti stacks, the flank wear was 1038% larger than that of drilling Tionly. Wang et al. (2013) mentioned that the thrust force increases steadily as more holes are drilled as a result of an increase in the tool-workpiece contact zone in the thrust direction and due to edge rounding wear. Moreover, while drilling a stack comprising Ti and CFRP, the tool's lifespan extended approximately threefold compared to drilling Ti alone. This occurred because, as depicted in Figure 9, the carbon fibers in the CFRP layer brushed away the Ti adhesion and smoothed the cutting-edge during drilling of the CFRP/Ti stack. This minimized edge chipping, which would have otherwise happened while drilling the lower Ti layer due to the removal of adherent Ti layers (Wang et al., 2014). The uneven loading

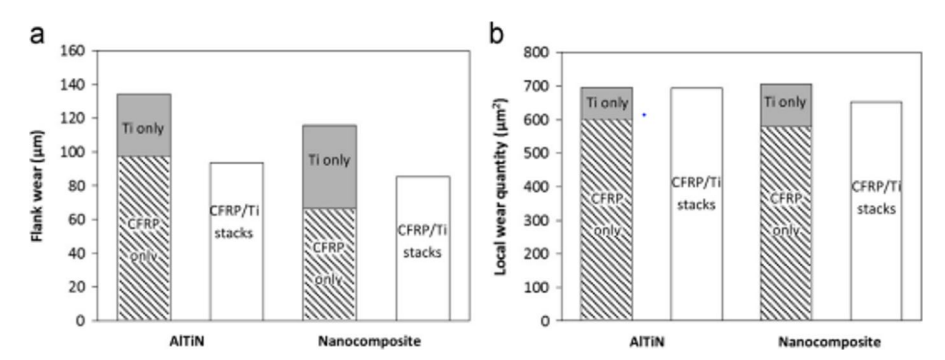


Figure 8. Comparison of Flank wear and Edge rounding wear (LWQ) of the AlTiN and nanocomposite coated drills at hole 40. (a) Flank wear and (b) Edge rounding wear (LWQ).

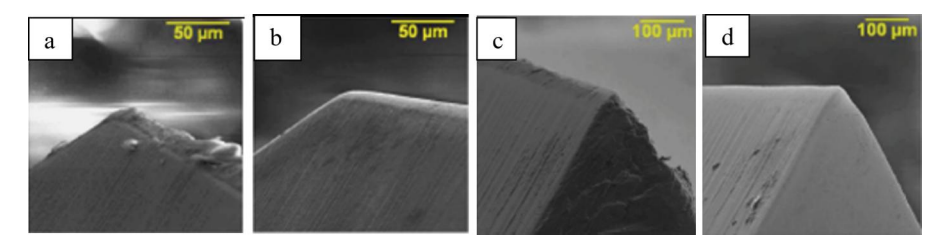


Figure 9. The SEM pictures of the drill cutting edges (a) near the chisel edge before and (b) after, near the margin before (c) and after (d) drilling into the top CFRP layer when drilling CFRP/Ti stack (Wang et al., 2014).

environment on the cutting edge is caused by the Ti adhesion's alternating adherence and removal. As a result, while drilling a CFRP/Ti stack, individual (CFRP and Ti) plate drilling processes are not independent but rather interact, and this kept the edges from chipping (Wang et al., 2014). Alonso et al., on the other hand, stated that adhesive and abrasive wear mechanisms happen concurrently while drilling stacks, and the combination of them favors quicker tool wear than cutting the components individually (Alonso Pinillos et al., 2019). Park et al. explored CFRP/Ti stack drilling using carbide and PCD tools (Park et al., 2011) and Ti/CFRP stack drilling using WC twist drills (Park et al., 2014). Both of these studies emphasized the cutting-edge abrasion caused by CFRP and adhesion caused by Ti on tool cutting edges and flank faces.

The creation of titanium alloy chips and burrs frequently results in a builtup adhesion layer on the cutting edges of the tool (Xu et al., 2020). Ti drilling is commonly associated with adhesion because of its strong chemical attraction to most tool materials (Zhang et al., 2008). The application of coatings such as titanium nitride (TiN) amplifies this effect (Hartung et al., 1982; Berger et al., 1998; Klocke and Krieg, 1999). During the Ti phase of CFRP/Ti drilling, when the cutting temperature rises sufficiently to trigger strong adhesive attraction, the WC drill tends to become softer. This is because the cobalt (Co) binder, responsible for binding the carbide grains together, softens, resulting in the WC drill also softening. Along with the abrasion caused by the hard titanium alloy, the flank wear is also prolonged by the removal of carbide grains from the cobalt binder as the titanium loses adhesion while cutting through the CFRP in the subsequent hole. It was mentioned by Komanduri and Reed that WC-Co with a low cobalt binder is better suited for drilling titanium compared to grades with higher cobalt content (Komanduri and Reed, 1983). The chemical reactivity of Ti rises with temperature and in turn increases the quantity of Ti adherence (Senthilkumar et al., 2013). Because significant Ti adhesion was not detected when drilling CFRP-Ti stacks at moderate speeds due to decreased heat generation, but it is clearly visible at high speeds due to greater heat generation (Park et al., 2014). Adhesion occurred promptly upon commencing titanium drilling, rapidly covering a significant portion of the flank surface, particularly at elevated spindle speeds (Senthilkumar et al., 2013; Xu et al., 2020). BUE reduces the sharpness of the cutting edge, and when these BUE break, the rate of chisel edge wear is significantly accelerated, leaving cutting carbon fibers with a "dull" edge at the hole entry (Xu et al., 2020). These problems are most obvious when the drill bit enters or leaves the CFRP and Ti layers (Gaugel et al., 2016). Because of the abrasiveness and high hardness of the reinforcing fibers, as well as the nonhomogeneous structure of the CFRP/Ti stack, rapid tool wear progression is common (Faraz et al., 2009; Rawat and Attia, 2009; Wang

et al., 2013; Çelik et al., 2015; Xu and Zhang, 2018). Excessive tool wear results in poor surface quality (Pecat and Brinksmeier, 2014).

Krystian et al. investigated drilling of CFRP/Ti stacks with three-flute and two-flute drills, as well as with two helix angles of 20° and 40°. When utilized at a higher feed rate, chipping of the primary cutting blade occurred in drills with a higher helix angle. However, the drill's cutting edge is stronger and less prone to chipping when the helix angle is lower, but it requires more cutting forces. Moreover, the two-flute drill bit, featuring a wider flute volume for chip removal and heat dispersion, generated the least cutting force and lowest cutting temperature compared to the three-flute drill (Wika et al., 2011). In another investigation, when drilling a CFRP/Ti stack, a 118° point angle drill exhibited higher chisel edge wear and flank wear rate than a 130° point angle drill, as shown in Figure 10. The increased chisel size on the tool flank leads to localized plastic deformation, contributing to higher thrust forces. The cutting forces are increased by plastic deformation because it increases the contact surface and, consequently, the friction between the drill and the workpiece. This raises the temperature of the tool and the workpiece at the cutting region. As a result, the tool flank's ductility improves (Senthilkumar et al., 2013). Garrick mentioned that, compared to typical PCD drills, K-land drills can extend tool life and improve hole quality (Garrick, 2007).

The performance and wear behavior of drill bits in aerospace applications, particularly in drilling CFRP/Ti stacks, are strongly influenced by the type of coating applied to the cutting tool. Various coatings—such as diamond-like carbon (DLC), titanium aluminum nitride (TiAlN), titanium aluminum chromium nitride (TiAlCrN), aluminum titanium silicon nitride (AlTiSiN-G) and diamond coatings—offer different levels of wear resistance

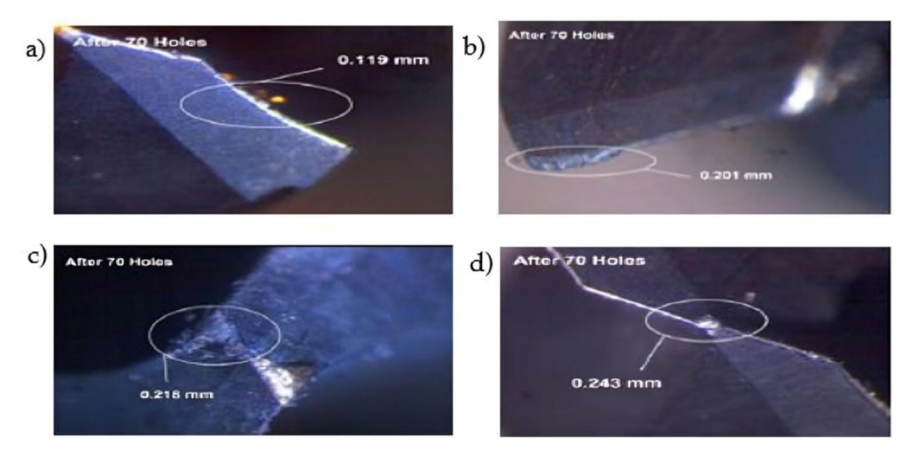


Figure 10. After drilling 70 holes, (a) Flank wear for 118° point angle drill (b) 130° point angle drill (c) chisel edge wear for 118° point angle drill and (d) 130° point angle drill bit (Senthilkumar et al., 2013).

and chip adhesion characteristics under varying cutting conditions (Jebaratnam, 2025).

Drill bits with DLC coatings commonly experience wear mechanisms such as abrasion, edge rounding and localized chipping. Despite these wear modes, DLC coatings generally provide good wear resistance due to their hardness and low friction properties, making them suitable for drilling composite materials like CFRP. They are particularly effective at reducing flank wear, which is a critical wear type that affects tool life and machining accuracy. TiAlN-coated drill bits exhibit wear in the form of abrasion and tend to suffer from aluminum particle adhesion during the drilling of CFRP/Ti stacks. The high cutting temperatures generated during drilling exacerbate this adhesion, potentially leading to material buildup on the tool edge and increased friction (Jebaratnam, 2025). Titanium aluminum chromium nitride (TiAlCrN) and titanium silicon (TiSi) coatings offer higher wear resistance and improved thermal stability compared to TiAlN. These coatings demonstrate reduced chip adherence and better abrasion resistance, particularly in challenging drilling scenarios where high temperatures and friction are present. Diamond-coated drills are highly effective in reducing wear, particularly flank wear, due to the superior hardness and low friction of the diamond layer. These coatings are ideal for drilling CFRP because they minimize delamination and tool wear. However, under specific conditions—such as drilling with minimum quantity lubrication (MQL)—diamond coatings can exhibit accelerated wear due to titanium chip accumulation, which can lead to coating failure (Jebaratnam, 2025).

Flank wear is a primary indicator of drill bit wear and is commonly used to assess tool life in aerospace applications. Studies indicate that DLCcoated drills tend to exhibit less flank wear compared to TiAlN-coated drills, highlighting the importance of selecting the right coating for each specific machining environment. Diamond coatings, while generally excellent at reducing wear, may still suffer from performance degradation under certain lubricating conditions, particularly when titanium chips accumulate on the tool surface. The interaction between CFRP and Ti layers in the stack also plays a critical role in determining tool wear and performance. For instance, the brushing effect of CFRP fibers on titanium fusion can cause localized wear or surface damage, further accelerating tool wear and reducing drill life (Jebaratnam, 2025).

Tool wear during drilling arises from mechanical and chemical interactions, including abrasion, adhesion and chipping, influenced by tool material, geometry and cutting parameters. Crater wear occurs on the rake face due to high feed rates and low spindle speeds, while flank wear, driven by abrasion, dominates during CFRP-Ti stack drilling. Chisel edge wear increases with lower relief angles and higher feed rates, while chipping wear arises from mechanical vibrations and high loads. Multi-material drilling faces challenges due to differing material responses—CFRP induces edge rounding wear, while Ti causes flank wear and adhesion. PCD tools are effective for CFRP but unsuitable for Ti at high speeds due to graphitization, while carbide tools handle Ti better but suffer adhesion issues. Drill geometry also affects performance; smaller helix angles and point angles reduce chipping but require higher cutting forces. Two-flute drills with wider flutes offer better heat dissipation and lower cutting forces than three-flute designs.

Manufacturing defects in CFRP/Ti stacks material

In the aircraft assembly process, drilling is a common machining technique used to create round holes of various depths and sizes. Three hundred thousand to three million holes may be present in commercial aircraft (El-Sonbaty et al., 2004; Abrão et al., 2008; Mouritz, 2012; Giasin, 2016, 2018; Giasin et al., 2016, 2017; Giasin and Ayvar-Soberanis, 2017). Drilling holes can provide significant challenges due to the vast differences in the mechanical and thermal properties of FRP and metal phases used in FMLs (Pawar et al., 2015). These include hole size, hole circularity, matrix distortion, delamination, exit burr effect, fiber shrinkage (Ezugwu and Wang, 1997; Abrão et al., 2007; Liu et al., 2012; Khashaba, 2013; Singh et al., 2013; Ben Soussia et al., 2014; Che et al., 2014) tool failure (Ramulu et al., 2001; Brinksmeier and Janssen, 2002; Kim and Ramulu, 2004, 2007; Vijayan et al., 2010; Park et al., 2011, 2014; Shyha et al., 2011) surface texture, presence of Ti burrs (Ramulu et al., 2001; Kim and Ramulu, 2004, 2007) and high machining costs (Xu, El Mansori, Voisin, et al., 2019; Xu, Ji, et al., 2019; Xu, Li, et al., 2019; Xu, Zhou, et al., 2019; Xu, et al., 2020). Different damages are dominant when using different sequences as shown in Figure 11. For example, scratches on the CFRP surface and spalling dominate while drilling in the CFRP/Ti sequence, but push-out

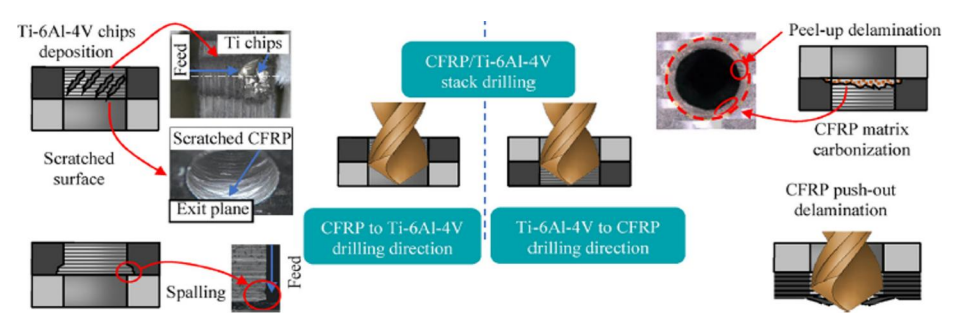


Figure 11. Surface integrity issues arise when drilling CFRP/Ti6Al4V stacked configurations with various stacking sequences (Rodriguez et al., 2023).

delamination and matrix carbonization are severe while drilling from the Ti/CFRP sequence. These issues represent about 60% of all part rejections (König and Graß, 1989; Komanduri, 1997; Hocheng, 2012; Mouritz, 2012; Vijayan et al., 2010; Giasin et al., 2015, 2020). In any cutting sequence, the space between the CFRP and Ti6Al4V layer should be avoided. Either the powdery chips produced by CFRP when drilling from Ti6Al4V to CFRP or the chips produced in the Ti6Al4V drilling operation when drilling from CFRP to Ti6Al4V will become trapped in the CFRP-Ti6Al4V interface's gap (An et al., 2020).

Drilling a CFRP/Ti stack from the CFRP side has a major problem where the Ti6Al4V chips erode the CFRP hole wall, which includes resin ablation, scratches and sticky chips (An et al., 2021). The titanium chips damage the CFRP surface in this configuration due to the difficulty of the titanium chip removal. Spalling may take place while the titanium chips are being evacuated and widen the hole at the base of the CFRP plate. This can be prevented by the Ti6Al4V plate put underneath the CFRP (Luo et al., 2019). Surface pits and heat degradation of the resin on the CFRP wall side are the key drilling problems when drilling through a CFRP/Ti stack from the Ti6Al4V direction (An et al., 2021). Delamination issues exist in this arrangement since the composite material is not supported at its back. Additionally, the epoxy matrix may carbonize as a result of the drill's high temperature after cutting the titanium phase, which often manifests as a discolored ring on the surface of the CFRP plate (119). Drill bits with unique geometries may be able to produce holes in CFRP/Ti stacks of excellent quality (Ad Vlot, 2001).

Delamination on the composite panel

The primary hole quality issues encountered during the drilling of CFRP panels include fiber pull-out and push-out delamination. According to Sandvik Coromant tool manufacturers, the maximum allowable delamination is 1 mm (Coromant, 2010). The mechanisms for chip formation at angles between 125° and 315° cause fiber pullout, matrix stripping and fiber matrix debonding (Eneyew and Ramulu, 2014). Delamination is one sort of damage that could arise in the interlaminar gap between adjacent layers in laminate parts (Rodriguez et al., 2023). Delamination could occur for one of two basic reasons at the metal composite interface (MCI). Firstly, bending tensions between the material point of contact and the drill bit (Erturk et al., 2019) or secondly, heat creation due to friction with CFRP particles or Ti chips cause delamination to occur (Park et al., 2018). Additionally, when subjected to cyclical loads, delamination will worsen and eventually shorten the service life of components (Xu et al., 2020).

Peel-up and push-out delamination are the two types of delamination flaws that can arise at the entrance and exit of CFRP, respectively (Zhang et al., 2001; Hocheng and Tsao, 2005; Li et al., 2022). Peel-up delamination happens where the drill enters the material, and it is brought on by an incomplete fiber fracture at the entrance. The tool's helix raises the upper layers of the composite, which are subsequently raised as shown in Figure 12a (Gao et al., 2022). Peel-up delamination is not as severe as push-out delamination. Push-out delamination develops when the drilling instrument pushes the laminate's final plies as it leaves the plate as shown in Figure 12b. Interlaminar debonding between neighboring plies of a composite is caused by thrust force, which causes push-out delamination at the composite hole's exit (Xu et al., 2020). Numerous investigations have shown that increased thrust forces caused by increased flank wear increase CFRP exit delamination (Gaugel et al., 2016; Raj and Karunamoorthy, 2016; Feito et al., 2018; Li et al., 2018), and Dahnel et al. (2020) mentioned that it made no difference to entry delamination. Researchers initially concentrated on employing aluminum at the bottom while drilling Ti/CFRP/Al stacks to reduce CFRP hole delamination. In the following research, machining of CFRP/Ti stacks without the backing of other metals was adopted (Mori et al., 2011; Park et al., 2011; Pecat and Brinksmeier, 2014; Wang et al., 2014). Push-out delamination tends to be more severe than peel-up delamination due to the insufficient support at the CFRP exit (Xu et al., 2016).

Ramulu et al. (2001) showed that the optimal stacking order is metal on the bottom and CFRP on top to reduce delamination during drilling. The bottom titanium alloy plate's supporting function prevents the laminate from deflecting at the CFRP exit, resulting in minimal exit delamination damage (Xu et al., 2016). An et al. (2020) backed up this claim and said that it is also unaffected by cutting parameters. Some other studies (Tashiro et al., 2011; Xu, Zhou, et al., 2019; An et al., 2020) also noted

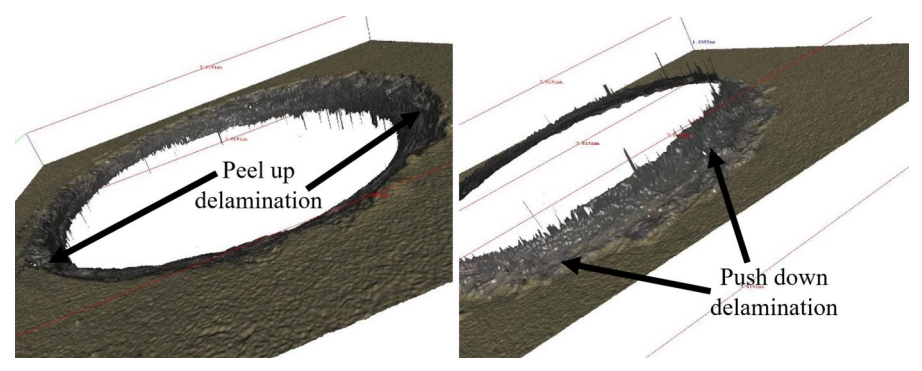


Figure 12. (a) Peel up at the entrance panel and (b) push down delamination at the exit panel (Mathavan, 2023).

that, when drilling a CFRP/Ti panel, the exit hole has considerably more damage since it is dependent on the drill's thrust force, cutting speed, tool shape and wear condition. However, due to the loss of support at the exit while drilling from the Ti6Al4V layer, CFRP hole exits show substantial delamination faults.

Researchers have noted the opposite outcomes as well. Delamination is more significant at the entrance than at the exit, according to the delamination factor (for feed ranging between 0.03 mm/rev and 0.09 mm/rev). Such unexpected results are attributed to the forces exerted by the Ti chips causing the CFRP layers to be pulled out at the hole entrance (Boutrih et al., 2022). During the titanium alloy drilling in the CFRP to Ti sequence, the high-temperature Ti chips significantly contribute to the delamination at the entrance of CFRP (Li et al., 2022; Jebaratnam, 2025). When cutting through the titanium phase, significant delamination damage begins at the interface zone and the CFRP phase once the tool reaches the intermediate cutting depth in the titanium. This ultimately results in delamination at the interface. On one side, the forced extrusion of CFRP material by the plastically deformed titanium alloy intensifies subsurface damage on the entry side of the CFRP. On the other side, the lack of support causes external forces on the free surface to worsen subsurface damage on the exit side of the CFRP (Jebaratnam, 2025). Additionally, material that is located close to the CFRP's entrance has low resistance to bending deformation, and it may consequently result in more severe entrance peel-up delamination. But most studies up to this point have ignored entrance delamination triggered by the titanium alloy drilling stage and concentrated on push-out delamination defects (Ramulu et al., 2001; Qi et al., 2014). This is because the chips with high temperatures weaken the matrix's bonding and also damage CFRP mechanically, which makes the material's delamination faults worse (Movahhedy et al., 2000; Fan and Wang, 2021).

According to Xu and Mansori, when drilling CFRP/Ti at a CFRP to Ti sequence, delamination appears to be increasing with the increase in feed (Isbilir and Ghassemieh, 2013; Xu and El Mansori, 2016) and declining with speed (Isbilir and Ghassemieh, 2013), whereas drilling from Ti to CFRP, it rises with both tool feed and cutting speed (Xu and El Mansori, 2016). Additionally, they mentioned that, in the CFRP \rightarrow Ti sequence, the delamination factor ranges between 1.01 and 1.08, while in the Ti → CFRP sequence, it was 1.05-1.15 for feed rates below 1 mm/rev. An et al. mentioned that, in the CFRP -> Ti sequence, the delamination coefficient ranges between 1.5 and 2.5, while in the Ti \rightarrow CFRP sequence, it was less than 1.0 (An et al., 2020). They also mentioned that 1D and 2D delamination coefficients were affected by the cutting parameters in a way that increased with the rise in the feed and declined with the rise in the cutting speed (An et al., 2020). When drilling a CFRP/Ti stack, with the rise in feed rate, the delamination factor rises regardless of the cooling method (dry or MQL cooling) or coating used (PVD TiAlN coated or CVD diamond coated) (Xu et al., 2020). This is because, when the feed rate is low, the hole wall has reduced thermal-mechanical deterioration due to low temperature and a small section modulus in bending. According to a different study, when the feed rate is amplified from 0.025 mm/rev to 0.100 mm/ rev under both dry and MQL conditions, the magnitudes of the delamination factors increase by about 116.96% and 37.98%, respectively (Xu, Ji, et al., 2019). When utilizing MQL, the delamination factors seem to be significantly more than those attained when using dry machining. This is closely related to the rise in CFRP thrust forces under the MQL situation, whereby a greater thrust force frequently causes more extensive delamination damage (Hocheng and Tsao, 2005, 2006).

Additionally, drilling-induced damage may be influenced by CFRP fiber orientation (Boutrih et al., 2022). The configuration of the angle between the cutting direction and fibers is 90 or less than 0 is the most crucial one for cutting a long fiber composite, according to prior studies (Wang et al., 1995; Zenia et al., 2015). In this structure, material removal is started along the fiber axis, then after the fiber shears, secondary breakup occurs along the free edge. As the fibers separate from the matrix, significant flaws may then spread throughout the material. Thus, there may be a relation between the fiber/matrix's debonding during the CFRP panel and delamination formation at the inter-material contact. Delamination occurs as a result of the fracture spreading from the composite surface to the contact. This assumption is based on a similarity to crack propagation observed in coated tools, where the stress exerted by the workpiece on the tool surface speeds up crack growth until it reaches the interface between the substrate and the coating, causing delamination (Nouari and Ginting, 2006; Bounif et al., 2021). When UD-CFRP is used at speeds above 15 m/s, entrance delamination decreases with increased feed, whereas exit delamination increases with increased feed because the feed rate has a much greater impact on the degree of defect in UD-CFRP than MD-CFRP (Boutrih et al., 2022). Although it is anticipated that the reduction in feed rate will reduce the likelihood of delamination and burr formation, material removal rate (MRR) will be significantly impacted (Sorrentino et al., 2018; Boutrih et al., 2022). Park et al. compared the delamination between CFRP/Ti and CFRP drilling. They discovered that drilling CFRP only produced an average delamination of less than 2 mm, whereas drilling CFRP-Ti stacks produced a broad range of delamination ranging from 1.5 mm to 13 mm (Park et al., 2014). Ti adhesion at the drill edges may be the cause of the large entrance delamination observed during the drilling of stacks. Dahnel et al. (2020)

also claimed that the amount of CFRP delamination caused by drilling only the CFRP was 22% and 62% lower than that caused by drilling the stacks with a single shot and two shots of drilling, respectively.

When considering the type of tools used, the interface delamination caused by double-point angle drill and candlestick drill is significantly less than that caused by the twist drill. This is due to the fact that most heat generated by twist drills and double-point angle drills is transmitted to the drilled surface after the primary cutting edge is sliced, causing interface damage. The tip construction of the candlestick drill, despite the workpiece receiving heat from the primary cutting edge, may cut through the material with the maximum cutting temperature (Qiu et al., 2021).

There are three types of delamination: type I, type II and type III. Type I delamination occurs when fibers bend toward the machining line, type II when the fibers protrude from the machined edge and type III takes place when fibers run parallel to the machined edge (Colligan and Ramulu, 1992). As a result of the rake face's extrusion action, the fiber will bend and break when the angle of fiber orientation at the entrance is around 135°. This type I of delamination happens when the peel-up force is higher than the strength of the bond between the fiber and the matrix. These are areas where the surface layer fibers are fractured inward from the cut edge, resulting in visible gaps in fiber alignment along the edge (Colligan and Ramulu, 1992). Type II delamination contains intact fibers that extend beyond the cut edge and may separate from the adjacent layer at a certain distance from the part's edge. Loose fibers partially connected to the machined edges, creating a fuzzy appearance on the upper or lower edge of the machined surface, create type III delamination (Colligan and Ramulu, 1992). Increased feed rates result in increased instantaneous cutting thickness per unit cutting edge, increased fiber-to-rake face contact area and enhanced peeling force and extrusion impact, aggravating type I and type III delamination (Li et al., 2022). The schematic diagrams of all types of delamination are shown in Figure 13.

Therefore, the optimal stacking order for drilling CFRP/Ti stacks is CFRP on top and titanium on the bottom to minimize exit delamination, as the titanium layer supports the laminate during drilling. However, significant delamination has been observed at both the entrance and exit, depending on cutting conditions and sequence. Drilling from CFRP to Ti results in reduced delamination at the CFRP exit but increased damage at the entrance due to thermal and mechanical effects of high-temperature Ti chips. Conversely, drilling from Ti to CFRP increases delamination at the exit, particularly with higher feed rates and cutting speeds. Entrance delamination, often overlooked in studies, is exacerbated by Ti chips weakening the CFRP matrix.

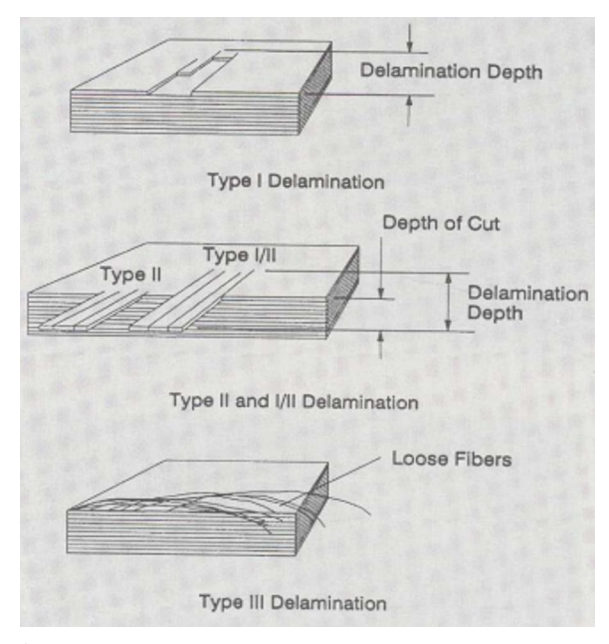


Figure 13. Types of delamination (Colligan and Ramulu, 1992).

Burr formation on Ti panel

The compression in the hole's center typically causes the burr development at the exit (Hassan et al., 2017), and the allowable burr height at the interface of drilling stack-up materials must not exceed 150 µm (Dornfeld and Min, 2010; Franke, 2018). Titanium burrs are created by the drilling force that punctures and fractures the material, causing the production of irregular metal extensions like sharp edges and "ring"-shaped materials at the hole entrance and exit as shown in Figure 14. The fatigue performance of the cut workpiece and the functionality of the finished assembly are both negatively impacted by the burr formations (Aurich et al., 2009). The key factor contributing to the production of metallic burrs, according to Dornfeld et al., is the heat effect (Dornfeld et al., 1999). Greater feed rates encourage greater cutting temperatures, which cause the titanium alloy to soften thermally. Because the softened titanium alloy is more ductile, burr height tends to be more significant (Xu et al., 2020; Qiu et al., 2021). Burr development may lead to electrical component short circuits, reduced component fatigue life and serve as a fracture initiation point (Ko et al., 2003). Before assembling the panel, a deburring step is necessary as a preventative measure if a burr forms at the hole's exit. This adds roughly 30% to the total assembly process time (Min et al., 2001; Avila et al., 2005).

Ramulu et al. (2001) reported the least burr height development, and Xu and El Mansori (2016) recorded the least burr width development at the hole edge with increasing feed rate. Few other researchers have also noted

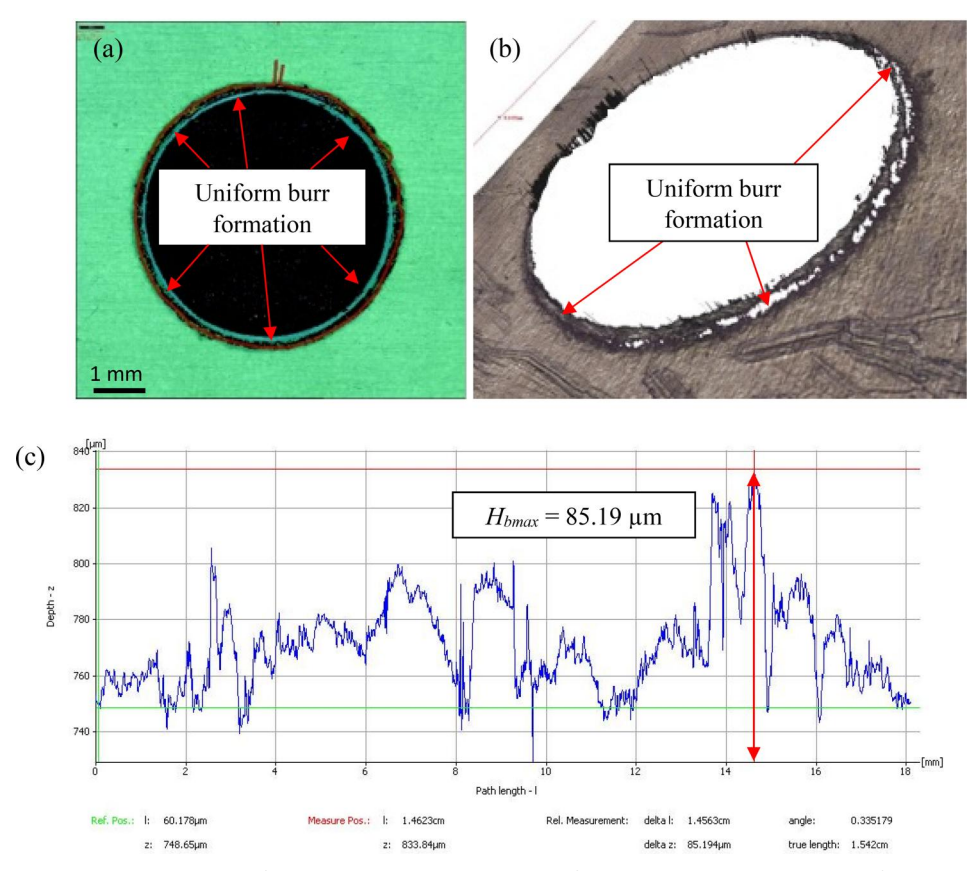


Figure 14. The process for measuring maximum burr formation: (a) observing burr formation in 2D, (b) identifying maximum burr formation using Alicona IFM and (c) measuring the maximum burr formation (Mathavan, 2023).

that, as speed (Gao et al., 2021) and feed (Kim et al., 2013) increase, exit burr heights increase. According to Isbilir et al., the roughness of drilled hole surfaces and burr height increase as feed rate rises and decrease as cutting speed rises (Isbilir and Ghassemieh, 2013). For dry and MQL conditions, the burr height rises by 154.53% and 45.94%, respectively, when the feed rate is raised from 0.025 mm/rev to 0.100 mm/rev. Further, they demonstrated that the MQL can produce burr heights that are lower than those produced by dry drilling (Isbilir and Ghassemieh, 2013). This is explained by the MQL conditions' ability to reduce titanium hole drilling temperatures, which reduces the development of burr flaws (Xu, Ji, et al., 2019). Further, Xu et al. observed that uncoated carbide drills resulted in higher drilling temperatures and larger burrs when machining CFRP/Ti stacks, primarily due to inadequate frictional contact and low thermal conductivity. On the other hand, diamond-coated drills produced lower burr heights because of their superior wear resistance, enhanced heat dissipation



and reduced mechanical loads, irrespective of the process parameters (Xu et al., 2020).

Drill bits with unique geometries may be able to produce holes in CFRP/ Ti stacks of excellent quality (Aurich et al., 2009). For example, twist drill and candlestick drill create "caps." The twist drill's "cap" has an irregular shape as a result of uneven force. However, the "cap" of the candlestick drill with a brim is due to its tip structure (Qiu et al., 2021). When comparing, the double-point angle drill produced the highest burr height, while the candlestick drill produced the lowest burr height in a way that the burr height produced by double-point angle drill is 6-8 times larger compared to candlestick drill and that produced by the twist drill is double the height produced by candlestick drill (Qi et al., 2014, 2021). The candlestick drill can effectively prevent burr formation because of its outside corner tip structure. Since the drilling thrust force of a twist drill is greater than that of a candlestick drill, it is easier for a twist drill to create burrs (Qiu et al., 2021). But a wide point angle of 140° in the standard twist drill causes the drilling lips to engage with the material earlier while drilling, which starts the cutting operation sooner and reduces burr development (Rodriguez et al., 2023). Xu and Mansori mentioned that uncoated drill bits with small chisel edges (0.11 mm) and small point angles (135°) and helix angles (20°) produced greater burr width at high feed rates compared to coated drill bits with big chisel edges (0.22 mm) and large point angles (140°) and helix angles (27.2°) (Xu and El Mansori, 2016). According to Dahnel et al. (2020), an increase in the number of drilled holes caused flank wear and Ti burr height to gradually increase. Kim et al. (2013) mentioned that exit damages, such as the development of titanium burr caps, did not occur when the PCD tools were used for drilling.

When the drilling sequence is taken into account, the Ti→CFRP drilling results in a lower defect extent than the CFRP→Ti drilling. The bottom CFRP phase had a supporting role in making the exit Ti layer more rigid, which made it easier to reduce the exit Ti burr defect (Xu and El Mansori, 2016).

Burr formation in CFRP/Ti stack drilling is primarily influenced by factors like drilling force, heat generation, tool geometry and drilling sequence. Higher feed rates and cutting temperatures contribute to increased burr height due to the thermal softening of titanium. MQL drilling reduces burr formation compared to dry drilling by lowering temperatures. Tool coatings, such as diamond coatings, help minimize burrs by improving wear resistance and heat dissipation. Drill geometry also plays a crucial role, with candlestick drills producing the least burrs and double-point angle drills generating the highest. A wider point angle in twist drills helps reduce burr development. Additionally, the Ti→CFRP drilling sequence results in lower burr defects than CFRP→Ti drilling due to the supporting role of the CFRP phase in stabilizing the titanium exit layer.

Hole surface roughness

The assessment of drilling quality in a composite panel is dependent on hole surface roughness, as it is a significant parameter (Abrão et al., 2007; Aamir et al., 2019). When the surface roughness is above the predetermined concerns encountered while drilling composites. The allowed hole surface roughness is less than 3.2 µm for CFRP and less than 1.6 µm for metal parts (Zhang et al., 2015). The drill bit shape and drilling parameters have a substantial impact on the hole surface roughness (Giasin et al., 2015). The wall of the drilled hole for a composite panel must be free of any surface imperfections in order to ensure an excellent degree of hole surface roughness, whereas the hole for a titanium panel should have a shining surface. Several hole surface roughness components are shown in Figure 15. According to earlier studies (Krishnaraj et al., 2012; Mahdi et al., 2020; Sui et al., 2020; Yuan Jia et al., 2020), reducing hole surface roughness is more challenging in the composite part due to its heterogeneous properties compared to the metal portion. Additionally, because composites

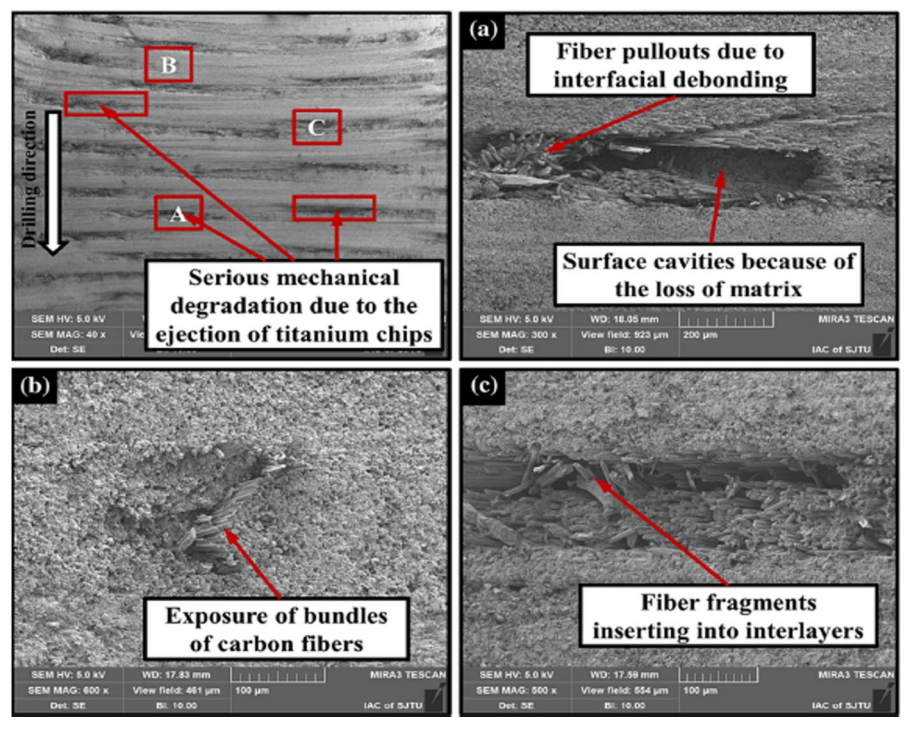


Figure 15. Morphologies of the composite hole walls formed by the TiAIN-coated drill bits under the dry cutting condition ($V_c = 30 \text{ m/min}$ and f = 0.025 mm/rev) (Xu et al., 2020).

have a poorer measurement reliability than metals, it is important to interpret the roughness of CFRP with caution (Kuo et al., 2018).

During the drilling process of the CFRP/Ti stack, the irregularly shaped Ti6Al4V chips are compressed by the CFRP hole wall, resulting in significant damage to the CFRP panel during titanium chip removal (Park et al., 2011). Brinksmeier et al. observed that the surface wall of the composite material exhibited indications of wear due to thermal degradation of resin (Brinksmeier and Janssen, 2002). The resin is thermally deteriorated when the hot titanium chips vacate through the flutes, leaving behind helical grooves on the hole surface (An et al., 2021). Surface roughness is reduced when the matrix smearing is decreased (Park et al., 2018). Furthermore, the overall quality of the finished surface is severely harmed by the titanium microchips that are embedded in the wall. Since drilling from the Ti6Al4V to the CFRP side produced regular spiral Ti6Al4V chips, the surface quality of the CFRP hole-wall is greatly enhanced, and there are no noticeable scratches on the surface. On the other hand, surface pit flaws resulted because the machining temperature exceeds the resin's vitrification point, accelerating the debonding of fibers from the resin and the subsequent pulling out of fibers (An et al., 2021). Xu et al. reported that the CFRP surface roughness values in the Ti→CFRP cutting sequence (CFRP phase Ra = $0.4 - 2.0 \,\mu m$ and Ti phase $0.279 \,\mu m - 1.331 \,\mu m$) were drastically reduced from those found in the CFRP→Ti cutting sequence (Ti phase Ra = $0.373 \,\mu\text{m} - 1.301 \,\mu\text{m}$ and in CFRP phase Ra = $1.146 \,\mu\text{m}$, $4.919 \,\mu\text{m}$), although there was no discernible difference in the Ti surface (Xu and El Mansori, 2016).

Yuan et al. performed tests to investigate a unique tool construction with cutting depth control. The findings suggested that the tool design had an impact on improving Ti/CFRP hole accuracy and drilling quality (Yuan Jia et al., 2020a, 2020b). According to Xu et al., a large chisel edge length combined with a wide point and helix angle drill decreases CFRP surface roughness compared to a small chisel length combined with a small point and helix angle drill, while having no discernible impact on Ti surface polish (Xu and El Mansori, 2016). Qiu et al. mentioned that, when machining a CFRP/Ti stack, the candlestick drill causes the least amount of surface damage when compared to the twist drill and double-point angle drill (Qiu et al., 2018, 2021). Kim et al. (2015) demonstrated that the hole surface was greatly impacted by the marginal face.

Kuo et al. observed while using CVD diamond-coated drills that fewer holes with unsatisfactory surface quality were made on Ti/CFRP/Al stacks when the cutting parameters were increased (Kuo et al., 2014). According to Xu et al., cutting speed has a negligible effect on surface roughness, while the feed rate notably increases hole surface roughness (Xu and El

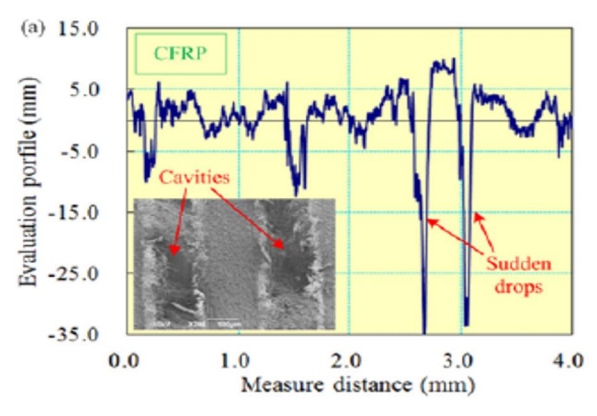


Figure 16. Hole surface roughness illustration in CFRP layer (Wang et al., 2015).

Mansori, 2016). They added that a modest cutting speed and low feed rate can lessen the hole surface roughness, while Park et al. mentioned that low cutting speed in conjunction with intermediate feed meant only slight adhesive effects on the hole surface (Park et al., 2011). In view of the effect of tool material, the burr height and surface roughness of carbide drills were almost 7.5 times lower than those of HSS-Co and HSS drills (Ramulu et al., 2001; Kim and Ramulu, 2004). Additionally, it was discovered that carbide drills performed better than HSS-Co and HSS drills in terms of tool life, surface abrasion and heat-induced damages (Ramulu et al., 2001). Figure 16 shows the change in the surface roughness profile measured along the length of a CFRP panel. The sudden drops are caused by the cavities, which are formed by fiber pullouts due to interfacial debonding, epoxy loss on CFRP surfaces, the softened matrix being smeared at the tool-work boundary due to excessive drilling temperatures and the ejection of titanium chips or fiber fragments inserting into interlayers.

As a whole, hole surface roughness is a crucial parameter in assessing drilling quality for composite panels, influenced by drill bit shape, cutting parameters and machining sequence. During CFRP/Ti stack drilling, hot titanium chips can degrade the resin, leading to surface defects such as pits, grooves and embedded microchips. The Ti→CFRP drilling sequence results in smoother CFRP surfaces compared to the CFRP→Ti sequence. Tool geometry plays a significant role, with larger chisel edges, wider point and helix angles and candlestick drills reducing surface damage. Cutting speed has minimal impact on surface roughness, whereas higher feed rates increase it. Carbide drills outperform HSS-Co and HSS drills in reducing burr height and surface roughness while improving tool life and durability. Optimized cutting conditions and advanced tool coatings, such as CVD diamond, help maintain superior hole quality by minimizing fiber pullouts, resin degradation and chip-induced defects.



Hole diameter error

Poor workpiece surface quality is one of the specific problems with the machining of CFRP/Ti6Al4V stacks (Ghassemieh, 2012; Isbilir and Ghassemieh, 2013; Kim et al., 2015; Unai et al., 2019). Many aspects such as tool geometry and material (Pawar et al., 2015; Zitoune et al., 2016), cutting parameters (Kim and Ramulu, 2004; Zitoune and Collombet, 2007; Feito et al., 2014) and cooling condition (Gisip et al., 2009; Giasin et al., 2015) affect the hole quality while drilling a CFRP/Ti stack. Therefore, proper selection of tool material/geometry, cutting parameters, use of coolants, use of coatings and drilling sequence are required to obtain a highquality hole. Both increase and decrease in hole diameter is recorded with the increase of feed rate in CFRP/Ti stack drilling. When the feed rate is raised during dry drilling at spindle speeds between 1,000 rev/min and 2,000 rev/min, the hole diameter decreases (Park et al., 2018; Kumar and Gururaja, 2020). On the other hand, larger holes are obtained under dry drilling due to the expansion of the workpiece at a quicker rate as a result of the elevated drilling temperature (Jia et al., 2020). For aerospace applications, the specified hole tolerances require a diameter variation of no more than 30 µm in material stacks composed of composites and aluminum or titanium alloys (Brinksmeier and Janssen, 2002; Zitoune et al., 2010).

According to Zitoune et al., the hole diameter difference between the Ti6Al4V panel and the CFRP panel during the CFRP to Ti drilling sequence rises as the feed rate is elevated. This is because Ti6Al4V chips become thicker with increased feed rate, which improves Ti chips' capability to resist bending deformation and encourages defects to the CFRP panel in the form of matrix degradation and fiber pull-outs at the layer's drilled hole surface (Giasin and Ayvar-Soberanis, 2017). Smaller feed rates are therefore preferable in industrial production to minimize damage to the CFRP panel (An et al., 2020). According to An et al., when drilling in a CFRP -> Ti6Al4V drilling sequence, regardless of the cutting speed and with a feed rate of 0.12 mm/rev, the diameter of the CFRP exit (6.6 mm) is larger than that of the Ti panel (6.38 mm), nominal diameter (6.35 mm) and CFRP entry. Contrarily, the entrance and exit hole diameters of the CFRP panel are a consistent size when applying the Ti→CFRP sequence under all the applied conditions and are less than that of the Ti6Al4V panel (Xu and El Mansori, 2016) For instance, the hole diameter of Ti6Al4V is always 0.02-0.03 mm greater than that of the CFRP panel and 0.02 mm greater than the nominal drill diameter. An et al. discovered that the CFRP layer's hole diameter is around 0.01 mm smaller than the drill diameter in the Ti → CFRP sequence (An et al., 2020). Further, in the CFRP → Ti sequence, the hole diameter is 6.4 mm to 6.6 mm, while in the Ti → CFRP sequence, the hole diameter is less than 6.4 mm, given that

the drill diameter is 6.35 mm. According to Xu and Mansori (2016), in the CFRP → Ti sequence, the hole diameter varies between 6.37 mm and 6.4 mm in the Ti panel and 6.36 mm and 6.42 mm in the CFRP panel, while in the Ti → CFRP sequence, the hole diameter varies between 6.28 mm and 6.43 mm in the Ti panel and 6.1 mm and 6.42 mm in the CFRP panel. The smaller hole diameter variation in the Ti \rightarrow CFRP sequence is attributed to the evacuation of metal chips early before the drill bit enters into the CFRP panel. But larger hole diameter variation in the CFRP -> Ti sequence is due to the blockage of chips while exiting from the hole. The spring-back effect while processing CFRP panels results in the undersized CFRP panel holes compared to metal panels (Zitoune et al., 2010; Boutrih et al., 2022). The hole diameters generated in this cutting order are partially large and partially undersized, substantially depending on the applied cutting parameters, according to Xu and Mansori (2016), who also used this cutting sequence. They mentioned that this is due to the discrepancy between the thermal expansion coefficient and the elastic modulus of Ti6Al4V and CFRP. Normally, when drilling Ti6Al4V, a lot of cutting heat is produced, and the linear thermal expansion coefficients of CFRP and titanium alloy are, respectively, -0.1×10^{-6} /°C and 7.89×10^{-6} / °C, and their respective elastic moduli are 295 GPa and 118.5 GPa (Zhou et al., 2016; Kim et al., 2017). Xu et al. discovered that using Ti→CFRP encourages lesser drilling forces, fewer stack-up diameter mistakes, lowered Ti burr extents, and enhanced surface roughness because Ti chip evacuation issues are avoided (Xu, Zhou, et al., 2019) and while using low cutting speed and low feed rate (Xu and El Mansori, 2016).

Additionally, Xu et al. discovered that regardless of the chisel length, helix angle, or point angle of the drill bits, the resulting hole size in either the Ti or CFRP panel is greater than the nominal diameter of 6.35 mm (Xu and El Mansori, 2016). This is because, during chip evacuation, Ti chips rub against the surface of the CFRP and during rotation out of the hole, the attached Ti chips cause scratches and a delamination impact on the hole (Boutrih et al., 2022).

According to findings by Kim et al., optimal process conditions for achieving the desired hole quality and minimizing process costs when drilling Gr/Bi-Ti involve utilizing high feed rates and low speeds with carbide drills, while employing low feed rates and low speeds with HSS-Co drills (Kim and Ramulu, 2004; Kim et al., 2005). Kim et al. (2013) also discussed drilling a hybrid composite laminate made of titanium and graphite using a PCD tool and discovered that the feed is the most crucial parameter in hole size mistakes. Prabukarthi et al. found that a spindle speed of 1000 rev/min and a feed rate of 0.13 mm/rev resulted in an acceptable hole diameter deviation (Prabukarthi et al., 2013). Contradictorily, An et al.

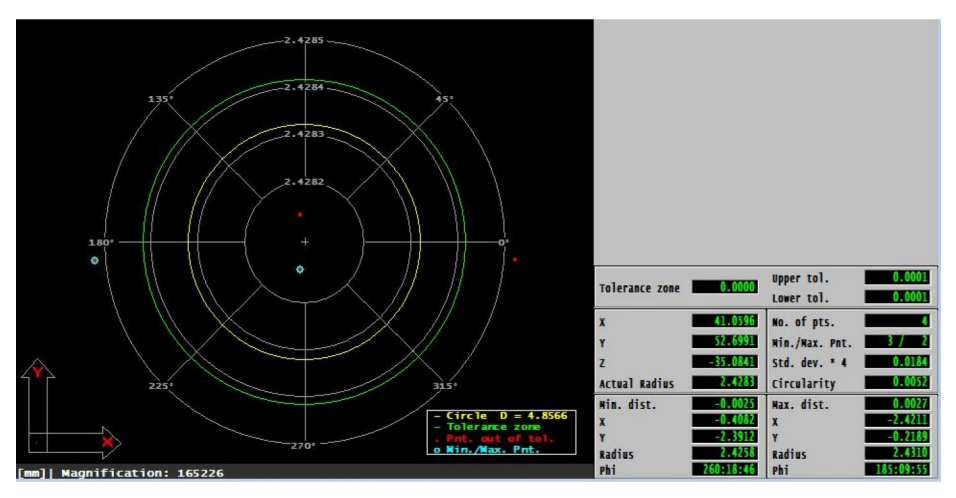


Figure 17. Details appear on the screen for hole diameter measurement for a hole (Mathavan, 2023).

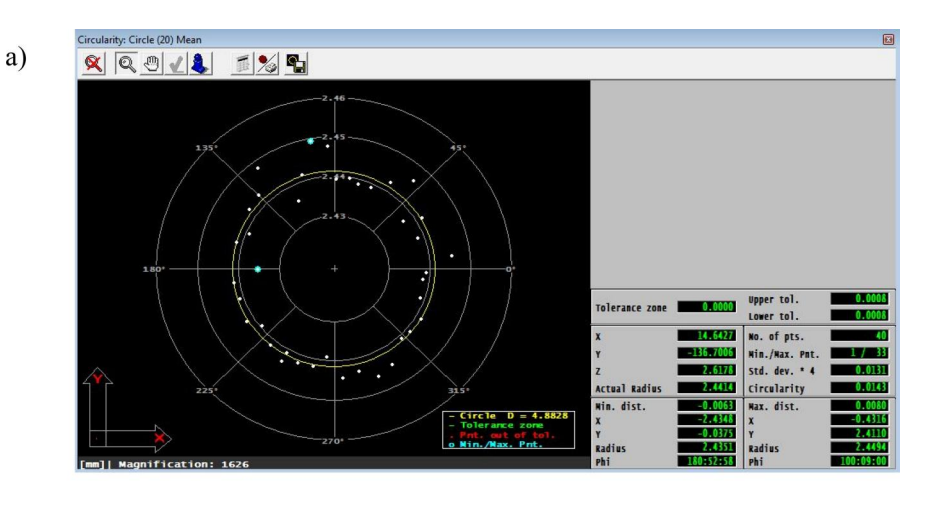
mentioned that, irrespective of the drilling parameters used, the diameter and roundness of the Ti6Al4V layer remain nearly unaffected (An et al., 2020). According to Park et al. (2011), tool wear lowers machining quality and increases hole size. Figure 17 shows the sample measurement of hole diameter using a coordinate measuring machine.

Machining CFRP/Ti6Al4V stacks presents challenges in achieving high hole quality, influenced by tool geometry, cutting parameters, cooling conditions and drilling sequence. Hole diameter variations occur with changing feed rates, where higher feed rates generally reduce hole size in dry drilling but can also enlarge holes due to thermal expansion. The CFRP→Ti sequence causes larger CFRP exit diameters and more defects, while the Ti→CFRP sequence results in better hole consistency, reduced burr formation and improved surface roughness. The thermal expansion coefficient differences between CFRP and Ti6Al4V contribute to diameter deviations, with Ti chips causing surface damage during evacuation. Studies show that optimal hole quality is achieved using carbide drills at high feed rates and low speeds, whereas HSS-Co drills perform better at low feed rates and speeds. Feed rate significantly affects hole size errors, with some studies recommending a spindle speed of 1000 rev/min and a 0.13 mm/rev feed for minimal deviations. However, tool wear remains a key factor in increasing hole size and reducing machining quality.

Poor hole integrity

The term "hole integrity" refers to the achievement of the stated dimensions for a hole in compliance with the drawing specifications. The circularity and cylindricity of a hole are two indications used to evaluate its

quality. Both indications should be kept at a least value to avoid disrupting the assembly process. However, because composite layers are anisotropic, the cylindricity errors in CFRP holes are much greater than those in titanium holes. As a result, the surfaces of the CFRP holes become substantially rougher. According to Xu et al., the cylindricity errors during stack drilling are approximately the same under both dry and MQL conditions. They further mentioned that, under dry and MQL conditions, the average cylindricity errors of the titanium holes are 3.81 and 7.21 times lower than those of the CFRP holes, respectively (Xu, Li, et al., 2019). An et al. (2020) also mentioned that, at 0.06 mm/rev, the circularity of the CFRP exit is 46 µm, which is significantly bigger than the roundness of the Ti6Al4V (6 µm) and the CFRP entry (12 µm). Studies done to determine the angle of the drill structure have revealed that drilling Ti/CFRP stacks with relatively smaller point angles (135°), shorter chisel edges and 30° helix angles could have less roundness deviation (Ashrafi et al., 2013; Senthilkumar et al., 2018). Moreover, Xu and Mansori mentioned that, at the same feed rates, an uncoated drill bit with a small chisel length and a small point and helix angle produced holes that were rounder than a coated drill bit with a big chisel length and a high point and helix angle (Xu and El Mansori, 2016). They further suggested using a parametric combination of a low cutting speed and low feed rate to reduce hole roundness error (Xu and El Mansori, 2016). Additionally, they stated that the hole roundness in the CFRP panel is not much impacted by the drilling sequence, but in the Ti panel, in the CFRP \rightarrow Ti sequence the hole roundness error is 0.005 - 0.013 mm, while in the Ti \rightarrow CFRP sequence it was 0.01 mm to 0.03 mm. Contradictorily, An et al. mentioned that, in the CFRP \rightarrow Ti sequence, the hole roundness error is 0.07 mm, while in the Ti \rightarrow CFRP sequence, it was less than 0.01 mm (An et al., 2020). In terms of hole circularity and hole cylindricity, holes drilled with diamond-coated drill bits performed two times better than holes drilled with diamond-like carbon (DLC)-coated drill bits (Kuo et al., 2014). The primary cause of hole cylindricity error is the creation of elevated cutting temperatures at increased spindle speeds as a result of tool rubbing against the workpiece. This might soften the matrix material and cause the hole's cylindricity to thermally deform (Giasin and Ayvar-Soberanis, 2016). Figure 18a shows a sample measurement of hole circularity, and Figure 18b shows cylindricity, respectively. The circularity measurement (0.0143 mm) shown in Figure 18a is the addition of minimum (0.0063 mm) and maximum (0.0081 mm) variation in distance of the circles drawn from the actual circle, which in other words can be stated as the difference between the minimum (radius $= 2.4351 \,\mathrm{mm}$) and maximum (radius = $2.4494 \,\mathrm{mm}$) inscribed circles. Additionally, the X, Y, and Z coordinates of the actual circle can also be obtained when measuring



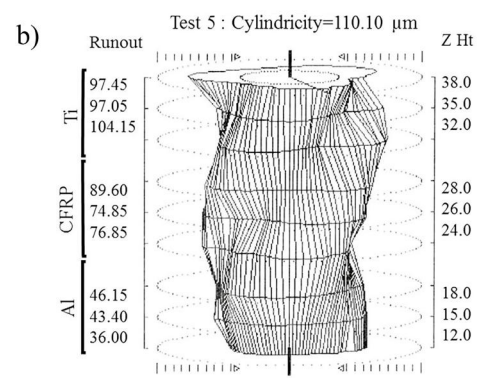


Figure 18. A sample of (a) circularity error (Mathavan, 2023) and (b) cylindricity error (Kuo et al., 2018).

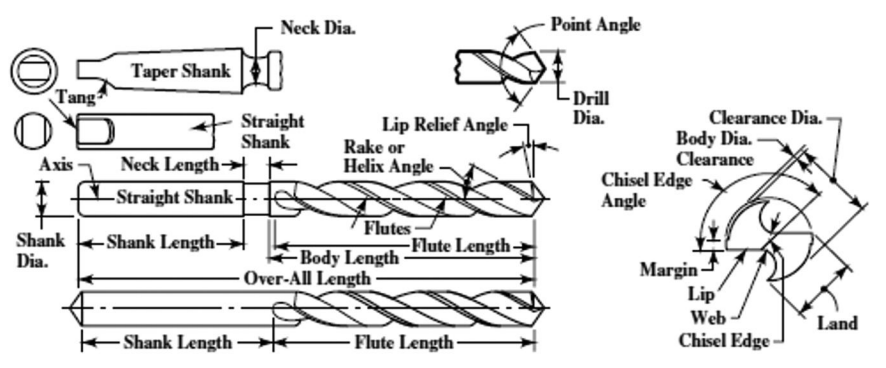


Figure 19. Geometry of a conventional twist drill (Erik Oberg et al., 2004; Senthilkumar et al., 2013; Wika et al., 2011).

circularity. The cylindricity shown in Figure 18b is measured at top, middle and bottom points for each panel.

Hole integrity refers to maintaining the specified dimensions, with circularity and cylindricity as key indicators of quality. Due to the anisotropic

nature of composite layers, CFRP holes exhibit significantly greater cylindricity errors and rougher surfaces than titanium holes. Circularity errors are also higher at the CFRP exit compared to the Ti6Al4V panel and CFRP entry. Studies suggest that using a smaller point angle (135°), shorter chisel edge and 30° helix angle reduces roundness deviation. Uncoated drills with small chisel lengths and low point/helix angles produce rounder holes than coated drills with larger chisel lengths and higher angles. Additionally, diamond-coated drills yield better circularity and cylindricity than DLC-coated drills. Hole cylindricity errors primarily result from increased cutting temperatures at high spindle speeds, which soften the matrix and cause thermal deformation.

Table 1 shows the summary of the work done so far by several researchers in terms of workpiece and the drilling sequence, the drilling environment used such as dry, MQL cooling, cryogenic cooling, etc., the vast range of parameters occupied under cutting speed and drill feed, the impact of drill bit geometries such as point angle, helix angle, chisel edge, etc., and the application of different coatings such as TiAlN, AlTiN, diamond, etc. The table is designed to show how various factors affect the hole quality and performance indicators.

Strategies for minimizing manufacturing defects

Optimizing drilling parameters

The machining process and resultant hole quality are significantly impacted by the chosen drilling parameters. Optimal selection of these parameters for distinct material layers plays a vital role in enhancing tool life, improving machining efficiency and ultimately reducing costs. Numerous researchers (Ramulu et al., 2001; Kim and Ramulu, 2004, 2007; Ghassemieh, 2012; Isbilir and Ghassemieh, 2013; Kim et al., 2013) have explored the impact of several parameters on drilling FRP/Ti stacks.

It's commonly noted that cutting speed has minimal impact on the generation of thrust force during the drilling of hybrid FRP/Ti composites. Conversely, the feed rate demonstrates a significant influence. This is attributed to the increased material volume that the drill must remove per revolution and the higher cutting resistance encountered during machining with an elevated feed rate, which consequently results in a rise in thrust force. Simultaneously, the increased feed rate results in a shorter engagement time between the tool and workpiece. This decreased tool-work contact time contributes to reduced heat liberation during drilling in the Ti panel, consequently minimizing the formation of exit Ti burrs (Ramulu et al., 2001; Kim and Ramulu, 2004, 2007; Kim et al., 2013). Research indicates that lower feed rate and higher cutting speed are advantageous in reducing thrust force during CFRP drilling, effectively minimizing burrs

Table 1. Summary of researches conducted on CFRP/Ti stack up drilling.

lable I. Summary	lable 1. Summary of researches conducted on CFRP/11 stack up drilling.	stack up drilling.		
Work piece	Tool	Parameters	Analysis	Author
CFRP/T16Al4V	TiAIN-coated carbide twist drills with diameter of 6.35 mm. The drill has two flutes, 0.22 mm-length chisel edge, 27.2° helix angle and 140° point angle.	Cutting speed $(\nu_c)=30$ m/min, feed rate $(f)=0.03,0.06,0.09,0.12,0.15$ mm/rev	Drilling forces, delamination, burr formation, cutting sequence, surface morphology	(Xu et al., 2019)
Ti6Al4/CFRP/Al7050	Uncoated, C7 coated and CVD diamond coated WC drills with diameter = 6.35 mm helix angle 30° point angle = 130°	Flood cutting = 15 L/min spray mist = 3 bar environment. Feed (mm/rev) = 0.05, 0.1, 0.15, Speed (m/min) = (20/40, 40/80, 60,120)	Hole size, hole roundness, hole cylindricity, burn height, hole edge quality, surface roughness (R _a), swaff morphology.	(Shyha et al., 2011)
CFRP/TI6Al4V	Solid carbide drills with a diameter = 4.83 mm, point angle = 120°, helix angle = 30°, CVD and PVD coatings of AlCrN, AlTiN, TiAIN/TISIN	Speed = 15 m/min, feed = 0.075 mm/rev, frequency = 1, 5 oscillation/rev, amplitude = 0.115mm LFVAD Cooling = MQL	Tool wear & tool life, adhesions at the cutting edges, Process temperature, cutting force, chip formation, hole quality	(Pecat and Brinksmeier, 2014)
CFRP/T16Al4V	PVD TITAIN-coated and CVD diamond coated WC drills with diameter = 6mm, helix angle = 30°, point angle = 140°	Cutting speeds = 15, 30, 45 and 60 m/min, feed rates = 0.025, 0.050, 0.075 and 0.100 mm/rev. MQL = 5 to 15 mL/h and dry conditions	Thrust force, delamination damage, tool wear	(Xu et al., 2020)
CFRP/TI6Al4V	TiAIN-coated, and diamond-coated drill. diameter = 6mm helix angle = 30° point angle = 140°	MQL = 15 mL/h and a compressed air pressure of 0.6 MPa, cutting speed (Vc) = 15, 30, 45 and 60 m/min feed rate (f) = 0.025, 0.050, 0.075 and 0.100 mm/rev	Effect of coating, effect of cooling on drilling torque, specific cutting energy consumption, surface morphology, bur height	(Xu et al., 2020)
CFRP/TI6Al4V	Uncoated cemented carbide drill diameter = 6.35 mm, helix angle = 30°, point angle = 140° and cutting-edge length =34 mm	Cutting speed, vc(m/min) = 10, 20, 30, 40; Feed rate, f(mm/rev) = 0.03, 0.06, 0.09, 0.12 Sequence – CFRP to Ti, Ti to CFRP, Dry machining	Hole diameter and roundness error, hole surface	(An et al., 2020)
				(penuituo)

Author	(Kim et al., 2015)	(Xu et al., 2020)	(Unai et al., 2019)	(Kumar et al., 2013)	(Senthilkumar et al., 2018)	(continued)
Analysis	Entrance delamination, hole diameter, roundness, hole surface roughness, CFRP hole profile, CFRP-TI inter-plate damage and	es, ights, morphologies,	Je,	vear, ın,	Hole diameter, roundness, delamination, burr height, thrust force, chip formation and tool wear.	
Parameters	WC: 6,000 rpm in CFRP, 800 rpm in Ti WC: 2,000 rpm in CFRP, 400 rpm in Ti PCD:2,000 rpm in CFRP, 300 rpm in Ti Feed 0,0762 mm/rev in CFRP, 0.051 mm/rev in Ti Mist coolant = 16 mL/min	Cutting speed (V _c) = 20, 35, 50, 65 m/ min feed rate (f) = 0.015, 0.030, 0.045, 0.060 mm/rev	Spindle speed $= 796 \text{ rpm}$, feed $= 0.02 \text{mm/rev}$	Spindle speed of 612 rpm and feed of 0.05mm/rev, spindle speed 1,826 rpm and feed of 0.05 mm/rev	Spindle speed rpm = 895, 1,000, 1,800, Feed rate mm/rev = 0.05, 0.08, 0.1 Flow rate mL/hr = 25, 50, 75	
Tool	WC twist drill, PCD twist drill of diameter = 9.525 mm	Uncoated tungsten carbide and diamond-coated drills with diameter $= 6.35 \mathrm{mm}$	Uncoated WC; 2 flute non stepped, 2 flute stepped and 3 flute stepped. diameter = 586 mm , helix angle = 30° , point angle = 130° .	WC drills with A (point angle = 118°, helix angle = 20°, Chisel edge thickness = 1.215 mm) B (point angle = 130°, helix angle = 30°, Chisel edge thick = 0.45 mm)	TiAIN Coated WC, TG1 (point angle = 130°, helix angle = 35°), TG2 (point angle = 135°, helix angle = 30°) TG3 (point angle = 140°, helix angle = 34°)	
Work piece	CFRP/Ti6A14V	CFRP/Ti6Al4V	CFRP/Ti6Al4V	CFRP/Ti6Al4V	CFRP/Ti6Al4V	

rs Analysis Author	n) 15, 30, 45, Drilling sequence,
Parameter	Cutting speed, v_c (m/min) 15
Tool	4V Diameter = 6.35 mm,
Work piece	CFRP/Ti6Al

Author	(Xu and El Mansori, 2016)	(Fernández-Pérez et al., 2019)	(Shyha et al., 2010)	(Xu et al, 2019)	(Shao et al., 2019)
Analysis	Drilling sequence, Thrust force, Chip formation, surface roughness, hole size accuracy, delamination, Tool life,	Tool wear, Effect of lubrication, Hole diameter, hole surface quality, burr,	Tool life, thrust force, Torque, Effect of cooling	Drilling forces, surface morphologies of composite holes, hole defect extents, hole geometrical accuracy and drill wear signatures	Thrust force, interface temperature, hole diameter, hole edge morphology, tool wear, chip formation, surface roughness, torque
Parameters	Cutting speed, v _c (m/min) 15, 30, 45, 60 Feed rate, f (mm/rev) 0.03, 0.06, 0.09, 0.12, 0.15	Cutting speed (m/min) = 15/70/15 Feed = 0.05mm/rev	Cutting speed = 20/40 m/min, 40/80 m/min and 60/120 m/min. feed rate = 0.05, 0.10 and 0.15 mm/rev. Wet 15 L/min and Spray mist cutting fluid ~50 mL/min) with the mineral oil lubricant ~10 mL/min with compressed air ~3 har	Dry and MQL of 6 bar and a 15 mL/h oil flow rate, feed rate (mm/rev) = 0.025, 0.050, 0.075 and 0.100, Cutting Speed m/min = 15, 30, 45, 60	Fixed feed rate = 0.01 mm/r, Spindle speed (r/min) = 1,000, 1,500, 2,000, 2,500, 3,000, 3,500 Ultrasonic vibrations assisted (UAD) F= 18.687kHz, Dry cutting
Tool	Diameter = 6.35 mm, Uncoated WC with point angle = 135° helix angle = 20° chisel edge = 0.11 mm (B) PVD TIAIN Coated twist drill with point angle = 140° helix angle = 27.2° chisel edge = 0.22 m	Diamond coated carbide substrate K10, two cutting edges point angle = 140° , diameter = 7.6 mm	Uncoated WC drills, CVD diamond coated WC and a hard metal C7 coated WC. helix angle = 30° point angle = 130° Diameter = 6.35	Uncoated WC twist drills diameter = 6 mm helix angle = 30° point angle = 140°	Two-flute uncoated WC twist drills diameter = 7.5mm
Work piece	CFRP/TI6AI4V	Ti6AlV/CFRP/TI6AlV	Ti6Al4V/CFRP/Al 7050	Ti6Al4V/CFRP	Ti6Al4V/CFRP

Work piece	Tool	Parameters	Analysis	Author
CFRP/Ti6Al4V	WC Diameter = 6mm Point angle = 118° Helix angle = 20°	Rotational speed N (rpm) = 2,000 and 3,000; Feed rate f (mm/rev) = 0.025, 0.05 and 0.075; Amplitude, A (µm) 3, 4.5 and 5.5; Frequency, F (Hz) 1.500 and 2.150	Comparison between HF-VAD and LF-VAD, thrust force, cutting temperature and exit burr height	(Hussein et al., 2019)
CFRP/TI6AI4V	Solid carbide Diameter = 7.938mm Cutting edges (N) = 2 Core diameter (d) = 1.9 mm Point angle (ϕ) = 128/155° Helix angle (β) = 16° CD 1 EVAD and HEVAD	Cutting speed of CFRP = 120 m/min and Ti = 20 m/min. Feed (f) = 0.05 mm/rev for Ti; 0.06 mm/rev for CFRP Amplitude (A) = 0.06 mm Oscillation frequency = 2.5 osc/rev MOI = 5 har pressure	Thrust force, Cutting edge geometry, Comparison of CD, LFVAD and HFVAD	(Yang et al., 2019)
CFRP/Ti6Al4V/ Al2024	Diameter = 6mm Conventional Drilling and Helical Machining	Sprindle speed (rpm) = 2,500, 3,000, 3,500; 3,500; 2,500;	Thrust force, Interface temperature, Comparison of helical milling and CD	(Sun et al., 2020)
CFRP/TI6Al4V	LFVAD and CD Uncoated WC drill bits diameter $= 6.35 \mathrm{mm}$ point angle $= 140^\circ$ helix angle $= 30^\circ$	Oscillation frequency = 1.5 osc/rev amplitude = 0.20 mm Cutting speed = 10, 20, 30, 40 m/min. Feed (f) = 0.015, 0.030, 0.045 and 0.060 mm/rev	Thrust force, Temperature, Surface morphology, Hole quality, Tool wear, Hole diameter and	(Xu et al., 2019)
CFRP/Ti6Al4V	TiAIN-coated drill Diameter = 6mm point angle = 140° , helix angle = 30° , rake angle = 10°	MQL = 15 mL/h and 0.6 MPa, dry Cutting speed (m/min) = 15, 30, 45 and 60 Feed rate (mm/rev) = 0.025, 0.050, 0.075 and 0100	Specific cuting energy, Hole morphology, Comparison of dry and MQL conditions	(Ji et al., 2020)
		200		(continued)

Table 1. Continued.

Work piece	Tool	Parameters	Analysis	Author
CFRP/Ti6Al4V	Diameter = 6mm WC Point angle = 118° Helix angle = 20°	Cutting speed N (rpm) = 2,000, 3,000 Feed rate f (mm/rev) = 0.025, 0.05, 0.075 0.075 Amplitude Am (mm) = 0.07, 0.1, 0.16, 0.25, 0.48 Frequency F = 2.5 cydes/rev (83.33 Hz at 2,000 rpm and 125 Hz at 3,000 rpm. Dry cutfing	Comparison of LFVAD and CD on Thrust force, cutting temperature, delamination, hole size, circularity, surface roughness and chip morphology	(Hussein et al., 2018)
CFRP/Ti6Al4V	Diameter $= 6.1 \text{mm}$ WC 2-flutes twist drills	Feed rate = 0.05 mm/rev and cutting speeds = 2.5 50 and 75 m/min, UAD work with fixed ultrasonic amplitude and frequency of 5.7 µm and 39 kHz	Comparison of UAD and CD on thrust force, tool wear	(Dahnel et al., 2016)
CFRP/Ti6Al4V	Uncoated solid tungsten carbide with two cutting edges. diameter $= 6.35 \text{ mm}$, point angle $= 140^{\circ}$, helix angle $= 30^{\circ}$	Spindle speed, n [rpm] = 1,000 Cutting speed, V [m/min] = 20 Feed rate, f [mm/rev] = 0.015, 0.030, 0.045, 0.060 Amplitude = 0.2 mm Forced air-cooling Oscillation 1.5 osc/rev	Comparison of UAD and CD on drilling forces, cutting temperatures, chip formation and tool wear	(Li et al., 2019)
CFRP/Ti6Al4V	Diameter = 7.5 mm uncoated WC twist drills with threaded shank	Spindle speed, <i>n</i> [rpm] = 1,000, 2,000, 3,000 Feed rate, <i>f</i> [µm/rev] = 5, 10, 15 Frequency (f) = 18.687, Amplitude (a) = 10 µm	Comparison of UAD and CD on drilling and interface temperature, hole morphology, delamination	(Shao et al., 2021)
CFRP/Ti6Al4V	A four-facet twist drill bit with diameter $= 9.56 \text{ mm}$ and point angle $= 118^{\circ}$	Feed rate = 0.05/0.1/0.15/0.2 mm/rev Cutting speed = 200/300/400/500 rev/ min 200/300/400/500	Thrust force and torque	(Jia et al., 2020)
(Gr/Bi)/Ti6Al4V	HSS, HSS-Co, carbide twist drills	Spindle speed = 325, 660, 1,115, 1,750, 2,750 rpm feed rate = 0.03, 0.08, 0.13, 0.12, 0.25 mm/rev	Drilling forces, Hole production, Tool wear, Hole damage, Surface topography	(Ramulu et al., 2001)

ameters 660, 1,115, 1,750 rpm On 13,0.20,0.25 mm/rev 10, 20 m/min Hole quality, Tool wear 10, 20 m/min Hole quality, Tool wear 10, 40 m/min An workpiece quality, Tool wear 10, 40 m/min An min An				
HSS-Co, split-Point, carbide drills Spindle speed = 660, 1,115, 1,750 pm Dilling process optimization, feed rate = 0.08,0.13,0.20,0.25 mm/rev Hole quality, Tool wear (Uncosted, TBs, diamond) feed rate = 0.15 mm (Uncosted, TBs, diamond) feed rate = 0.015 mm (Uncosted, TBs, diamond) feed rate = 0.000, 6.000 pm (TB) fool wear feed rate = 0.0762 (CFRP), 0.0500 mm/rev (TB) fool wear feed rate = 0.0762 (CFRP), 0.0500 mm/rev (TB) fool wear feed rate = 0.0762 mm/rev (CFRP); do 0.000 pm (TB) fool wear feed rate = 0.0762 mm/rev (CFRP); do 0.000 pm (TB) fool wear feed rate = 0.0762 mm/rev (CFRP); do 0.000 pm (TB) fool wear feed rate = 0.0762 mm/rev (CFRP); do 0.000 pm (TB) fool wear feed rate = 0.0762 mm/rev (CFRP); do 0.000 pm (TB) fool wear feed rate = 0.0762 mm/rev (CFRP); do 0.000 pm (TB) fool wear feed rate = 0.0762 mm/rev (CFRP); do 0.000 pm (TB) fool wear feed rate = 0.0762 mm/rev (CFRP); do 0.000 pm (TB) fool wear feed rate = 0.0762 mm/rev (CFRP); do 0.000 pm (TB) fool wear feed rate = 0.0762 mm/rev (CFRP); do 0.000 pm (TB) fool wear feed rate = 0.0762 mm/rev (CFRP); do 0.000 pm (TB) fool wear feed rate = 0.0762 mm/rev (CFRP); do 0.000 pm (TB) fool wear feed rate = 0.0762 mm/rev (CFRP); do 0.000 pm (TB) fool wear feed rate = 0.0762 mm/rev		Parameters	Analysis	Author
Twist drill, Step drills (Uncoated, Tills, diamond) (Indicated, Tills, Tills) (Indicated, Tills) (Indiling, Total, Spender, Tills) (Indiling, Total, Tills) (Indiling, Tills) (Indiling, Total, Tills) (Indiling, Total,	arbide drills	Spindle speed = 660, 1,115, 1,750 rpm feed rate = 0.08,0.13,0.20,0.25 mm/rev	Drilling process optimization, Hole quality, Tool wear	(Kim and Ramulu, 2004)
Twist drill, step drill Cutting speed = 40 m/min Thermal and mechanical loads, Diameter = 16mm Cutting environment: MQL WC twist drill, step drill Cutting environment: MQL WC twist drills Spindle speed = 2000, 6000 rpm Diameter = 9.525 mm drill point angle = 138° (CFRP) n = 800, 400 rpm (Ti) Tool wear, feed rate = 0.0762 (CFRP), 0.508 mm/, rev (Ti) Tool wear WC, PCD drills Spindle speed = 2,000, 6,000 rpm Diameter = 9.525 mm (CFRP) and 0.400, 800 rpm (Ti) Tool wear (CFRP) and 0.0508 mm/rev (Ti) Tool wear (CFRP) and 0.0508 mm/rev (Ti) Tool wear (CFRP); 400, 800 rpm (Ti) and 5urface roughness, drill point angle = 140° feed rate = 0.051 mm/rev (Ti) and 4500 rpm (CFRP); 400, 800 rpm (Ti) and 4500 rpm (CFRP); 400, 800 rpm (Ti) and 4500 rpm ATTN twist drills Spindle speed = 1.400 rpm (Ti) and 4500 rpm (CFRP); 400, 800 rpm (Ti) and 5urface roughness drill point angle = 140° feed rate = 1.19 and 450 mm/min Takin, Tisin and TiAIC/TTSi-coated farte = 0.2 mm/min drills Cauting environment: dry and mist-Hole quality water = 6 mm Cutting environment: dry and mist-Hole quality	, nond) 30°	Cutting speed = 10, 20 m/min feed rate = 0.15 mm Cutting environment: dry and oil mist conditions	Workpiece quality, Tool wear	(Brinksmeier and Janssen, 2002)
WC twist drills We twist drills Diameter = 9.525 mm drill point angle = 135* Leed rate = 0.0762 (CFRP),0.0508 mm/ Helix angle = 28* Cutting environment: dry and wet WC, PCD drills Cutting environment: dry and wet CIFRP): 300, 400, 800 rpm (Ti) Cutting environment: mist WC, BAM-coated drills Cutting environment: mist WC, BAM-coated drills CIFRP): 400, 800 rpm (Ti) CIFRP): 400 soft mm/rev AITN twist drills Diameter = 8 mm Af7 mm/min (Ti) CIFRPD: 400 rpm (Ti) CIFRPD: 300, 400 soft pm (Ti) CIFRPD: 400 rpm (Ti) CIFRPD:		Cutting speed = 40 m/min feed rate = 5 mm/min Cutting environment: MOI	Thermal and mechanical loads, Surface microstructure	(Brinksmeier et al., 2011)
WC, PCD drills Diameter = 9.525 mm drill point angle = 135° Helix angle = 28° C(FRP); 300, 400, 800 rpm (TI) drill point angle = 135° Lutting environment: mist WC, BAM-coated drills Cutting environment: mist WC, BAM-coated drills Cutting environment: mist WC, BAM-coated drills Cutting environment: mist WC, BAM-coated drills C(FRP); 400, 800 rpm (TI) Tool wear, Tool wear, Tool wear Tool wear, Spindle speed = 1,400 and 4,500 rpm Tool wear, Tool wear	m 35°	Spindle speed = 2,000, 6,000 rpm (CFRP) n = 800, 400 rpm (Ti) feed rate = 0.0762 (CFRP),0.0508 mm/ rev (Ti)	Drilling forces, Tool wear, Hole quality	(Park et al., 2014)
WC, BAM-coated drills Spindle speed = 2,000 rpm (CFRP); 400, 800 rpm (Ti) Tool wear, (CFRP); 400, 800 rpm (Ti) Tool performance feed rate = 0.051 mm/rev Spindle speed = 1,400 rpm (Ti) and Jameter = 8 mm drill point angle = 45	m 35°	Spindle speed = 2,000, 6,000 rpm (CFRP); 300, 400, 800 rpm (Ti) feed rate = 0.0762 mm/rev (CFRP); 0.0508 mm/rev (Ti)	Drilling forces, Tool wear	(Park et al., 2011)
AITIN twist drills Diameter = 8 mm drill point angle = 140° helix angle = 45° Cy-coated carbide drills Diameter = 6 mm AST mm/min (Ti) Cy-coated carbide drills Diameter = 6 mm AST mm/min (Ti) Cy-coated carbide drills Diameter = 6 mm AST mm/min (Ti) Cy-coated carbide drills Diameter = 6 mm AST mm/min (Ti) Cy-coated carbide drills Diameter = 6 mm AST mm/min (Ti) Cy-coated carbide drills Feed rate = 119 mm/min (Ti) Diameter = 6 mm AST mm/min (Ti) Cy-coated carbide drills Feed rate = 119 mm/min (Ti) Diameter = 6 mm AST mm/min (Ti) Cy-coated carbide drills Feed rate = 119 mm/min (Ti) Diameter = 6 mm AST mm/min (Ti) Cy-coated carbide drills Feed rate = 119 mm/min (Ti) Tool wear	s	Spindle speed = 2,000, 6,000 rpm (CFRP); 400, 800 rpm (Ti) feed rate = 0.051 mm/rev	Tool wear, Tool performance	(Park et al., 2012)
C7-coated carbide drills Spindle speed = 1,400 and 4,500 rpm Drilling forces, Diameter = 6 mm Spindle speed = 188 m/min TiAlN, TiSiN and TiAlCr/TiSi-coated Cutting speed = 18.8 m/min Drilling forces, Cutting environment: dry and mist-Hole quality C1-coated carbide drills feed rate = 1,400 and 4,500 rpm Drilling forces, C1-coated carbide drills feed rate = 1,400 and 4,500 rpm Drilling forces, C1-coated carbide drills feed rate = 1,400 and 4,500 rpm Drilling forces, C1-coated carbide drills feed rate = 1,400 and 4,500 rpm Drilling forces, C1-coated carbide drills feed rate = 1,400 and 4,500 rpm Drilling forces, C1-coated carbide drills feed rate = 1,400 and 4,500 rpm Drilling forces, C1-coated carbide drills feed rate = 1,400 and 4,500 rpm Drilling forces, C1-coated carbide drills feed rate = 1,400 and 4,500 rpm Drilling forces, C1-coated carbide drills feed rate = 1,400 and 4,500 rpm Prilling forces, C1-coated carbide drills feed rate = 1,400 and 4,500 rpm Prilling forces, C1-coated carbide drills feed rate = 1,400 and 4,500 rpm Prilling forces, C1-coated carbide drills feed rate = 1,400 and 4,500 rpm Prilling forces, C1-coated carbide drills feed rate = 1,400 and 4,500 rpm Prilling forces, C1-coated carbide drills feed rate = 1,400 and 4,500 rpm Prilling forces, C1-coated carbide drill feed rate = 1,400 and 4,500 rpm Prilling forces, C1-coated carbide drill feed rate = 1,400 and 4,500 rpm Prilling forces, C1-coated carbide drill feed rate = 1,400 and 4,500 rpm Prilling forces, C1-coated carbide drill feed rate = 1,400 and 4,500 rpm Prilling forces, C1-coated carbide drill feed rate = 1,400 and 4,500 rpm Prilling forces, C1-coated carbide drill feed rate = 1,400 and 4,500 rpm Prilling forces, C1-coated carbide drill feed rate = 1,400 and 4,500 rpm Prilling forces, C1-coated carbide drill feed rate = 1,400 and 4,500 rpm Prilling forces, C1-coated carbide drill feed rate = 1,400 and 4,500 rpm Prilling forces, C1-coated carbide drill feed rate = 1,400 and 4,500 rpm Prilling forces, C1-coat	.04	Spindle speed = 1,400 rpm (Ti) and 4,500 rpm (CFRP) feed rate = 119 mm/min (CFRP) and 457 mm/min (Ti)	Drilling forces, Delamination, Burrs, Surface roughness, Tool wear	(Isbilir and Ghassemieh, 2013)
TiAIN, TiSIN and TiAICr/TiSi-coated Cutting speed = 18.8 m/min Drilling forces, drills feed rate = 0.2 mm/rev Tool wear, Diameter = 6 mm Cutting environment: dry and mist-Hole quality	ills	Spindle speed = $1,400$ and $4,500$ rpm feed rate = 119 and 457 mm/min	Drilling forces, Tool wear, Surface roughness	(Ghassemieh, 2012)
	Cr/TiSi-coated	Cutting speed = 18.8 m/min feed rate = 0.2 mm/rev Cutting environment: dry and mistwater cooling	Drilling forces, Tool wear, Hole quality	(Fujiwara et al., 2012)

Table 1. Continued.

	_
7	∹
•	~
(υ
-	3
•	=
•	=
+	_
2	=
(2
t	
`	_
_	_
۴	
	11
_	=
	7
T-15	=
ď	v
г	_

Work piece	Tool	Parameters	Analysis	Author
CFRP/TI6AI4V	TiAIN, TiAICr/TiSi coated drills Diameter = 6 mm	Cutting speed = 9.4, 18.8 m/min feed rate = 0.1, 0.2 mm/rev Cutting environment: dry and watermist cooling	Cutting forces, Tool wear, Hole quality, Cutting environment comparison	(Tashiro et al., 2011)
CFRP/Ti6Al4V	K ₂ 0 uncoated drill Diameter = 12 mm drill point angle = 140° helix angle = 30°	Spindle speed = 2,652 rpm (CFRP); 265 rpm (TI) feed rate = 0.05 mm/rev (CFRP); 0.2 mm/rev (TI)	Drilling forces, Tool wear	(Poutord et al., 2013)
Ti6Al4V/CFRP/ Al7050	DLC and CVD diamond drill Diameter = 6.38 mm drill point angle = 140° helix angle = 30°	Cutting speed = 30 m/min (TI); cutting speed = 120 m/min (CFRP, AI) feed rate = 0.08, 0.15 mm/rev	Thrust force, Torque, Tool wear, Hole accuracy, Burr formation	(Kuo et al., 2014)
CFRP/Ti; CFRP/AI		Variable cutting conditions, nature of materials, feed rate, spindle speed, etc.	Effects of different input factors on hole diameter	(Carvajal et al., 2011)
CFRP/Ti6Al4V, Ti6Al4V, CFRP	Uncoated, AITIN coated and nano crystalline AITIN grains surrounded by Si ₃ N ₄ matrix coated WC drills Diameter = 9.525 mm drill point angle = 135° helix angle = 25°	For CFRP spindle speed = 6,000 rpm, feed rate = 0.0762 mm/rev For Ti spindle speed = 500 rpm, feed rate = 0.0508 mm/rev 16 mL/min Mist coolant	Drilling forces, Tool wear mechanisms inCFRP-only, Ti-only and CFRP/Ti drilling	(Wang et al., 2014)
CFRP/Ti	TiAIN coated twist drill Diameter = 6 mm drill point angle = 120° helix angle = 20°	Cutting speed = 10 , 25 m/min, feed rate = 0.05 , 0.1 mm/rev	Drilling-force models Predicted forces Measured forces	(Matsumura and Tamura, 2013)
CFRP/Ti6Al4V	Uncoated cemented carbide drill with the diameter 6.35 mm, helix angle = 30°, point angle = 140° and cutting-edge length = 34 mm	Cutting speed = 10 m/min , feed rate = 0.06 mm/rev	CFRP to TI, TI to CFRP sequence, Hole quality, fatigue, Quasi static tensile strength.	(An et al., 2021)
CFRP/Ti		Spindle speed = 612 rpm, 1,826 rpm feed = 0.05mm/rev, 0.05 mm/rev. Spindle speed (r/min) = 400, Feed rate (mm/r) = 0.03, 0.04, 0.05, 0.06 Conventional drilling CD, CVAD (Highfrequency = 34.91 kHz, 3µm, lowfrequency 33.33 Hz, 20 um)	Flank wear, chisel edge wear, delamination, burr height, tolerance, chip morphology Delamination	(Senthilkumar et al., 2013) (Li et al., 2022)
				(00000000)

Work piece	Tool	Parameters	Analysis	Author
CFRP/Ti6AIV	Uncoated solid carbide drill,	Dry cutting.	Machining forces, dimensional accuracy,	(Boutrih et al.,
	diameter $= 4.17$ mm,	Cutting speed Vc (m/min) = 15, 30,	surface integrity and finally hole quality	2022)
	2 cutting edges,	45, 65;		
	chisel edge $= 0.11 \mathrm{mm}$	Feed rate f (mm/rev) = 0.03, 0.06,		
	helix angle $=20^{\circ}$,	0.09, 0.12		
	point angle $= 135^{\circ}$.	Sequence – CFRP to Ti, Ti to CFRP		
Ti6Al4V/CFRP/	Coating – Uncoated and TiAIN/TiN	Feed (mm/rev) $= 0.05$, 0.08		(Kuo et al., 2018)
AA7050	coated WC twist drills.	With and without pecking		
	Relief angle $= 14^{\circ}$,	Cutting fluid – water-based emulsion		
	helix angle $=30^\circ$	delivered internally at a flow rate of		
	Point angle $= 140^\circ$	30 L/min and a pressure of 70 bar,		
	Diameter $= 6.35 \text{mm}$	containing 7–8% soluble mineral oil		
CFRP and Ti6Al4V	TiAIN coated carbide twist drills	Speed = 1,000, 1,500, 2,000 rev/min		(Cao et al., 2023)
plate	UD CFRP	Feed = 50mm/min		

and delamination defects. Conversely, when drilling titanium alloy, a higher feed rate and lower cutting speed are preferable to reduce cutting temperature, mitigate tool wear and reduce exit burr height in the titanium alloy (Park et al., 2011; Wang et al., 2014; Jiaying et al., 2022). Therefore, when considering the CFRP/Ti stack-up drilling, the choice of drilling parameters must account for the specific requirements of the CFRP, titanium alloy and interface machining stage (Ramulu et al., 2001; Denkena et al., 2008; Park et al., 2011).

For drilling composite panels, it is generally recommended to employ a low feed rate (0.01-0.05 mm/rev) with a relatively high cutting speed (150-200 m/min) to minimize delamination (Mkaddem et al., 2013; Sheikh-Ahmad, 2015). Conversely, for titanium phase machining, a high feed rate (0.05-0.1 mm/rev) with a low cutting speed (10-30 m/min) is advisable; however, these circumstances are detrimental to composite parts because the high axial force causes delamination (Ramulu et al., 2001; Sharif and Rahim, 2007). Moreover, specific scenarios might benefit from a cutting condition comprising a low cutting speed and a moderate feed rate, enhancing CFRP/Ti drilling and ensuring an admirable hole surface finish for both CFRP and Ti phases (Park et al., 2014). Additionally, research by Soo et al. (2019) highlighted that increasing the feed rate resulted in improved hole accuracy, with diameter fluctuation not exceeding 15 µm. Zitoune et al. observed that drilling with a low feed rate (f = 0.05 mm/rev) resulted in the formation of continuous chips, and increasing the spindle speed from 1,050 to 2,750 rev/min had no discernible effect on chip shape and size (Zitoune et al., 2010).

The selection of drilling parameters significantly influences machining efficiency, tool life and hole quality in CFRP/Ti stacks, requiring tailored approaches for each material layer. Cutting speed has minimal effect on thrust force, whereas feed rate has a substantial impact, with higher feed rates increasing thrust force but reducing tool-work contact time, thereby minimizing heat and exit burrs in titanium. Lower feed rates (0.01-0.05 mm/rev) and higher cutting speeds (150-200 m/min) are recommended for CFRP to reduce delamination, while higher feed rates (0.05-0.1 mm/rev) and lower cutting speeds (10-30 m/min) are ideal for titanium to lower cutting temperatures and mitigate burrs. Balancing these parameters for interface machining can enhance hole quality for both materials. Additionally, moderate feed rates and low cutting speeds can improve surface finish in stack drilling, while higher feed rates may enhance hole accuracy without significant diameter fluctuations. Chip formation and behavior also vary with feed rates and spindle speeds, further influencing the overall drilling performance. Table 2 shows different combinations of feed and speed and the impact of them on various outcomes.

Table 2.	Influence	of	speed	and	feed	on	various	machining	outputs	while	drilling	CFRP/Ti
stack.												

Speed	Feed	Result	Reference
Increase	Decrease	Continuous metal chip	(Kim et al., 2005)
Increase	Increase	continuous metal chip	(Ramulu et al., 2001), (Kim and Ramulu, 2004)
	Decrease	CFRP Continuous chip	(Kim et al., 2005)
	Increase	CFRP Dust chip	(Kim et al., 2005)
Increase		Entry delamination increased	(Abrão et al., 2007)
Increase		Exit delamination increased	(Abrão et al., 2007)
Increase	Decrease	Optimum for CFRP panel	(Ramulu et al., 2001), (Liu et al., 2012) (Kuo et al., 2018)
Increase	Increase	Optimum for Ti panel	(Ramulu et al., 2001), (Kurt et al., 2008)
Decrease	Increase	Thrust force increase	(Xu et al., 2016)

Customizing tool geometry

Selecting an optimal tool for CFRP/Ti stack drilling presents a notable challenge, primarily because each phase of machining shows distinct wear patterns. For example, when drilling CFRP panels, the cutting tool undergoes noticeable wear on its edges, causing edge rounding and the flank experiences considerable wear due to the abrasive nature of the reinforcing fibers (König and Graß, 1989) and the major wear modes are abrasion, chipping and fracture induced by mechanical and thermal loads (Xu et al., 2014). Conversely, when drilling Ti panels, severe adhesion of Ti chips combined with highly localized temperature concentrations at the tool-chip interface easily leads to edge chipping, adhesion wear and tool breakage. Therefore, cutting tools for hybrid CFRP/Ti drilling should possess exceptional toughness, high hardness, superior wear resistance, high thermal conductivity and favorable chemical inertness. Various tool materials, such as high-speed steel, coated tools, carbide tools and super hard materials like PCBN or PCD, have been examined for this purpose (Lantrip, 2008). For composite/ metal drilling, carbide tools with low cobalt content are preferred due to their higher hardness and improved abrasion resistance. However, research by Xu and El Mansori (2016) indicates that the geometric properties of the tool have a greater impact on FML drilling than the material composition.

Specially designed tool geometries have demonstrated significant potential in achieving improved hole quality while drilling stacks (Zitoune et al., 2016; Altin Karataş and Gökkaya, 2018). Researches on these tool geometries incorporate characteristic angles (e.g., helix angle, clearance angle, point and) (Senthilkumar et al., 2013, 2018; Xu and El Mansori, 2016), edge configurations (Zitoune et al., 2016), tool diameter (Zitoune et al., 2010) and tool shapes (e.g., twist, double point, candlestick, etc) (Pawar et al., 2015; Soo et al., 2019; Unai et al., 2019). Figure 19 illustrates the typical structure of a conventional twist drill. Smaller geometric properties of the drill, such as helix angle, point angle and chisel edge length, typically lead to better hole quality, including improved circularity, reduced delamination, enhanced surface roughness and precise hole size, compared to

larger ones (Zitoune et al., 2010; Senthilkumar et al., 2013, 2018; Xu and El Mansori, 2016). Zitoune et al. suggested utilizing drills with diameters of 6 mm or less for drilling multi-material stacks because larger diameters result in significant increases in chip cross-sectional area and longer chisel edge lengths (Zitoune et al., 2010). Won and Dharan emphasized that when the feed rate is low, 40% of the total cutting force originates from the chisel edge, increasing to 60% when the feed rate is high (Won and Dharan, 2002). Therefore, for drilling multi-material stacks, it is preferable to use a drill with a diameter of 6 mm or less. Moreover, it was noted that drill bits with a narrow chisel-edge width could decrease force generation and mitigate delamination damage during drilling (Sheikh-Ahmad, 2015).

In drilling FML stacks, Aydin and Nalbant achieved optimal performance with a helix angle of 130° (ErmanAydın, 2020). Literature suggests that higher drill point angles (130° $< \sigma <$ 140°) are more effective for drilling metal (Kelly and Cotterell, 2002), whereas lower drill point angles (75° < σ < 118°) are preferable for drilling FRP (Chen, 1997; Seeholzer et al., 2019). Kuo et al. (2014) revealed that employing a two-stage point design for a drill bit could improve its 'self-centering' capability, thereby reducing tool deflection and ensuring excellent hole accuracy. Garrick argued that drill bits featuring a unique K-land design, typically employed in cutting Ti alloy, could strengthen the cutting edges, rendering the tool suitable for power-feed drilling in CFRP/Ti stacks. In the author's experiments, veined PCD drills with a modified K-land design exhibited extended tool life and enhanced hole quality when compared to conventional geometric PCD drills (Garrick, 2007).

Multiple researches have established that stepped drills are highly effective in drilling CFRP/titanium alloy structures. Stepped drills play a crucial role in distributing mechanical load during drilling, leading to improved hole quality and reduced tool wear. Alonso et al. (Unai et al., 2019) compared the impact of flute count and geometry in stepped drills on interface drilling quality, as depicted in Figure 20a. The findings revealed that a three-flute step drill, in contrast to a double-edge step drill and a regular twist drill, significantly reduces tool wear, minimizes thermal damage at the interface and notably decreases CFRP delamination at the stack interface. Moreover, the burr height measurements for stepless drills were approximately twice as high as those recorded for two-fluted stepped drills. However, Xia and Mahdavian (2005) observed that during metal drilling, the second step of a step drill bit consistently generates continuous and large-sized chips. This poses challenges as these unbroken metal chips must traverse a longer removal route, particularly through the upper CFRP layer, where there is a risk of potential tearing damages. Hence, to facilitate chip breaking and removal as well as minimize cutting temperature, Wang et al.

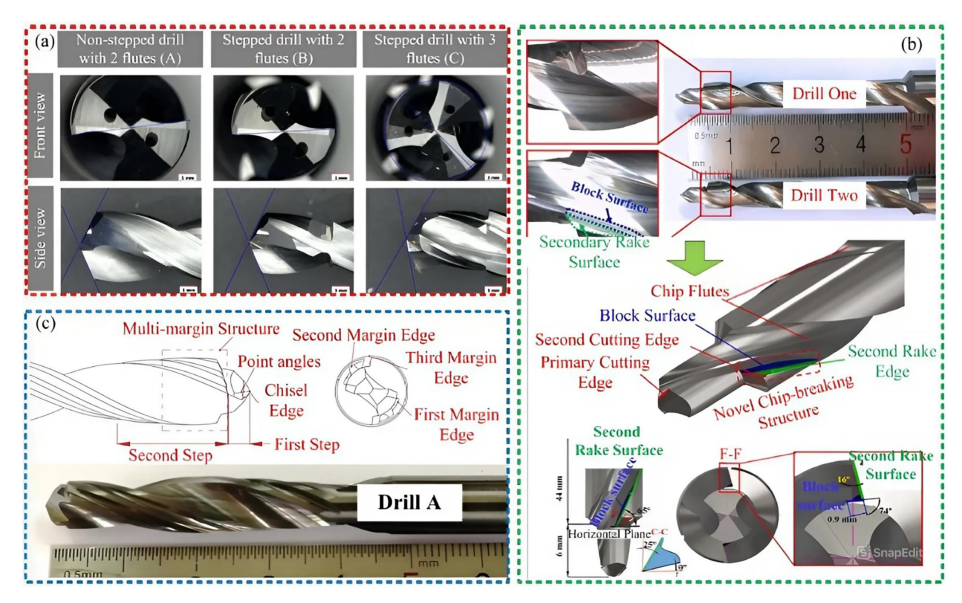


Figure 20. Novel tool structure for CFRP/Ti (Al) stacks: (a) the stepped drill with different number of flutes and geometry (Unai et al., 2019), (b) a new stepped drill with a chip breaking structure (Wang et al., 2021) and (c) a multi-cutting-edge twist drill (Yuan Jia et al., 2020).

(2021) innovated a modified stepped drill featuring a chip-breaking design based on chip fracture theory as illustrated in Figure 20b. This novel design incorporates a block surface on the inner side of the secondary cutting edge's rake surface. This addition of a block surface adjacent to the rake surface effectively restricts lateral chip movement, thereby reducing the chip curl radius, increasing chip surface strain and potentially leading to chip breakage. Furthermore, Yuan Jia et al. (2020) introduced a multicutting-edge twist drill specifically tailored for drilling titanium alloy/CFRP structures in the opposite stacking sequence, as depicted in Figure 20c. The multi-cutting-edge configuration serves to reduce both radial and axial cutting depths, effectively alleviating the tool's pressure on the hole wall during machining and minimizing pressure in the outlet direction. Consequently, this design significantly enhances machining precision for laminated apertures while reducing CFRP exit delamination and titanium alloy burr height.

Therefore, it can be said that drilling CFRP/Ti stacks presents challenges due to distinct wear patterns in each material: CFRP's abrasiveness causes edge rounding and flank wear, while Ti's high adhesion and heat generation lead to chipping and tool breakage. Optimal tools require toughness, hardness, wear resistance, thermal conductivity and chemical inertness. Carbide tools with low cobalt content are preferred for their abrasion resistance, but tool geometry plays a more significant role. Key geometric features include helix and point angles, chisel-edge width and flute design, with smaller diameters (≤6 mm) and narrow chisel edges reducing



delamination and cutting forces. Higher point angles (130°-140°) suit metal drilling, while lower angles (75°-118°) are better for FRP. Advanced designs like two-flute drills with large helix angles, stepped drills and multi-cutting-edge twist drills improve chip removal, reduce wear and enhance hole quality. Innovations like modified stepped drills with chipbreaking designs further optimize performance by reducing thermal damage, delamination, and burr formation in CFRP/Ti stacks.

Selecting drill bit material

Hardness, toughness, wear and heat resistance are the main factors that determine a drill's lifespan. A high-quality drill should be able to withstand high temperatures without breaking, rupturing, or wearing out (Prajapati et al., 2015; Hari Nath Reddy et al., 2021). In theory, for the cutting tool to effectively cut through the workpiece, its hardness needs to be higher than that of the workpiece. A bit's resistance to stress load, vibration-induced chipping and cracking, misalignment, runouts and other drilling process flaws increases with its toughness. Increasing the toughness of drill bits while maintaining their hardness is a prominent trend in their development phases.

High-speed steel (HSS) is typically utilized in drilling applications since it is less expensive than other materials like tungsten carbide, ceramic, or polycrystalline diamond (PCD). According to Liu et al., the main reason why HSS or carbide drill bits have become popular is because they operate better at high cutting speeds than other drill bits (Liu et al., 2012). HSS drills were often employed in a number of studies, making it the most widely used tooling material because of its affordability and increased toughness (Davim and Reis, 2003a; Tsao and Hocheng, 2007). But HSS is not advised for composite drilling applications because of its poor wear resistance when drilling on highly abrasive materials like CFRP (Geier et al., 2019; Geng et al., 2019). In contrast to other tooling materials, HSS with the maximum hardness deforms at about 700 °C (Davim and Reis, 2003b; Astakhov et al., 2008).

In the case of tungsten carbide, the cobalt matrix is added together by the sintering process in carbide materials, which are composed of carbide particles (tungsten carbides, titanium, tantalum, or some mix of these). The carbide particle size that is often utilized for cutting can be categorized respectively as less than 0.8 μm, 0.8 μm to 1.0 μm, 1 μm to 4 μm and more than 4 µm for micro grains, fine grains, medium grains and coarse grains (Lin and Chen, 1996; Hassan, 2020). The characteristics of carbide tools are greatly impacted by the quantity of cobalt present. Depending on the desired toughness and hardness, the cobalt percentage of the sintered tungsten carbide rod for the drill bit will vary between 3% and 20%. The toughness of the drill bit increases as the cobalt concentration rises, but the strength and hardness may deteriorate. For the identical composite materials, tungsten carbide bits outperformed HSS at low speed and feed while drilling at high temperature in terms of wear resistance, delamination and improved surface finish (Lin and Chen, 1996). When the radius away from the corner was measured after the drilling procedure, there was hardly any wear visible on the carbide drills' flank surface, while the HSS bit had significant wear (Shyha et al., 2009).

When considering ceramic tool material, maintaining high hardness (and hence abrasive wear resistance) at high temperatures is the key benefit of employing them. The high temperature that results from the tool and workpiece coming into contact weakens all tool materials during the drilling operation, but ceramic materials can function since they wear off considerably more slowly. One of the key advantages of ceramic cutting tools is their chemical stability (Çelik et al., 2015). Compared to the majority of ferrous materials, including super-alloys, ceramic materials are therefore perfect. There are two basic varieties of ceramics. The first is aluminum oxide, which is generally applied to strong steel and is brittle yet wearresistant. The other one is silicon nitride, which is used specifically on cast iron and is comparatively soft and durable. The configuration of a variety of ceramic materials known as Si-AlONs, which mix silicon nitride and aluminum oxide, is now the most important breakthrough. The harder the material, the greater the ratio of aluminum oxide; nevertheless, the more silicon nitride needed, the tougher the material must be (Çelik et al., 2015). It now seems that ceramic tools will benefit greatly from the new field of nanotechnology. Nowadays, the most sophisticated ceramics are micrograin materials, while the most recent advancements are focused on moving toward nanograins (Çelik et al., 2015). The main benefit of this technique is that when more grain area is exposed to bonding, the strength increases with the smallest particle size. Increased resistance to damage and improved wear characteristics are the outcomes of the strength gain. Coating applications are seldom used for ceramic materials because of the poor adherence between the coating materials and the ceramic substrate.

The hardest material for cutting tools is polycrystalline diamond, where diamond particles in a metal matrix make up the PCD cutting tool. Compared to tungsten carbide, which has a hardness of 1,600-2,200 HV, PCD has a far higher Vickers hardness (HV) of 6,000. According to Karpat and Bahtiyar, PCD is appropriate for high-speed drilling and cutting of very abrasive materials like CFRP (Karpat and Bahtiyar, 2015). According to Garrick et al. and Heath et al., they have created a veined drill that can drill titanium stacks and carbon composites in a single stroke (Heath, 2001;

Garrick, 2007). The helical PCD drill geometry performed the best overall cutting when compared to other tungsten carbide drills; nevertheless, when delamination is taken into account, it is more susceptible to variations in feed rate. Heath et al. asserted that because PCD can tolerate very abrasive carbon fiber-reinforced polymers (CFRP), it is a more robust tool that may be used to drill composite materials. But when combined with composites, PCD is too brittle to withstand the high cutting forces of metals like titanium (Heath, 2001; Garrick, 2007). According to Butler-Smith et al., there are notable benefits of core drilling using PCD drill. A novel core drill design reduced drilling temperature, thrust force and surface deterioration by 26%, which decreased the likelihood of delamination during composite drilling (Butler-Smith et al., 2015). The PCD tool was mainly claimed to have greater cutting efficiency while processing typical composites because of its low heat conductivity and strong wear resistance (Ferreira et al., 1999; Kim et al., 2015). When used in stack-up drilling, the PCD coating may also offer exceptional wear resistance and successfully lessen the excessive chip adhesion that occurs during metal component drilling (Park et al., 2012). Due to their great abrasion resistance, PCD tools are typically chosen for cutting composites (An et al., 2013, 2014). Build-up edge and build-up layer are the primary issues while drilling a stack material with metal components. When drilling a metallic item, the chips that are created during the drilling process can readily fuse to the drill's cutting edge, creating a layer that causes the tool to fail too soon (Zitoune et al., 2010, 2012). One of the materials that may be utilized to drill the stack material at the lowest drilling temperature is PCD because of its strong wear resistance, low friction characteristics and low thermal conductivity. However, when drilling a metallic item with high-speed machining, a PCD drill can readily fracture because of the material's inherent brittleness. In contrast to tungsten carbide materials, it is advised that PCD drills be used at a somewhat narrower range of cutting parameters. In contrast to high-speed steel (HSS), PCD has the least acceptable toughness property because of its abrupt deformation at 600 °C (Davim and Reis, 2003b; Astakhov et al., 2008).

On the whole, it can be said that the lifespan of drills depends on hardness, toughness, wear and heat resistance, with tougher, harder drills being key for improved performance. High-speed steel (HSS) is commonly used for its affordability and toughness but lacks wear resistance, especially for abrasive materials like CFRP. Tungsten carbide, with its cobalt matrix and varying cobalt content, offers superior wear resistance, toughness and performance under high temperatures compared to HSS. Ceramic tools, known for their hardness and thermal stability, excel in high-temperature applications but are brittle, with advancements in nanotechnology

enhancing their strength and wear resistance. Polycrystalline diamond (PCD) tools, the hardest cutting material, provide exceptional wear resistance and cutting efficiency for abrasive composites but are brittle and less suited for high cutting forces or metallic materials like titanium.

Application of cooling technology

Metalworking fluids (MWFs) are used to machine tough-to-cut materials because they reduce cutting temperatures, reduce friction between the workpiece and tool and improve chip removal. These factors significantly extend tool life and reduce surface quality and machinability issues (Krolczyk et al., 2019). When using cutting fluid during drilling, the hole size decreases as the coolant helps to dissipate some of the cutting heat (Park et al., 2011). However, they pose risks to both the environment and employees (Wang et al., 2022). Due to moisture absorption, composite materials like CFRPs lose their interlaminar strength as well (Almudaihesh et al., 2020). Turner et al. examined the impact of various MWFs on the mechanical characteristics of CFRPs and demonstrated that swelling of the composite resulted from water absorption in both water- and oil-based coolants. This consequently resulted in the tested specimens' mechanical strength declining (Turner et al., 2015). In contrast, Tetsuya et al. revealed that, while drilling CFRP/Ti6Al4V stacks with cemented carbide drills, employing water-mist cooling can enhance the precision of the hole diameter in the CFRP layer (Tashiro et al., 2011).

Minimum quantity lubrication

During dry drilling, since the drill edges aren't cooled or lubricated by the cutting fluid, the hot, sharp-edged metallic chips generated during subsequent titanium drilling induce notable mechanical wear and thermal degradation on the surface of the carbon/epoxy. This exacerbates the severity of the composite flaws (Xu et al., 2020). According to Min et al., the morphologies of the drilled composite phase are substantially smoother under the minimum quantity lubrication (MQL) conditions (Ji et al., 2020). In order to reduce friction at the tool-chip interface with less lubricant (500 mL/h), oil atomization is used in MQL to provide highly localized lubrication (Madarkar et al., 2018; Masoudi et al., 2018), which lowers the cutting temperature (Hamran et al., 2020) and conserves the energy lost to friction to reduce the power usage (Ji et al., 2020; Xu et al., 2020). When drilling CFRP/metal stacks, MQL can be used to reduce high drilling temperatures, delay tool wear and prevent metal from sticking to the cutting edge, especially when the metallic panel is titanium (Hassan et al., 2022). Due to the lubricant's moistening effect, which causes the composite chip dust to soak up the lubricant and stick at the drill edges, the majority of the chip adhesion under MQL conditions is composed of powdery composite debris (Perçin et al., 2016). In contrast, dry machining results in highly worn drill surfaces with large amounts of titanium chips firmly fused on the primary, secondary and drill chisel edges. It suggests that poor cutting conditions are predominating during stack drilling since the severe adherence of titanium might lead to BUE or even peeling off of the adhered chips, which accelerates drill edge chipping or fracture (Xu, Ji, et al., 2019). Utilizing MQL reduced the rate of tool wear by preventing BUE from forming on tool faces due to high cutting temperatures (Brinksmeier and Janssen, 2002).

Dry and flood cooling have traditionally been the two mediums for machining; and more recently, attention has been paid to MQL as a cooling medium. The experimental diagram for MQL is shown in Figure 21. The machining quality of CFRP/Ti6Al4V stacks was first studied by Senthilkumar et al. under MQL conditions (Senthilkumar et al., 2018). The authors conducted a number of test runs using different MQL variants and noted that a lower flow rate resulted in improved machining quality. Under the established process conditions, a number of MQL drilling experiments were conducted by different authors with a compressed air pressure of 0.6 MPa and coolant flow rate of 15 mL/h (Xu, Ji, et al., 2019; Ji et al., 2020; Xu et al., 2020). It was found that low oil flow rates and high air pressures work well together to produce MQL drilling with greater machining quality (Iskandar et al., 2013; Meshreki et al., 2016). Nam and Lee examined the effects of using nanofluid MQL conditions and compressed air in micro-drilling of Ti6Al4V alloys (Nam and Lee, 2018). According to the findings, the nanofluid MQL may more successfully enter the cutting area and make best use of the ball bearing effects, which would result in a large reduction in friction.

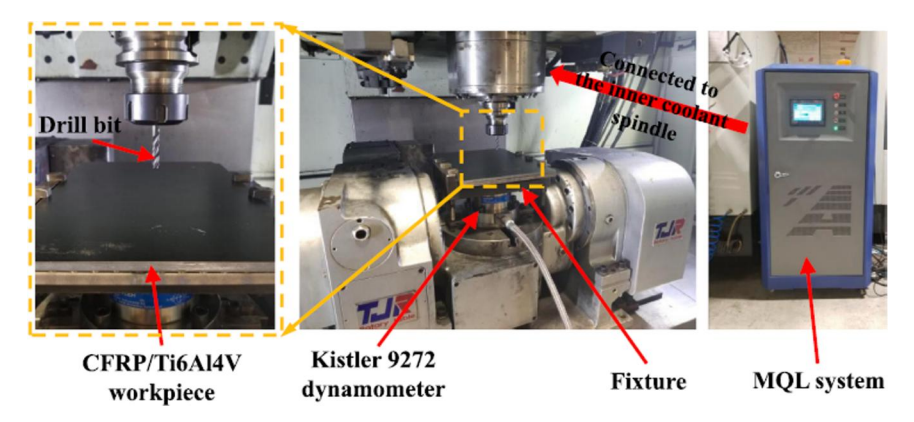


Figure 21. Experiment set up with MQL (Xu et al., 2020).

According to Seo et al. (2021), MQL machining increased cutting force and accordingly delamination because the material didn't soften as a result of lower cutting temperatures. Typically, the MQL environment produces greater thrust forces than dry machining (Meshreki et al., 2016; Xu et al., 2020); for instance, it produces CFRP panel thrust forces that are 12.71% higher than those attained during dry drilling circumstances at $V = 15 \,\text{m/}$ min and $f = 0.100 \,\mathrm{mm/rev}$ (Xu, Ji, et al., 2019). Two elements can explain these phenomena. First, since the lubricants' wetting properties make the powdery particles that have been removed from the composite panel easy to clog along drill edges, increasing the frictional effort needed to eliminate composite chips (Xu, Ji, et al., 2019). Second, the cooling effects brought on by the MQL oil supply stop the composite polymer matrix from softening and plasticizing, preserving the brittle characteristics of the carbon/epoxy system and exhibiting greater mechanical resistance to the drill cutting edges, particularly the chisel edge (Xu et al., 2020). While drilling the Ti6Al4V layer, MQL conditions also fall short of reducing drilling forces since they encourage thrust forces that are on par with those attained in a dry drilling environment. Two elements can explain these phenomena. First of all, titanium alloy is a typical tough-to-cut material and when MQL is used, the cutting zone's temperature is lowered, which diminishes the impact of thermal softening and induces a cooling effect on the chips expelled from the drilled hole, thereby elevating the friction between each chip and the hole wall. Second, to drill the tough titanium alloy, the sharpness of the cutting edge should be maximized. However, the oil-induced adhesion of CFRP chips causes a significant rounding of the cutting edge and worsens the drill bit's abrasive wear, which is quite unfavorable and increases the cutting load (Xu et al., 2020). Additionally, regardless of whether there are CFRP or Ti6Al4V layers present, the drilling speed has a negative impact on the growth of thrust forces in the majority of drilling scenarios. The incident is linked to softening of the workpiece due to high speeds, which lowers the cutting resistance to evacuate additional softened pieces (Krishnaraj et al., 2012; Xu et al., 2014, 2020). It is found that both MQL and dry drilling methods benefit from a parametric combination of high cutting speeds and low feed rates for reducing thrust forces (Xu, Ji, et al., 2019).

Although using MQL reduced tool wear and enhanced the surface morphologies of the drilled holes, it did not solve the issues of delamination (Xu, Ji, et al., 2019) and hole cylindricity (Xu et al., 2020). When compared to dry machining, MQL environments typically result in substantially smoother composite surfaces with lower levels of drilling-induced flaws (Xu et al., 2020). This shows how well the cutting oil penetrates the toolwork interface, lubricates, cools and cuts holes, minimizing the occurrence of different forms of thermal and mechanical-driven defects over the material removal process (Xu, Ji, et al., 2019). Due to the efficient cooling and lubricating properties of the MQL atmosphere, the titanium chip evacuation does not create visible scratch marks or thermal deterioration on the cut composite holes (Rahim and Sasahara, 2010).

One of the first to use MQL while machining multilayer composite stacks was Brinksmeier and Janssen (2002). They discovered that while drilling composite/metal stacks, the usage of MQL could significantly decrease the diameter difference and reduce tool-metallic chip adherence. When the MQL environment is used, composite hole diameters are typically more consistent and nearer to the nominal diameter. However, in dry drilling and MQL drilling, increasing either the cutting speed or feed rate tends to impact the titanium chips' scratching on the composite holes (Xu et al., 2020) and increase the CFRP hole diameter (Xu, Ji, et al., 2019). Additionally, for both the dry and the MQL circumstances, in the CFRP panel, the exit hole diameters show the highest values, succeeded by those of the middle hole and the entrance hole (Xu et al., 2020). In metallic panel, the MQL conditions frequently result in undersized holes that are

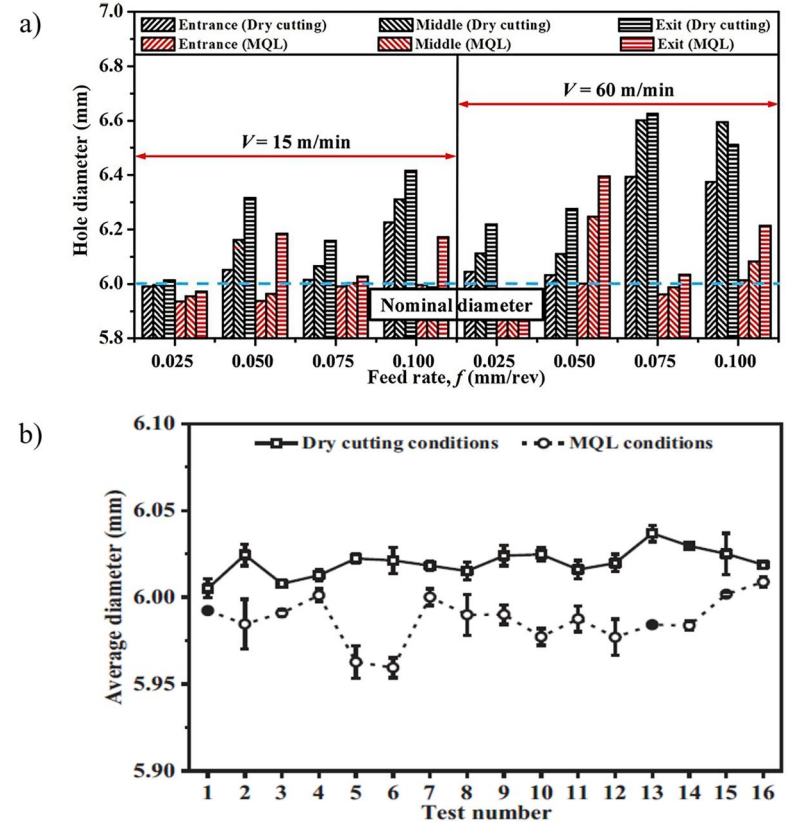


Figure 22. Comparison of hole diameters for the (a) CFRP phase and (b) titanium phase between the dry and MQL conditions (Xu, Ji, et al., 2019).

less than the nominal diameter in the titanium phase, as shown in Figure 22 (Xu, Ji, et al., 2019). This occurrence results from the cooling shrinkage of the hole's diameter following the drilling procedure (Xu et al., 2020). The multilayer composite/metal stacks should be drilled at the lowest cutting speed and feed rate to obtain the most consistent titanium hole diameters (Xu, Ji, et al., 2019).

When considering cylindricity on a titanium panel, the MQL has a negative impact, causing an error increase of 28.03% for the drill with the TiAlN coating and of 106.54% for the drill coated with diamond. But in CFRP panel, it decreased the average cylindricity errors by 16.11% and 15.08%, respectively, for TiAlN and diamond-coated tools (Xu et al., 2020). When considering burr height, the occurrence is reduced because titanium chips become firm and crisp, making it simpler to break off and remove from the hole walls since the titanium panel's cutting temperature is greatly reduced under the MQL condition due to the lubricating and cooling phenomena (Xu et al., 2020).

Cryogenic cooling

MQL and cryogenic cooling are eco-friendly methods to lower the cutting temperature among the several other methods (Yildiz and Nalbant, 2008). Due to their cleaner, safer and more environmentally friendly qualities, cryogenic coolants have drawn the most interest from researchers since MQL, when used at high cutting speeds, negatively affects the precision of machined parts (Bhowmick and Alpas, 2008). An experimental setup of cryogenic cooling is shown in Figure 23. Usually, liquid gases like liquid nitrogen (LN₂) and liquid carbon dioxide (LCO₂) are used as coolants in cryogenic cooling. These fluids reduce cutting temperatures and reduce workplace pollution because the gases after use get mixed into the atmosphere (Rodríguez et al., 2021). The methods of heat extraction, however, are highly dissimilar for these two gases. LN₂ is sprayed over the cutting zone at -196 °C, and when the liquid phase evaporates, it draws heat away

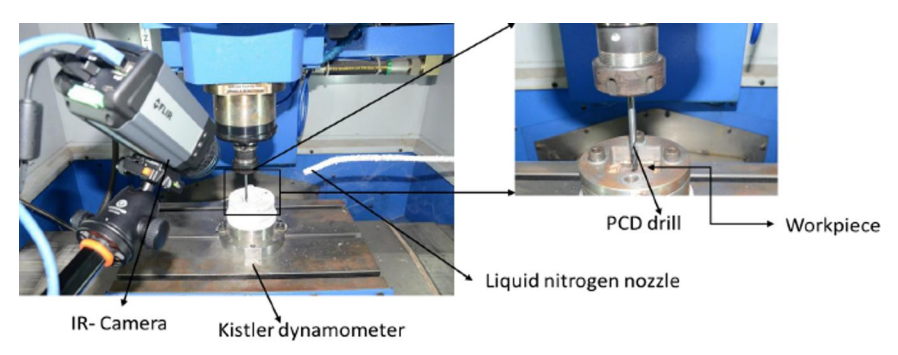


Figure 23. Experimental setup for cryogenic drilling (Kumar, 2018).

from the cutting zone. LCO₂ is kept at ambient temperature and 57 bar of pressure, and after a quick expansion caused by the Joule-Thomson effect, the temperature is reduced (down to -78.5 °C) when the liquid is ejected to ambient pressure. Dry ice and gaseous CO₂ coexist in a two-phase flow as a result, and the solid phase sublimates to lower the temperature (Liu et al., 2021). Additionally, the increased injection pressure results in a cushioning effect at the tool-material interface, reducing friction (Klocke et al., 2011). Further, they strengthen the hole quality and lengthen the tool life (Pu et al., 2009; Pusavec et al., 2010). For drilling and other types of machining, cryogenic coolant is chosen over normal coolant because of its various advantages, such as higher productivity, increased chip breaking, better surface finish, lower cost and worker health (Yildiz and Nalbant, 2008; Kumar, 2018). A number of research projects concentrated on drilling single materials like CFRP (Xia et al., 2016), titanium (Jerold and Kumar, 2013; Ahmed and Kumar, 2016) and CFRP/Ti stack-up panels (Kim et al., 2015) examining the success with regard to force, torque, tool wear, chip morphology and hole quality.

According to tests on CFRP/Ti drilling, forces and torque obtained during cryogenic drilling are greater than those obtained in dry conditions because the stiffness of CFRP and hardness of Ti increase due to their tensile strength and young's modulus as the temperature decreases (Basmaci et al., 2017; Kumar, 2018). Increased thrust force and torque are a problem that raises the likelihood of delamination (Xia et al., 2016), which results from CFRP hardening as a result of the extremely low LN2 temperature (Khanna et al., 2019). Impero et al. (2018), however, stated that this cooling method in CFRP/Ti6Al4V stacks meant a loss in torque and thrust force. The functionality of Ti6Al4V/CFRP/Ti6Al4V stacks in dry and LN₂ drilling conditions was also examined by Kumar et al. (2020), and they found that the torque was 7-25% lower (Kumar, 2018) and thrust force was 33-54% higher under the LN₂ condition compared to the dry state. This reduction in torque should be due to the lubrication action of the LN₂ film formed in the tool-work interface. They further mentioned that the CFRP hole surface was smoother and there were fewer fiber pull-outs, fiber matrix debonding (Kumar, 2018) and protruding fibers (Isbilir and Ghassemieh, 2013). When drilling CFRP/Ti6Al4V with DLC-coated solid carbide tools, it was found that LN₂ cryogenic cooling outperformed wet cooling for CFRP drilling, reducing the average thrust force by 17% in the CFRP panel. Similarly, thrust force during titanium drilling was also lower under cryogenic conditions compared to wet cooling (Umberto, 2019). When drilling CFRP/Ti stacks with a cemented WC drill under LN₂ cryogenic conditions, the forces on the CFRP are significantly higher compared to dry and MQL conditions. This increase is due to the low machining temperatures causing

matrix hardening in the CFRP, which results in higher cutting forces (Jiaying et al., 2022). According to Prisco, LN₂ cryogenic cooling has opposing effects on the two main factors influencing cutting forces (Umberto, 2019). On one hand, the reduced workpiece temperature increases its shear strength, leading to higher cutting forces. On the other hand, cryogenic cooling reduces adhesion between the tool rake and the chip due to chip hardening at lower temperatures, which lowers friction (Pradeep Kumar and Shakeel Ahmed, 2017). Additionally, the reduced temperature enhances chip breakability, which is crucial for evacuating chips from confined spaces, such as during drilling. In deep hole drilling, the benefits of reduced friction and improved chip breakability outweigh the increased shear strength. Additionally, compared to those under dry conditions, entry delamination, hole diameter error, surface roughness and entrance and exit burr heights were all reduced (Kumar, 2018; Kumar et al., 2020), but exit delamination was a little larger (Kumar, 2018). The use of cryogenic cooling results in a drop in temperature at the site of chip creation, which lowers plastic deformation as seen by the Ti panel's ductility and elongation and thereby lowers the burr height (Biermann and Hartmann, 2012). The rationale for the enhanced hole surface is that lowering the cutting zone temperature reduces thermal damages like debonding and smearing on the hole surface and changes the material's characteristics from ductile to brittle (Kumar, 2018).

Rodriguez investigated the drilling performance in CFRP/Ti6Al4V stacks using LCO₂ as the cutting fluid as shown in Figure 24 (Rodríguez et al., 2021). The findings demonstrated that tool tip temperature is greatly reduced, hole diameter values deviate less than 0.5% from nominal values, and CFRP layer surface integrity is preserved when CO₂ cryogenic cooling is used during drilling. Delamination is minimized because the composite

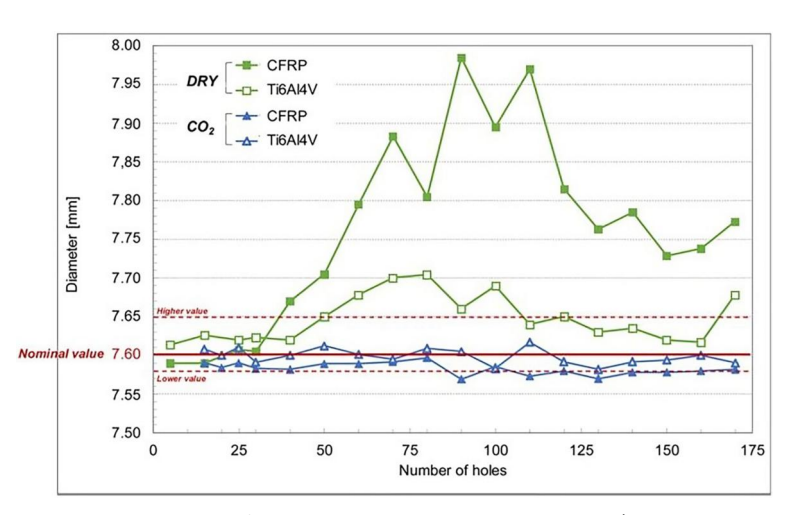


Figure 24. Diameters obtained after drilling CFRP-Ti6Al4V stacks (Rodríguez et al., 2021).

matrix stiffens at low temperatures, reducing the likelihood of cracking (Rodríguez et al., 2021). This also prevents burned areas during CO2 cryogenic drilling, unlike dry drilling, where burned areas are common. This phenomenon is attributed to the cutting temperature, which remains below 0 °C under CO₂ cryogenic conditions but can exceed 300 °C in dry conditions (Rodríguez et al., 2021). Although delamination factors increase almost linearly with the number of holes drilled using a WC tool across all conditions, they are lower under cryogenic conditions compared to dry and MQL conditions (Jiaying et al., 2022). Further, using LCO₂ results in a 50% increase in spindle power consumption in the first hole; however, it reduces edge damage to the drilling tools, thereby extending their lifespan. This effect is attributed to the material's decreased ductility and increased fragility at lower temperatures, which reduces the dislocation mobility of the material grains. As a result, torque increases, leading to higher spindle power consumption (Rodríguez et al., 2021).

The surface quality of machined holes improved with the use of cryogenic coolant, particularly when drilling at higher spindle speeds with a PCD-tipped bit on CFRP/Ti stacks. This improvement is due to the reduction in cutting zone temperature, which prevents thermal damage to the hole surface and alters material properties from ductile to brittle (Kumar, 2018). In contrast, maximum feed marks or smearing were observed during dry drilling with a PCD-tipped bit on CFRP/Ti stacks due to the elevated cutting zone temperatures (Kumar, 2018). However, under MQL and cryogenic conditions, the hole surfaces appeared smoother, likely due to the polishing effect of adhering CFRP powders or the lower temperatures achieved under cryogenic conditions (Jiaying et al., 2022). Furthermore, burr height was not influenced by cutting parameters but was instead dependent on cooling conditions. Drilling with DLC-coated solid carbide tools under LN₂ cryogenic cooling resulted in a higher burr height compared to wet conditions (Umberto, 2019). However, when LN₂ was used as a coolant with a PCD-tipped bit, exit burr height was reduced due to the lower temperature at the chip formation area, which minimized plastic deformation. Burr formation is largely influenced by the material's plastic deformation, as determined by its ductility and elongation properties (Kumar, 2018). Additionally, when drilling with DLC-coated solid carbide tools, the average hole diameter for both CFRP and titanium is largely unaffected by drilling parameters but is influenced by the cooling method (Umberto, 2019). Drilling under LN2 cryogenic cooling produces smaller hole diameters compared to wet cooling. This undersizing effect is attributed to the spring-back phenomenon (Kim et al., 2015). Table 3 shows the comparison between MQL and cryogenic cooling on various outputs related to CFRP/Ti drilling.

Table 3. Comparison between cryogenic cooling and MQL cooling.

Aspect	Cryogenic cooling	MQL Cooling			
Nature	Uses extremely low temperatures (e.g., liquid nitrogen) to cool the cutting tool and workpiece.	Utilizes a minimal amount of lubricant delivered in aerosol form to the cutting area.			
Cooling efficiency	Excellent cooling capacity due to extremely low temperatures, minimizing heat in high-speed drilling.	Moderate cooling effect; suitable for medium-speed operations and light machining.			
Tool wear reduction	Significantly reduces tool wear due to better control of cutting temperatures.	Reduces tool wear but not as effective as cryogenic cooling in high-friction applications.			
Surface quality	Achieves smoother surface finish due to reduced thermal damage and chip adhesion.	Provides good surface quality but may leave slight residue or require post-cleaning.			
Chip evacuation	Helps prevent chips from adhering to the tool due to cold temperatures.	Effective chip evacuation due to lubricant flow but may clog under heavy chip loads.			
Environmental impact	Environmentally friendly if using liquid nitrogen; no toxic waste or disposal issues.	Environmentally friendly due to minimal lubricant usage, but some oil mist may be present.			
Operational Cost	High due to the cost of cryogenic equipment and liquid nitrogen supply.	Low to moderate, depending on lubricant costs and MQL system setup.			
System Complexity	Requires specialized equipment for liquid nitrogen storage and delivery.	Simple system with easy installation and operation.			
Suitability for CFRP/Ti	Highly effective for CFRP/Ti drilling due to better control of heat at the composite-metal interface.	Effective but may struggle with higher temperatures generated during CFRP/Ti drilling.			
Defect Mitigation	Reduces delamination, burr formation and surface roughness due to better temperature control.	Can help reduce delamination and burrs but not as effective as cryogenic cooling.			
Application Versatility	Limited primarily to high- performance machining and aerospace applications.	Versatile for a wide range of machining operations, from general machining to aerospace.			

Minimum quantity lubrication (MQL) and cryogenic cooling are ecofriendly machining methods that reduce cutting temperatures and improve drilling performance in CFRP/Ti6Al4V stacks. MQL uses oil atomization to provide localized lubrication, reducing tool wear and enhancing surface morphology, though it can increase thrust forces and delamination due to chip adhesion and reduced matrix softening. Cryogenic cooling, using liquid nitrogen (LN₂) or liquid carbon dioxide (LCO₂), cools the cutting zone efficiently, improving hole quality and reducing burr height, delamination and thermal damage, though it can increase thrust forces and torque due to material hardening at low temperatures. Cryogenic cooling also minimizes hole diameter error and tool wear, enhancing machining quality and tool life, making it a promising alternative for drilling composite/metal stacks.

Application of coating technology

Using a variety of coating materials is another potential method to improve the interface zone's heat flow conditions, drilled hole quality and tool wear conditions (Jebaratnam, 2025). But the use of coated tools in CFRP/Ti machining is uncommon despite the limited study that has been done to examine the impacts of coating due to the low resistance of coating materials to the harsh brushing effects of CFRP (Hartung et al., 1982; Berger et al., 1998; Klocke and Krieg, 1999). ASTM B348 Grade 5 standard Ti6Al4V titanium alloy (ASTM B348-83) has poorer abrasion resistance compared to soft 300 series stainless steel. Anodizing titanium alloys in sliding systems followed by treatment with a dry film lubricant coating of molybdenum disulfide (MoS₂) and/or polytetrafluoroethane (PTFE) can notably reduce wear (Budinski, 1991). Contrarily, titanium alloy's tendency for adhesion results in chip accumulation at the cutting edges, and the application of wear-resistant coatings propels this effect (Hartung et al., 1982; Berger et al., 1998; Klocke and Krieg, 1999). Therefore, it is believed that the impact of tool coating during CFRP/Ti panel drilling is minimal compared to cutting parameters and environment (Shyha et al., 2010). However, those who experimented with coated tool drilling discovered that, in drilling CFRP/Ti stacks, the coatings stopped edge chipping before they wore off since edge-rounding and edge chipping are the main causes of tool failure in uncoated WC tools during CFRP/Ti stack drilling (Wang et al., 2014).

Studies on CFRP, Ti6Al4V and CFRP/Ti6Al4V stack were carried out by Isbilir and Ghassemieh using an AlTiN-coated WC drill bit (Isbilir and Ghassemieh, 2013). The authors made the conclusion that various stack sequences and cutting parameters had an impact on the torque, thrust force, burr development and drilling temperature. They stated that between the first and fifteenth holes, the thrust force increased by 56.6% and 37.8% in CFRP and Ti6Al4V, respectively. When drilling a CFRP/Ti6Al4V stack with nano-crystalline AlTiN grains embedded in amorphous silicon nitride (Si₃N₄) coated drill (C7), Ghassemieh reported that the thrust force increased by 12.5% and 37.5% in Ti6Al4V and CFRP, respectively, and the torque increased by 18% and 25% in Ti6Al4V and CFRP, respectively, between the first and fourteenth holes. In both situations, the rise in CFRP is continuous and linear, whereas the rise in Ti varied (Ghassemieh, 2012). Additionally, it was discovered that delamination increased by 85% and grew exponentially between the first and 24th holes. Moreover, throughout the process of drilling 15 holes, the surface roughness in both panels was far lower than the acceptable industry limit. In CFRP, the hole surface roughness was less than 2.3 μm, while in Ti6Al4V, it was less than 0.4 μm (Ghassemieh, 2012).

Tashiro et al. (2011) experimented with drilling a stack made of CFRP and Ti6Al4V with TiAlN and TiAlCr/TiSi-coated drills. The coating strength of TiAlCr/TiSi (50 GPa) is 30% greater than that of TiAlN (35 GPa) and the life of the drill with the TiAlCr/TiSi coating was longer

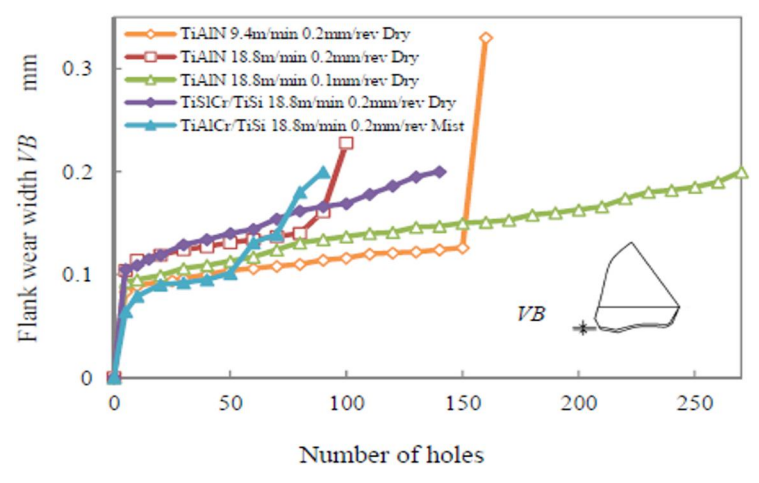


Figure 25. Flank wear width with different coating (Tashiro et al., 2011).

than the drill with the TiAlN coating. Additionally, water-mist cooling does not extend drill life because, with a TiAlCr/TiSi-coated tool, only 90 holes could be drilled in water-mist cooling while 140 holes could be drilled in a dry process with just 0.2 mm of flank wear as shown in Figure 25 (Tashiro et al., 2011). They added that, in both CFRP and Ti panels, a TiAlCr/TiSi coated tool produced less thrust force with water mist cooling than with dry cooling. Both TiAlN and TiAlCr/TiSi-coated drills exhibit nearly identical and stable torque values over the course of the trial involving 250 holes in CFRP. When using a tool coated in TiAlN, the torque in Ti panels increases gradually; however, when using a tool coated in TiAlCr/TiSi, the torque increases quickly in both wet and dry conditions. In addition, the hole diameter made by both drills in the CFRP panel is bigger than the hole diameter made in the Ti panel. In Ti panels, the drill coated with TiAlCr/TiSi generated greater diameters than the tool coated with TiAlN, and the difference between the two was minimal (Tashiro et al., 2011). However, in the case of CFRP, the hole diameter formed by the TiAlNcoated drill is greater than the diameter produced by the TiAlCr/TiSicoated drill. Furthermore, when the number of holes increases, the TiAlCr/ TiSi coated drill exhibits minimal variation, whereas the TiAlN-coated tool had a variation of 0.5 mm from the nominal diameter at the 100th hole (Tashiro et al., 2011). Kuo et al. (2014) also mentioned that, after drilling roughly 70 holes, Ti/CFRP/Al exhibits a 0.04 mm diameter tolerance using DLC and diamond-coated drill bits.

According to Xu et al., the surface roughness values generated by the drill with the physical vapor deposited (PVD) TiAlN coating are discovered to be only marginally less than those produced by the drill without coating, though the TiAlN coating's outstanding mechanical and physical qualities mitigate the high friction of tool-chip interaction during the drilling

operation (Xu and El Mansori, 2016). They also mentioned that the TiAlN coating's outstanding wear resistance and keeping sharp cutting edges for drilling either CFRP or Ti phase holes are the reason why the TiAlN-coated drill is observed to provide better hole diameter tolerance than that with an uncoated drill (Xu and El Mansori, 2016). However, uncoated drill bits with small chisel lengths, small point angles and small helix angles outperformed TiAlN-coated drill bits with large chisel lengths, large points and large helix angles when it came to the formation of Ti exit burrs and CFRP delamination. This finding suggests that tool geometry has a higher impact on CFRP/Ti drilling than tool coating. This may be because a tiny chisel length with a small point and helix angle encourages lower thrust force as the torque is largely impacted by the drill point angle and helix angle, and the chisel edge is believed to contribute 50% to 60% of the overall thrust force creation (Xu and El Mansori, 2016). In another research, the uncoated carbide drill outperformed the AlTiN and nanocomposite and C7 (nanocrystalline AlTiN grains surrounded by Si₃N₄ matrix) coated drills when drilling CFRP/Ti stacks (Wang et al., 2014). When drilling began, the value of the force produced by the uncoated tool was less than that of the coated tool. This might be because coated tools have somewhat larger radiuses than uncoated tools due to coating application (Wang et al., 2014). Throughout the drilling of 80 holes, the torque in the CFRP panel did not change significantly, but it increased for all three tool types in the Ti panel, going from a 400-500 Ncm interval to a 650-800 Ncm interval (Wang et al., 2014). Instead, the C7- coated drill and AlTiN-coated drill had 21.4% and 26.6% greater flank wear than the uncoated tool at the 120th hole. Edge rounding wear is measured by local wear quantity (LWQ), which was shown to be minimal with uncoated tools and maximal with tools coated in TiAlN (Wang et al., 2014).

Kuo et al. mentioned that when drilling a stack panel with a TiAlNcoated carbide drill with a 140° point angle, the quality of the stack's surface was examined. The findings demonstrated that Ti6Al4V layers had adherent material because of compressive tool stresses while CFRP layers had surface voids as a result of fiber/matrix losses (Kuo et al., 2014). Brinksmeier et al. conducted an experiment on the machining of multilayer materials made of CFRP, titanium and aluminum (Brinksmeier and Janssen, 2002). The primary issues with multi-material drilling were identified as CFRP delamination, metal burr formation, heavy tool wear and variations in measured diameters between each material.

Different cutting sequences were tried by Xu et al., such CFRP→Ti6A4V stacks and Ti6Al4V→CFRP stacks (Xu, El Mansori, Voisin, et al., 2019). Additionally, they experimented with various varieties of polycrystalline diamond (PCD) drills as well as coated and uncoated sintered carbide drills. The findings demonstrated that the tool tip acquired a higher starting temperature in the case of the Ti6Al4V→CFRP stack and that the drilling thrust force was lower. A drill with diamond coating produced less heat than one without (Xu, El Mansori, Voisin, et al., 2019). Xu et al. also tested with TiAlN-coated drill on both sequences. They found that the Ti -> CFRP machining generated a little bit less thrust force and torque magnitudes than those generated in the CFRP \rightarrow Ti cutting sequence (Xu and El Mansori, 2016). In both the sequences the thrust force is amplified with the feed rate. The surface roughness on CFRP with a CFRP → Ti sequence is larger than that of a Ti → CFRP sequence, while on Ti, a Ti \rightarrow CFRP sequence produced comparatively poorer results than a CFRP → Ti sequence (Xu and El Mansori, 2016).

When drilling a Ti/CFRP/Al stack, Kuo et al. noted that TiAlN/TiNcoated tools generated 90-148 holes before they reached the tool life criteria of 0.30 mm flank wear, whereas 180 holes were produced by the uncoated drills with a flank wear of not more than 0.23 mm (Kuo et al., 2018). Since tool coating was discovered to be the primary reason influencing the hole diameter with PCR of 64.5% and 57.5% in Ti and CFRP, respectively, the TiAlN/TiN-coated drills, irrespective of their lower tool life, often produced improved hole diameter accuracy as a result of less wear at the peripheral corners of the drill. The uncoated drill produces entrance and exit burrs that are higher than those produced by drills coated with TiAlN/TiN, suggesting that coating reduces friction at the toolworkpiece interface and thereby reduces temperature, which in turn resulted in reduced burr height. Regardless of the lower flank wear level, holes drilled with the uncoated tool showed worse cylindricity throughout the whole stack. This may have happened because the tool's margin and periphery had seen more wear, which reduced its ability to effectively withstand imbalanced forces and prevent tool deflection during drilling. However, there was no discernible difference between coated and uncoated tools' hole surface roughness (Kuo et al., 2018).

With uncoated, chemical vapor deposited (CVD) diamond-coated, and C7-coated tungsten carbide tools, Shyha et al. performed drilling tests on a Ti/CFRP/Al panel. The drilling trials were begun with the titanium component, moved through the CFRP and ended with the aluminum at the base of the stack (Shyha et al., 2010). Because the Al and CFRP surfaces of the stack sustained significant damage due to the sharp Ti swarf sliding up the hole during chip removal (Brinksmeier and Janssen, 2002), the reverse direction to typical (Al/CFRP/Ti) practice was chosen. Uncoated tools provided the longest tool lives when cutting parameters were low, but as cutting parameters increased, CVD diamond-coated tools outperformed C7-coated tools. When using a CVD diamond-coated tool on CFRP and Ti

panels, the thrust force is greater than when using an uncoated tool; however, when utilizing wet cutting on Al panels, the thrust force is the opposite. Additionally, the uncoated drill failed at its first hole due to high feed and speed. Under spray mist cooling, the C7-coated tool produces less thrust force than the uncoated tool in all three panels (Shyha et al., 2010). Table 4 shows the quantitative comparison of the effects of different drill bit coatings on tool damage.

Therefore, it can be decided that the use of coated tools in CFRP/Ti drilling remains limited due to the harsh abrasive nature of CFRP and the adhesion tendency of titanium, which often accelerates coating wear. However, research highlights the potential benefits of coatings in reducing edge chipping and wear. Studies using coatings like AlTiN, TiAlN, TiAlCr/ TiSi and diamond coatings reveal varying impacts on thrust force, torque, surface roughness and tool life. Coated drills often enhance hole diameter accuracy and reduce burr formation, but tool geometry and cutting parameters have a greater influence on performance. TiAlCr/TiSi coatings demonstrate superior durability compared to TiAlN, producing less thrust force under water-mist cooling, while uncoated tools sometimes outperform coated ones in specific scenarios, such as with low cutting parameters. The sequence of drilling (e.g., CFRP → Ti or Ti → CFRP) also affects thrust force, torque and surface quality, with Ti → CFRP generally yielding lower thrust force but poorer titanium surface results. Although coated tools can improve wear resistance and maintain sharper cutting edges, uncoated tools often exhibit longer tool life and better resistance to edge rounding under certain conditions, emphasizing the complex interplay between coating, geometry, and cutting environment.

Developing advanced process

There are creative ideas and methods for drilling good holes in fiber metal stack materials like advanced cutting tools and coatings (Geier et al., 2019), optimized process parameters (Geier and Szalay, 2017; Balázs and Takács, 2020), application of support plates (Dogrusadik and Kentli, 2017), advanced technologies like helical milling, circular milling, wobble or tilted helical milling (Haiyan and Xuda, 2016; Durante et al., 2019; Pereszlai and Pereszlai et al., 2021), vibration assisted drilling (Hussein Geier, 2020; et al., 2018; Xu, Ji, et al., 2019; Xu, Zhou, et al., 2019), ultrasonic vibrationassisted drilling (Li et al., 2019) and peck drilling (Fernandez-Vidal et al., 2018) which are discussed by various researchers; however, their temporal and case horizons are frequently too narrow. So conventional drilling is still highly preferred (Sorrentino et al., 2018).

Table 4. Quantitative comparison of the effect of coatings on tool damage.

Reference	(Shyha et al., 2011)				(Wang et al., 2014)			(Xu et al., 2020)				(Xu et al., 2020)
Tool wear on last hole	Vb = 0.3 mm (310 holes)	Vb = 0.3 mm (197 holes)	Vb = 0.3 mm (268 holes)	Vb = 0.3 mm (92 holes)	$Vb = 104 \mu m (120 holes) LWQ 1.450 \mu m2$	Vb = 135 µm (120 holes) LWQ 1.650 µm ²	Vb = 145 μm (120 holes) LWQ 1.500 μm ²		I	I	I	ı
Thrust on last hole	1	ı	I	I	Ti = 1320 N; CFRP = 470N	Ti = 1,260 N; CFRP = 530 N	Ti = 1,400 N; CFRP = 510 N	CFRP = 140 N; Ti = 550 N	CFRP = 130 N; Ti = 500 N	CFRP = 125 N; Ti = 550 N	CFRP = 285 N; Ti = 1,200 N	ı
Thrust on first hole	1	ı	I	I	Ti = 410 N; CFRP =120N	Ti = 430 N; CFRP = 200 N	Ti = 420 N; CFRP = 120 N	CFRP = 65 N; $Ti = 180 N$	CFRP =70 N; $Ti = 300 \text{ N}$	CFRP = 45 N; $Ti = 250 N$	CFRP = 87 N; Ti = 550 N	
Torque on first hole	1	ı	I	I	Ti = 310 Nm; CFRP = 50Nm	Ti = 360Nm; CFRP = 45Nm	Ti = 450 Nm; CFRP $= 60 Nm$	I	I	I	ı	1
Torque on first hole	1	I	ı	I	Ti = 310 Nm; CFRP = 50Nm	Ti = 360 Nm; CFRP $= 45 Nm$	Ti = 450 Nm; CFRP $= 60 Nm$	I	I	I	I	I
Parameters	20/40 m/min; 0.05 rev/min	20/40 m/min; 0.05 rev/min	20/40 m/min; 0.1 rev/min	20/40 m/min; 0.15 rev/min	6,000 rpm and 0.0762 mm/rev feed rate were used in	CFRP panel. 500 rpm and 0.0508 mm/rev feed	rate were used in Ti. Coolant with a flow rate of 16 mL/min.	Speeds (Vc) – 15, 30, 45 and 60 m/min; Feed (f) of 0.025.	0.050, 0.075 and 0.100 mm/rev.	micro-cutting oil with a flow rate of		
Tool	Uncoated, 6.35 mm diameter (Wet) (Hole 1 and 310)	CVD diamond coated, 6.35 mm diameter (Wet) (Hole 1 and 156)	C7 coated, 6.35 mm diameter (Wet) (Hole 1 and 268)	Uncoated, 6.35 mm diameter (Spray mist) (Hole 1 and 64)	Uncoated	AlTiN coated	nc-AlTiN surrounded by Si ₃ N ₄ matrix coated	TiAlN coated; 6mm diameter (1–16 holes)	TiAIN coated (MQL); 6 mm diameter (1–16 holes)	Diamond coated; 6 mm diameter (1–16 holes)	Diamond coated (MQL); 6 mm diameter (1–16 holes)	(50)
Work piece	Ti6Al4V /CFRP/Al 7050	T7451; Each panel is 10 mm thick.			Ti6Al4V/CFRP; Ti 6.73mm, CFRP	7.54mm.		CFRP/Ti6Al4V; Thickness CFRP =	6.6mm and Ti6Al4V =	6.28 mm		

τ	ż
d	Ū
=	3
2	Ξ
Ψ	5
2	_
٠,	5
L	J
_	٠
`	ı
0	υ
3	2
40	0

Work piece	Tool	Parameters	Torque on first hole	Torque on first hole	Thrust on first hole	Thrust on last hole	Tool wear on last hole	Reference
CFRP/Ti6Al4V Thickness of CFRP =	Uncoated (CFRP to Ti); 6.35 mm (1– 16 holes)	Speed – 20, 35, 50, 65 m/min; Feed – 0.015, 0.03, 0.045, 0.06 mm/			CFRP = 76–132 N; Ti = 280–630 N			
9.16 mm and	Uncoated (Ti to CFRP); 6.35 mm	rev; Sequence CFRP $ ightarrow$	I	I	CFRP = $68-110 \text{ N}$; Ti = $255-440 \text{ N}$	I	I	
Ti6Al4V = 6.8mm	(1–16 holes)	Ti, Ti → CFRP	Diamond coated (CFRP to Ti); 6.35 mm (1–16 holes)	1	1	CFRP = 58-120 N; Ti = 240-500 N	1	
Diamond coated (Ti to CFRP); 6.35 mm (1-16		ı	1 1	CFRP = 49–104 N; Ti = 250–380 N	ı	ı		
noles) CFRP/Ti6Al4V	TiAlN coated (1–50	Speed – 1,000, rev/min, Feed 50 mm/min	I	I	CFRP = $63-90 \text{ N; Ti}$ = $240-380 \text{ N}$	I	$Vb=1063~\mu\text{m}$	(Cao et al., 2023)
CFRP/Ti6Al4V	TiAlN coated; 6mm	Cutting speed (Vc) – 15,	CFRP = 0.6 1.4Nm;	CFRP = 0.6 1.4Nm;		1	ı	(Xu et al., 2020)
$\begin{array}{ll} {\sf Thickness} \\ {\sf of \ CFRP} = \end{array}$	diameter (1–16 holes)	30, 45 and 60 m/ min; Feed rate (f) –						
6.60mm	TiAIN coated (MQL);	0.025, 0.050, 0.075	Ti = 1-3.5 Nm	Ti = 1-3.5 Nm	ı	ı	I	
and Ti6Al4V =	6 mm diameter (1–16 holes)	and 0.100 mm/rev; coolant flow rate of						
0.28mm	Diamona coated; 6mm diameter (1–16 holes)	13 mc/n	CFRF 0.3-1.5 NIII;	CFRF 0.3-1.5 NM;	I	I	I	
	Diamond coated (MQL); 6mm		Ti 0.5–2.2 Nm	Ti 0.5–2.2 Nm	ı	I	I	
CEDB/TICALAV	diameter (1–16 holes) TiAlCx/TiSi (Mi++).	10000	CEDB 05 12 Nm: Ti	CEDB 0.5 1.2 Nm: Ti	CEBB — 450.) (1000 – 550)	(140 holor)	(Tachico et al. 2011)
Thickness of CERP —	6mm diameter	speed = 10.0 III/IIIII, Feed=0.02 mm/rev	0.9–2.2 Nm	0.9–2.2 Nm	$T_1 = 450$, $T_1 = 1,500$	$T_1 = 1,820$	0.2 IIIII (140 II0les)	(1931110 et al., 2011)
3mm and Ti alloy = 9.5mm	TIAICr/TISI (Dry); 6 mm diameter (1–140 holes)		CFRP 0.4–1.2 Nm; Ti 0.8–3.9 Nm	CFRP 0.4–1.2 Nm; Ti 0.8–3.9 Nm	CFRP = 250; Ti = 1,300	CFRP = 500; Ti = 1,500	0.2mm (90 holes)	

	١
₹	1
ā	
-	
=	
2	_
Contin	
÷	
=	
_	è
U	ì
_	1
_	
_	
4	
a	
a	
a	
a	
a	

Reference		(Ghassemieh, 2012)	(Xu and El Mansori, 2016)			(continued)
Tool wear on last hole	0.23mm (100 holes)	1	1	1	1	
Thrust on last hole	CFRP = 530; Ti = 1,850	ı	1	1	1	
Thrust on first hole	CFRP = 430; Ti = 1,681	CFRP = 150–270; Ti = 700–850	CFRP = 80–200N; Ti = 220–650N	CFRP = 170–350N; Ti = 500–950N	CFRP = 140-320N; Ti = 500-920N	
Torque on first hole	CFRP = 0.2 Nm;	Ti = 2.26 Nm	CFRP = 0.01 Nm;	Ti = 2.24 Nm	CFRP = 0.2 Nm;	
Torque on first hole	CFRP = 0.2 Nm;	Ti = 2.26 Nm	CFRP = 0.01 Nm;	Ti = 2.24 Nm	CFRP = 0.2 Nm;	
Parameters		CFRP-4,500 rpm and 457.2 mm/min; Ti- 1,400 rpm and 119 mm/min	Cutting speed, vc (m/ min) 15, 30, 45, 60; Feed rate, f (mm/rev) 0.03, 0.06, 0.09, 0.12, 0.15; Cutting sequence CFRP — Ti.	Ti → CFRP		
Tool	TiAlN (Dry); 6mm diameter (1–100 holes)	d; 6mm er (1–24	6.35mm diameter uncoated tool, 0.11mm chisel edge, helix angle 20° and point angle 135°; CRP to Ti (1–20 holes)	6.35 mm diameter PVD TiAIN-coated twist drill, 0.22 mm-chisel edge, helix angle = 27.2° and point angle = 140°; CFRP to Ti sequence (1–20 holes)	6.35 diameter PVD TIAIN-coated twist drill with 0.22 mm-chisel edge, helix angle of 27.2° and point angle = 140°; Sequence Ti to CFRP (1–20 holes)	
Work piece		CFRP/Ti6Al4V	CFRP/Ti6A14; Each stack is 4 mm thick			

							Tool wear on last	
Work piece	Tool	Parameters	Torque on first hole	Torque on first hole Torque on first hole Thrust on first hole Thrust on last hole	Thrust on first hole	Thrust on last hole	hole	Reference
Ti-6Al4V/	Uncoated; 6.35mm	Uncoated; 6.35mm Feed rate 0.05–and	Ti = 2.25 Nm	Ti = 2.25 Nm	Ti = 1,800 N;	Ti = 1,620 N; CFRP 0.17 mm (180 holes) (Kuo et al., 2018)	0.17 mm (180 holes)	(Kuo et al., 2018)
CFRP/	diameter (1–180	0.08-mm rev at 90th			CFRP = 750 N;	= 680N; AI $=$		
AA7050		holes, 0.05 and hole			AI = 510 N	250 N		
Each layer								
10mm	TiAlN/TiN coated;		CFRP = 0.6-1.1Nm;	CFRP = 0.6-1.1Nm;	Ti = 2,050 N;	Ti = 1,860 N; CFRP	0.34 mm (160 holes)	
thick	6.35 diameter (1–		Ti = 2.4-3.9 Nm	Ti = 2.4-3.9 Nm	$CFRP = 810\;N;$	= 770N; AI $=$		
	160 holes, 0.05				AI = 530 N	280 N		
	and 0.08 mm/rev)							

Researchers investigated how drilling strategies, such as adaptive pecking, affected the cutting temperatures and chip morphology (Shyha et al., 2010). Researchers found that two-shot peck drilling produced a tool life of 75 holes, but drilling the CFRP/Ti stacks in single shot lasted only for 62 holes due to a higher rate of flank wear (Dahnel et al., 2020). Two-shot peck drilling produced fewer hole diameter errors in Ti panels than single-shot drilling, but the contrary was true for CFRP panels, where the two-shot peck drilling produced larger mistakes than single-shot drilling. These measured sizes are all more than the nominal diameter and up to 80 holes under the H7 industrial tolerance (Dahnel et al., 2020). Additionally, the entry delamination of two shots of peck drilling resulted in smaller CFRP entrance delamination for the first few holes (up to 20 holes), but as the number of holes increased, the delamination increased and became greater than that of single-shot drilling (Dahnel et al., 2020). Moreover, it was discovered that single-shot drilling of CFRP/Ti stacks produces a 30% higher burr height than two-shot peck drilling (Dahnel et al., 2020).

Since pre-drilling is the initial stage of the step drill and drilling is the final stage, modified step drills have improved surface quality, diameter tolerances and tool wear when drilling multilayer materials (Brinksmeier and Janssen, 2002). As a result, even though both the step drill and doublepoint angle tool demonstrated little thrust, good hole quality and minimal burr, the step drill performs drilling tasks better than the double-point angle drill (Wei et al., 2016). Many scholars became interested in the relation between tool wear, forces and torque (Park et al., 2011), trying to establish connections with the effect of process parameters on force and torque (Denkena et al., 2008). Step drilling with MQL on Al/CFRP/Ti stacks has been demonstrated by Brinksmeier and Janssen to provide improved chip removal, tool life, hole size and hole surface (Brinksmeier and Janssen, 2002).

According to Alonso et al., stepped geometries with more flutes result in reduced local wear quantity (LWQ) values and thrust forces (Unai et al., 2019). They added that the diameter of the holes rose linearly for the stepped tools in CFRP and Ti panels. However, because of the less pronounced wear progression, the increase for 40 holes in a three-fluted step drill (5 μm) is smaller than it is for a two-fluted step drill (10 μm). Another research group found that the diameter of the hole in CFRP is often smaller even when using conventional step drill bits and exceeds the acceptable accuracy (Tsao, 2008). In addition, the two fluted step drill's burr height values were higher than those found for the stepped drill with three flutes (Unai et al., 2019). Because the ultimate burr that forms during drilling with a step drill is the consequence of both drill bit steps, the nonstepped drill produced the least burr height. The tool point first creates a

main burr when it leaves the titanium plate. This procedure is comparable to that used in non-stepped tool drilling operations. Both the cut and uncut material and the primary burr that has already been developed are pushed out by the cutting edges when the tool step leaves the workpiece (Unai et al., 2019). Additionally, the three-fluted step drill caused the least delamination, while the non-step drill caused the greatest. According to Ko et al. and Li et al., machining with a step drill bit always results in the initial CFRP hole exit defects and those defects are expected to be prolonged when the rest of the drill bit contacts the drill-exit leftover material, causing additional defects to the final hole (Ko et al., 2003; Li et al., 2018). They further mentioned that, comparing the hole diameters of CFRP-Ti and CFRP-only stacks, it can be seen that the hole sizes for CFRP-only stacks are 5-7 μm lesser than the nominal tool diameter (Ko et al., 2003; Li et al., 2018). Re-sharpenable veined PCD drill was a new idea put up by Garrick for drilling holes of consistently high quality on CFRP/Ti stacks (Garrick, 2007).

Vibration-assisted drilling is another technique to promote high-quality drilling while machining CFRP/Ti6Al4V stacks. It can be classified as low frequency vibration assisted drilling (LFVAD), ultrasonic vibration-aided drilling (UVAD) and compound vibration-assisted drilling (CVAD). LFVAD and UVAD show considerable promise in decreasing cutting temperature and force, improving machining quality and extending tool life compared to conventional drilling (CD) (Yang, Chen, et al., 2020; Yang, Zhu, et al., 2020). In an experiment using CFRP/Ti6Al4V stacked material, the temperature of LFVAD was substantially lower than that of CD, according to Hussein et al. (2018). It was also noted by Pecat et al. that, in LFVAD, the measured temperatures are approximately 43% lower compared to CD when operating at the same cutting speed and feed rate with an equivalent material removal rate. It is due to the following reasons. The axial oscillations in vibration-assisted drilling create an interrupted cutting action, allowing the tool to cool during non-cutting intervals, with the actual contact time reduced by approximately 55% under the given parameters (Pecat and Brinksmeier, 2014). Additionally, the tool's lifting motion enables better lubrication of the borehole bottom, reducing frictional heat. Moreover, small metallic chips, which absorb most of the heat, are rapidly evacuated from the cutting zone, further contributing to temperature reduction. Hot metallic chips that damage CFRP's exit hole cause the majority of the heat in the cutting zone. In order to optimize small chip segment extraction, cutting temperatures must be lowered in order to prevent damage to titanium's burr and CFRP's borehole. Both the CFRP entrance and exit delamination faults were decreased as a result of an improvement in the chip removal mechanism and a decrease in the drilling

temperature (Li et al., 2022). When using LFVAD with the right operating parameters, the workpiece and tool will periodically come into contact and then separate, which can satisfy the geometric chip-breaking criterion. The discontinuous cutting mode of LFVAD may efficiently break and remove chips, decrease drilling temperature and decrease average thrust force and cutting time (Li et al., 2022).

Ultrasonic vibration aided drilling (UVAD) is the machining process where a workpiece or tool is subjected to a specific frequency of vibration. The experimental setup of UVAD is shown in Figure 26. Here, the properties of the rotation between the hole surface and tool produced by the ultrasonic vibration alter the tool-workpiece interaction (Wang et al., 2023). The amplitude in UVAD is minimal and frequently falls short of the requirements for chip breaking. However, because of the antifriction nature of ultrasonic vibration, the cutting edge's torque and cutting force are decreased and the conditions for heat dissipation are improved (Yan and Shao, 2011). The reason is because the cutting zone in UVAD can be opened at regular intervals, which will decrease heat production and encourage air to penetrate the workpiece-tool interface, lengthen cooling times and quicken heat dissipation (Wang et al., 2017). Additionally, due to ultrasonic vibration, which has the features of high-speed machining, UVAD has high instantaneous cutting speed and energy. This makes it easier to cut carbon fiber, which significantly lessens the delamination flaws in CFRP (Li et al., 2017) by accelerating the local fracture of carbon fibers in CFRP (Wang et al., 2018). In addition, Ti chips can be split into smaller

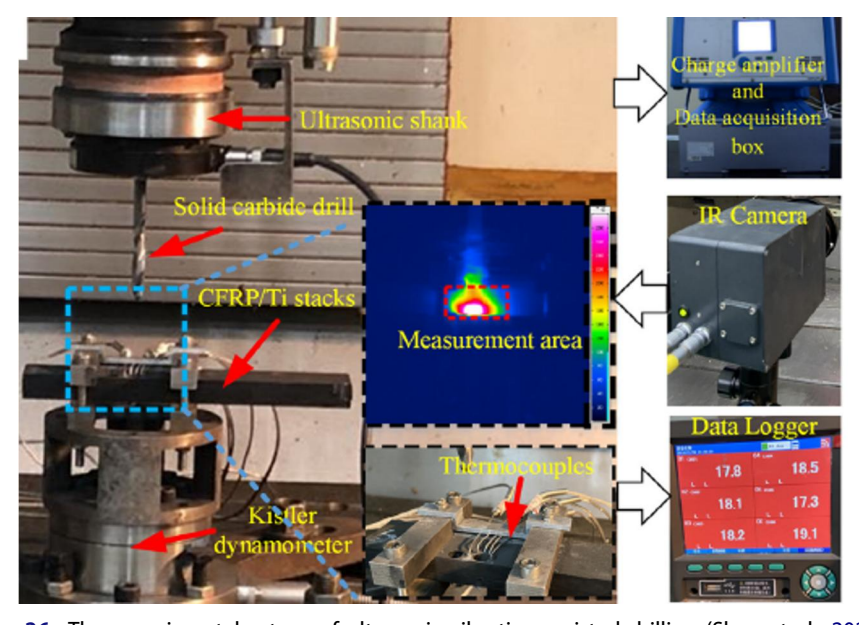


Figure 26. The experimental set up of ultrasonic vibration assisted drilling (Shao et al., 2021).

pieces than the traditional long ribbon Ti chips. Segmented chips are simple to remove, effectively resolving the issue of chip entanglement and reducing secondary damages to the wall of drilled CFRP holes (Xu and El Mansori, 2016). For the single-shot drilling of CFRP/Ti stacks with cutting fluid, Dahnel et al. employed the UVAD technique and examined the mechanisms of tool wear (Dahnel et al., 2015). Results showed that, in contrast to CD, tool wear in UVAD, such as titanium adhesion, abrasive wear and major edges chipping, may be efficiently reduced. Additionally, Dahnel et al. (2016) discovered that the intermittent cutting mode of UVAD, which was essential in weakening titanium adherence, resulted in lower thrust force and tool wear for UVAD at various cutting speeds than for CD. Onawumi et al. found that, at the lowest feed rate of 0.03 mm/rev, UVAD reduced thrust force by approximately 49% compared to CD. This reduction is attributed to the high forces typically required for the plastic deformation of the titanium alloy during material removal in CD. In contrast, UVAD's intermittent cutting action facilitated material removal through micro-chipping, leading to localized damage and deformation, thereby lowering the overall cutting forces (Onawumi et al., 2018). In order to drill CFRP/Ti stacks without cooling, Shao et al. used the UVAD method, which resulted in higher hole quality and productivity than CD (Shao et al., 2019). Additionally, Cong et al. discovered that the variable feed rate can produce better process effects during UVAD of CFRP/Ti stacks as compared to the constant feed rate (Cong et al., 2013). According to Onawumi et al., UVAD of stacks can provide better hole circularity and smaller burr height than CD while using less cutting force (Onawumi et al., 2018). They mentioned that, as the feed rate increased during UVAD, the hole diameter decreased. Further, UVAD demonstrated overall superior performance compared to CD, achieving a 50% reduction in burr formation. At lower cutting speeds, heat was generated more quickly, making the exit side of the titanium plate more ductile, which in turn reduced fracture and shear during drilling.

When compared to LFVAD, CVAD - which is also referred to as lowand high-frequency vibration-assisted drilling (LF/HF VAD) - can increase the chip-breaking zone to some degree and decrease the low-frequency amplitude of the critical chip- breaking condition, thereby reducing the impact of low-frequency vibration. The experimental setup of CVAD is shown in Figure 27. CVAD can expand the frequency and thickness range, which promotes the development of discontinuous, smaller chips (Li et al., 2022). The smaller chip has a greater surface area per unit volume in contact with the air, accelerating the chip's heat dissipation and allowing for a smoother discharge out of the hole to further lower drilling temperature. On the one hand, the matrix strength degradation brought on by high

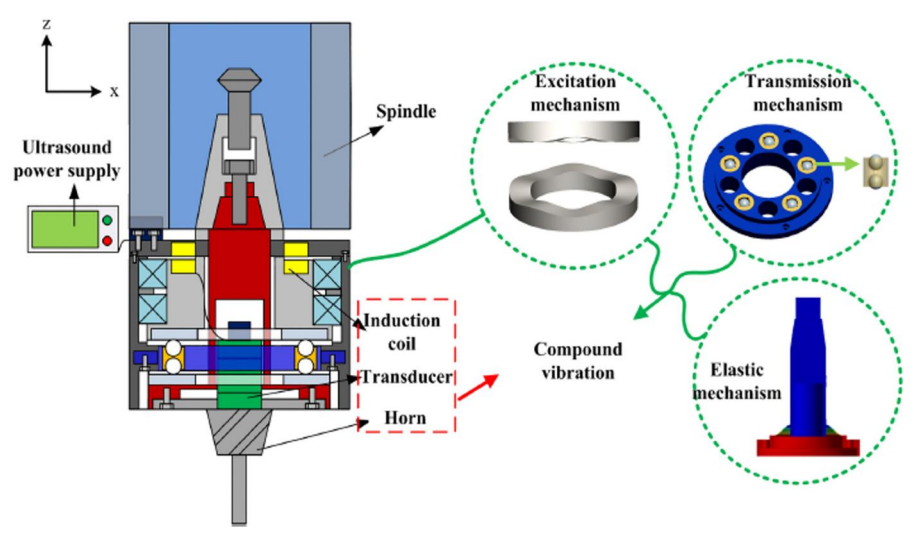


Figure 27. Working principal diagram of CVAD set up (Li et al., 2022).

temperature can be avoided by the dissipation of a significant portion of cutting heat (Li et al., 2022). On the other hand, effective chip evacuation can significantly lessen the chip's resistance against the hole wall. CVAD has a stronger potential relevance in preventing the thermal-mechanical damage produced by titanium alloy on CFRP while evacuation and delamination fault at the CFRP entrance. This occurs as a result of the CVAD, which converts drilling from continuous drilling to intermittent drilling, increasing the tool's duty cycle (Li et al., 2022). A temperature decrease of around 38% is attained, especially during the titanium alloy drilling with CVAD to shatter titanium alloy chips into smaller bits, which are then effectively expelled from the hole following the spiral groove. In addition to greatly reducing CFRP secondary damage in the titanium alloy machining phase, the rapid cutting speed impacted by longitudinal torsional ultrasonic vibration somewhat reduces entrance delamination during the CFRP drilling phase with CVAD (Li et al., 2022).

Helical milling (HM) is a hole-machining technique that makes use of milling tools with helical feed. By changing the diameter of the helical feed trajectory, this technique can be used for holes with various diameters (Pereira et al., 2017; Wang et al., 2020). Compared to traditional drilling, HM has a larger space for heat dissipation and chip removal (Jiaying et al., 2022). Because of the intermittent contact between the tool and the work-piece, the cutting temperature is lower in HM compared to CD, which enhances the quality of the CFRP hole surface (Sun et al., 2020). Wang et al. found that in CD and HM hole machining of CFRP/Ti stacks, HM resulted in better roundness in the CFRP panel, improved geometric precision for the titanium alloy panel holes and decreased roundness in the

transition area (Wang et al., 2021). Denkena et al. demonstrated that HM of CFRP/Ti stacks could improve the quality of the holes (Denkena et al., 2008). Due to the peripheral force distribution on CFRP/Ti stacks, HM outperforms conventional drilling in terms of reduced delamination and burr. Ge et al. investigated the HM of CFRP/Ti6Al4V stacks under cryogenic and MQL conditions, revealing that MQL lubrication can decrease friction between the tool and the hole surface (Jiaying et al., 2022).

For CFRP/Ti stacks to tightly verify the hole-making precision, two operations, including drilling and reaming, are necessary during industrial production. Though Ti6Al4V chips can readily leave a major scrape on the surface of a drilled CFRP hole when the machining sequence is CFRP \rightarrow Ti, in most circumstances the reaming procedure can still eliminate the created hole defects and enhance the uniformity of the hole quality of the stack structure. While using the Ti → CFRP drilling sequence can mitigate erosion damage caused by Ti6Al4V chips on the CFRP layer, it does not completely eliminate delamination damage during the reaming process (An et al., 2020). Thus, table 5 shows the advantages, disadvantages, and possible remedies for those disadvantages in single shot drilling of CFRP/Ti stack material.

Table 5. Advantages, disadvantages and possible solutions for disadvantages in single-shot drilling of CFRP/Ti stack material.

Advantages	Disadvantages	Remedies for disadvantages
Reduced Process Time & Cost: Since the drilling is done in a single pass, it minimizes the overall machining time and reduces drilling costs	Tool Wear & Shorter Tool Life: High-speed steel tools exhibit extreme wear, sometimes failing after a single hole due to the varying hardness of composite and metal layers	Optimized Tool Coating
Fewer Cutting Tools Required: Fewer tool changes are needed, which decreases tool inventory and maintenance costs	Hole Diameter Variability: Differences in the mechanical properties of composite and metal layers lead to substantial hole diameter differences across layers	Advanced Drill Geometry
Minimized Heat Generation & Chip Size: Single-shot drilling reduces the drill bit's temperature and produces smaller chips, which is crucial for maintaining hole quality, particularly in CFRP/Al stacks	Chip Adhesion Issues: Metal chip's may build up on the cutting edges, leading to Build-Up Layer (BUL) and Build-Up Edge (BUE), which accelerates tool wear	Optimization of Cutting Parameters
Improved Hole Tolerance: By optimizing drill geometry, hole tolerance of 25 µm can be achieved, preventing chip clogging and ensuring better hole quality	Surface Roughness Issues: The rubbing and abrasion of hot, sharp metal chips against the composite layer can degrade the hole surface quality	Use of Cooling and Lubrication
Better Alignment & Positioning: Reduces errors caused by repositioning the drill, ensuring improved alignment of holes in composite-metal stacks	Delamination & Burr Formation: The process may cause exit delamination in CFRP layers and burr formation in metal layers, which can impact the structural integrity and require additional deburring processes	Application of Vibration-Assisted Drilling



Concluding remarks

- Composite/metal stacking materials are being widely used as structural supports in aircraft sector designs. The simplest method of assembling parts during production operations to prevent positioning problems is single-shot drilling while stacking material sheets. In this review article, potential methods for high-quality drilling of CFRP/Ti stacks were reviewed. In a complex and dynamic production process, high-quality drilling is influenced by a variety of internal and external elements, including tool geometry, material, coating, cutting environment, drilling parameters, the characteristics of the workpiece and the drilling sequence. High interface temperature, high cutting force fluctuation, tool wear and chip erosion are issues that arise while drilling CFRP/Ti stacks. Suppression tactics are also discussed in this study in order to address these challenges.
- Owing to the dissimilar characters of the composite/metal system, drilling hybrid CFRP/Ti composite entails connected chip-separation modes and interrelated cutting behaviors. When comparing interface drilling to drilling the CFRP and Ti panels separately, interface drilling is often regarded as the most complex and challenging operation due to the interaction of multiple tools and the intense transfer of mechanical and physical reactions involved. Due to the differing material properties while cutting two distinct materials simultaneously, the tool-workpiece system is unstable, which worsens the production circumstances at the transition region of the laminated interface. The choice of machining parameters will be greatly impacted by the capacity to estimate the stability of the drilling system and forecast the cutting force during the drilling operation.
- Owing to the difference in production temperatures between Ti and CFRP, high temperatures that are challenging to regulate can quickly cause irreversible thermal damage in CFRP. Currently, the experimental approach is mostly employed to gauge the laminated interface's temperature. Due to the various heat production, dispersion and transmission mechanisms of various materials, additional research may be necessary to establish to accurately develop a model that can predict temperature at the interface and determine the impact of drilling parameters on the temperature.
- On CFRP/Ti stack drilling, tool wear mechanisms typically involve the connection and engagement of both metal-leading and composite leading wear modes. Even though different drill materials wear differently, from a global perspective, abrasive wear, flank wear, edge rounding wear and adhesion wear are often the primary wear patterns regulating the tool wear development. Additionally, during the cutting process of



- the stack interface, the temperature and stress distribution along the cutting edge are not even, which causes a variety of tool damage. Tool wear in turn leads to hole damage.
- Induced hole damage in CFRP/Ti drilling includes both polymeric flaws and metallic flaws. The interface damage is typically the most severe of them all. The primary sources of damage are thought to be poor bottom Ti plate stiffness, high interface temperature and erosion of Ti chips. To meet the requirements of the aerospace industry for the drilled holes, close tolerance must be attained in the areas of hole delamination, exit burr height, hole wall surface roughness and stack-up diameter deviation. Few researchers have studied hole circularity and hole cylindricity in CFRP/Ti stack- up drilling, which may create the impression that their importance is lower than it actually is. Therefore, in-depth study of these aspects is required.
- Variable parameter drilling can choose the best cutting parameters for various materials, enhance drilling performance and quality and decrease tool wear. For titanium panels, high feed rates and low cutting speeds are typically best, whereas CFRP panels benefit from low feed rates and high cutting speeds. Making the right processing parameter choices helps increase process stability, which benefits drilling accuracy and hole quality. Additionally, the creation of sophisticated variable parameter machining apparatus and systems is crucial for real-world engineering applications.
- A suitable machining environment may successfully decrease the cutting temperature, increase the tool's lifespan and enhance the drilling quality of CFRP/Ti stacks. The drilling of CFRP/Ti stacks has recently used more ecologically friendly cryogenic cooling and MQL technology. Two widely used coolants are liquid nitrogen and liquid carbon dioxide. Some significant benefits of cooling are fast cooling, quick chip evacuation, prevention of chip accumulation and improved chip breakage.
- Although various coatings have been created and tested, no studies have yet reported on the tribological characterization of these coatings for this application. To develop a superior coating, additional research on the bond strength, hardness and coefficient of friction of coated drill bits may be required.
- In drilling CFRP/Ti stacks, vibration-assisted drilling offers benefits such as lowering the interface temperature, reducing chip size and extending tool life. Particularly, the recently proposed HF-LF VAD provides a more evident machining effect.
- In the future, exploration of hybrid cooling methods (e.g., combining cryogenic cooling with MQL or high-pressure air) to improve temperature control, reduce tool wear and mitigate chip adhesion can be used.

Development of sustainable, environmentally friendly lubricants to meet regulatory requirements and reduce environmental impact may also be occupied. Further, an ideal drilling environment may be created by combining the application of coatings, cooling techniques, better tool geometry, and optimal drilling settings. This will enhance the hole quality and lengthen the tool life.

- The development of self-healing coatings and enhanced wear-resistant tools to focus on cost-effectiveness by increasing the lifespan of cutting tools would be a great solution to current challenges. Further, development of multi-functional tool coatings optimized for wear resistance, thermal insulation and self-lubrication will enhance tool life and reduce cutting forces. Additionally, developing tools and processes capable of performing drilling, reaming and deburring in a single operation will improve productivity and reduce secondary processes.
- With the trend toward machine learning and AI these days, predictive analytics and machine learning algorithms to analyze historical data to predict tool wear, optimize drilling sequences and improve hole quality may be occupied in the future to improve hole quality. Integration of automated drilling systems and robotic arms for consistent and precise drilling, reducing manual intervention and improving repeatability in aerospace manufacturing
- Integration of real-time monitoring systems using sensors and AI-based predictive algorithms to detect tool wear, chip buildup and surface defects during drilling may be used. Adaptive control systems that automatically adjust feed rates, cutting speeds and coolant flow to optimize drilling performance and extend tool life can be added while drilling.

Nomenclature

BUE Build-up edge BUL Build-up layer

CARALL Carbon-reinforced aluminum laminate **CFRP** Carbon fiber-reinforced polymer

CFRP/Al Carbon Fiber-Reinforced Polymer / Aluminum CFRP/Ti Carbon Fiber-Reinforced Polymer / Titanium

CVD Chemical vapor deposition

C7 Nano-crystalline AlTiN grains embedded in an amorphous matrix of sili-

con nitride (Si3N4)

DF Delamination Factor DLC Diamond like carbon Fiber metal composite **FMC GFRP** Glass fiber-reinforced plastic

GLARE Glass-reinforced aluminum laminate

HSS High speed steel

HSS-Co High Speed Steel with Cobalt

HP-LF MQL High Pressure Low Frequency Minimum Quantity Lubrication

Liquid Nitrogen LN2 LCO₂ Liquid carbon dioxide

LP-HF MQL Low Pressure High Frequency Minimum Quantity Lubrication

MD CFRP Multi directional Carbon fiber-reinforced plastic

MoS2 Molybdenum di sulfide

MQL Minimum Quantity Lubrication **PCBN** Polycrystalline cubic boron nitride

PCD Polycrystalline diamond **PCR** Partial Correlation Regression **PMC** Polymer Matrix Composite Physical Vapor Deposition **PVD**

Τi Titanium alloy

TiN Titanium nitride coating

TiAlCr Titanium aluminum chromium coating **TiAlN** Titanium aluminum nitride coating

TiSi Titanium silica coating

TiSiN Titanium silica nitride coating

UD CFRP Uni directional Carbon fiber-reinforced plastic

WC Tungsten Carbide

Author contributions

J. Joy Mathavan was involved in conceptualization, writing-original draft, formattingand editing; M. H. Hassan was involved in supervision and validation.

Disclosure statement

No potential conflict of interest was reported by the author(s).

ORCID

Joy Mathavan Jebaratnam http://orcid.org/0000-0002-3270-6185 Muhammad Hafiz Hassan http://orcid.org/0000-0002-8717-8973

Data availability statement

Data sharing not applicable to this article as no datasets were generated or analyzed during the current study.

References

Aamir, M.; Tolouei-Rad, M.; Giasin, K.; Nosrati, A. (2019). Recent advances in drilling of carbon fiber-reinforced polymers for aerospace applications: A review. The International Journal of Advanced Manufacturing Technology, 105(5-6): 2289-2308. doi: 10.1007/ s00170-019-04348-z.



- Abhishek, K.; Datta, S.; Mahapatra, S.S. (2015). Optimization of thrust, torque, entry, and exist delamination factor during drilling of CFRP composites. The International Journal of Advanced Manufacturing Technology, 76(1-4): 401-416. doi: 10.1007/s00170-014-6199-3.
- Abrão, A.M.; Faria, P.E.; Rubio, J.C.C.; Reis, P.; Davim, J.P. (2007). Drilling of fiber reinforced plastics: A review. Journal of Materials Processing Technology, 186(1-3): 1-7. doi: 10.1016/j.jmatprotec.2006.11.146.
- Abrão, A.M.; Rubio, J.C.C.; Faria, P.E.; Davim, J.P. (2008). The effect of cutting tool geometry on thrust force and delamination when drilling glass fibre reinforced plastic composite. Materials and Design, 29(2): 508-513. doi: 10.1016/J.MATDES.2007.01.016.
- Ahmed, L.S.; Kumar, M.P. (2016). Cryogenic drilling of Ti-6Al-4V alloy under liquid nitrogen cooling. Materials and Manufacturing Processes, 31(7): 951-959. doi: 10.1080/ 10426914.2015.1048475.
- Almudaihesh, F.; Holford, K.; Pullin, R.; Eaton, M. (2020). The influence of water absorption on unidirectional and 2D woven CFRP composites and their mechanical performance. Composites Part B: Engineering, 182: 107626. doi: 10.1016/j.compositesb.2019. 107626
- Alonso Pinillos, U.; Fernández Vidal, S.R.; Calamaz, M.; Girot Mata, F.A. (2019). Wear mechanisms and wear model of carbide tools during dry drilling of CFRP/TiAl6V4 stacks. Materials, 12(18): 2843. doi: 10.3390/ma12182843.
- Altin Karataş, M.; Gökkaya, H. (2018). A review on machinability of carbon fiber reinforced polymer (CFRP) and glass fiber reinforced polymer (GFRP) composite materials. Defence Technology, 14(4): 318-326. doi: 10.1016/J.DT.2018.02.001.
- An, M.; Xu, Q.L.; Cai, J.Y.; Chen, X.J. (2013). Experimental investigation on drilling force and hole quality when drilling of T800S/250F CFRP laminate. Advanced Materials Research, 797: 155-160. doi: 10.4028/www.scientific.net/AMR.797.155.
- An, Q.; Cai, X.; Xu, J.; Chen, M. (2014). Experimental investigation on drilling of high strength T800S/250F CFRP with twist and dagger drill bits. International Journal of Abrasive Technology, 6(3): 183-196. doi: 10.1504/IJAT.2014.060690.
- An, Q.; Dang, J.; Li, J.; Wang, C.; Chen, M. (2020). Investigation on the cutting responses of CFRP/Ti stacks: With special emphasis on the effects of drilling sequences. Composite Structures, 253: 112794. doi: 10.1016/j.compstruct.2020.112794.
- An, Q.; Zhong, B.; Wang, X.; Zhang, H.; Sun, X.; Chen, M. (2021). Effects of drilling strategies for CFRP/Ti stacks on static mechanical property and fatigue behavior of openhole CFRP laminates. The Journal of Manufacturing Processes, 64: 409-420. doi: 10.1016/ j.jmapro.2021.01.036.
- Anand, R.S.; Patra, K. (2017). Mechanistic cutting force modelling for micro-drilling of CFRP composite laminates. CIRP Journal of Manufacturing Science and Technology, 16: 55-63. doi: 10.1016/J.CIRPJ.2016.07.002.
- Anand, R.S.; Patra, K. (2018). Cutting force and hole quality analysis in micro-drilling of CFRP. Materials and Manufacturing Processes, 33(12): 1369-1377. doi: 10.1080/10426914. 2017.1401715.
- Arrazola, P.J.; Garay, A.; Iriarte, L.M.; Armendia, M.; Marya, S.; Le Maître, F. (2009). Machinability of titanium alloys (Ti6Al4V and Ti555.3). Journal of Materials Processing Technology, 209(5): 2223–2230. doi: 10.1016/j.jmatprotec.2008.06.020.
- Ashrafi, S.A.; Sharif, S.; Farid, A.A.; Yahya, M.Y. (2013). Performance evaluation of carbide tools in drilling CFRP-Al stacks. Journal of Composite Materials, 48(17): 1-14. doi: 10. 1177/0021998313494429.



- Astakhov, V.P.; Davim, J.P.; Davim, J.P. (2008). Tools (Geometry and Material) and Tool Wear BT - Machining: Fundamentals and Recent Advances. Springer London, London, 29-57. doi: 10.1007/978-1-84800-213-5_2.
- ASTM B348-83. Standard specification for titanium and titanium alloy bars and billets. Pennsylvania, United States.
- Aurich, J.C.; Dornfeld, D.; Arrazola, P.J.; Franke, V.; Leitz, L.; Min, S. (2009). Burrs-analysis, control and removal. CIRP Annals Manufacturing Technology, 58(2): 519-542. doi: 10.1016/j.cirp.2009.09.004.
- Avila, M.; Gardner, J.; Reich-Weiser, C.; Tripathi, S.; Vijayaraghavan, A.; Dornfeld, A. (2005). Strategies for burr minimization and cleanability in aerospace and automotive manufacturing. SAE Technical Papers. 2005-01-3327. doi: 10.4271/2005-01-3327.
- Balázs, B.Z.; Takács, M. (2020). Experimental investigation and optimisation of the micro milling process of hardened hot-work tool steel. The International Journal of Advanced Manufacturing Technology, 106(11-12): 5289-5305. doi: 10.1007/s00170-020-04991-x.
- Basmaci, G.; Yoruk, A.; Koklu, U.; Morkavuk, S. (2017). Impact of cryogenic condition and drill diameter on drilling performance of CFRP. Applied Sciences (Switzerland), 7(7): 667. doi: 10.3390/app7070667.
- Ben Soussia, A.; Mkaddem, A.; El Mansori, M. (2014). Rigorous treatment of dry cutting of FRP - Interface consumption concept: A review. International Journal of Mechanical Sciences, 83(Complete): 1-29. doi: 10.1016/j.ijmecsci.2014.03.017.
- Berger, U.; Janssen, R.; Brinksmeier, E. (1998). Advanced mechatronic system for manufacturing and repair of turbine blades. IFAC Proceedings Volumes, 31(15): 295-300. doi: 10. 1016/s1474-6670(17)40569-6.
- Bhowmick, S.; Alpas, A.T. (2008). Minimum quantity lubrication drilling of aluminiumsilicon alloys in water using diamond-like carbon coated drills. International Journal of Machine Tools and Manufacture, 48(12-13): 1429-1443. doi: 10.1016/j.ijmachtools.2008. 04.010
- Biermann, D.; Hartmann, H. (2012). Reduction of burr formation in drilling using cryogenic process cooling. Procedia CIRP, 3: 85-90. doi: 10.1016/j.procir.2012.07.016
- Boccarusso, L.; De Fazio, D.; Durante, M.; Langella, A.; Capece Minutolo, F.M. (2019). CFRPs drilling: comparison among holes produced by different drilling strategies. *Procedia CIRP*, 79: 325–330. doi: 10.1016/j.procir.2019.02.075
- Bonnet, C.; Poulachon, G.; Rech, J.; Girard, Y.; Costes, J.P. (2015). CFRP drilling: Fundamental study of local feed force and consequences on hole exit damage. International Journal of Machine Tools and Manufacture, 94: 57-64. doi: 10.1016/j. ijmachtools.2015.04.006
- Bounif, K.; Abbadi, M.; Nouari, M.; Selvam, R. (2021). A numerical approach for crackinduced damage in tungsten carbide cutting tools during machining. Engineering Failure Analysis, 128: 105617. doi: 10.1016/j.engfailanal.2021.105617
- Boutrih, L.; Makich, H.; Stief, P.; Dantan, J.; Etienne, A.; Siadat, A. (2022). Surface quality in dry machining of CFRP composite / Ti6Al4V stack laminate. Procedia CIRP, 108: 758–763. doi: 10.1016/j.procir.2022.03.117.
- Brinksmeier, E.; Fangmann, S.; Rentsch, R. (2011). Drilling of composites and resulting surface integrity. CIRP Annals Manufacturing Technology, 60(1): 57-60. doi: 10.1016/j.cirp. 2011.03.077.
- Brinksmeier, E.; Janssen, R. (2002). Drilling of multi-layer composite materials consisting of Carbon Fiber Reinforced Plastics (CFRP), titanium and aluminum alloys. CIRP Annals, 51(1): 87-90. doi: 10.1016/S0007-8506(07)61472-3.



- Budinski, K.G. (1991). Tribological properties of titanium alloys. Wear, 151(2): 203-217. doi: 10.1016/0043-1648(91)90249-T.
- Butler-Smith, P.W.; Axinte, D.A.; Daine, M.; Kennedy, A.R.; Harper, L.T.; Bucourt, J.F.; Ragueneau, R. (2015). A study of an improved cutting mechanism of composite materials using novel design of diamond micro-core drills. International Journal of Machine Tools and Manufacture, 88: 175-183. doi: 10.1016/j.ijmachtools.2014.10.002
- Byrne, G.; et al. (2021). Towards high performance living manufacturing systems a new convergence between biology and engineering. CIRP Journal of Manufacturing Science and Technology, 34: 6-21. doi: 10.1016/j.cirpj.2020.10.009.
- Çalışkan, H.; Küçükköse, M. (2015). The effect of aCN/TiAlN coating on tool wear, cutting force, surface finish and chip morphology in face milling of Ti6Al4V superalloy. International Journal of Refractory Metals and Hard Materials, 50: 304-312. doi: 10.1016/ j.ijrmhm.2015.02.012.
- Calzada, K.; Kapoor, S.; DeVor, R.; Samuel, J.; Srivastava, A. (2012). Modeling and interpretation of fiber orientation-based failure mechanisms in machining of carbon fiberreinforced polymer composites. The Journal of Manufacturing Processes, 14(2): 141-149. doi: 10.1016/j.jmapro.2011.09.005.
- Campos Rubio, J.; Abrao, A.M.; Faria, P.E.; Correia, A.E.; Davim, J.P. (2008). Effects of high speed in the drilling of glass fibre reinforced plastic: Evaluation of the delamination factor. International Journal of Machine Tools and Manufacture, 48(6): 715-720. doi: 10. 1016/j.ijmachtools.2007.10.015
- Cao, S.; Li, Y.; Zhang, K.; Hou, G.; Luo, B.; Liu, S.; Long, T.; Liu, P. (2023). Investigation of CFRP damages induced by the interface high temperature and mixed tool wear mechanism in drilling of thin-walled CFRP/Ti stacks. Composite Structures, 323: 117438. doi: 10.1016/j.compstruct.2023.117438.
- Carvajal, R.; González-R, P.L.; Lozano, S. (2011). Research study of factors affecting difference between hole diameters in hybrid metal-composite drilling. Proceedings of the Institution of Mechanical Engineers Part B Journal of Engineering Manufacture, 225(7): 991-1000. doi: 10.1177/2041297510393444.
- Çelik, A.; Lazoglu, I.; Kara, A.; Kara, F. (2015). Investigation on the performance of SiAlON ceramic drills on aerospace grade CFRP composites. Journal of Materials Processing Technology, 223: 39-47. doi: 10.1016/j.jmatprotec.2015.03.040
- Çelik, A.; Lazoglu, I.; Kara, A.; Kara, F. (2015). Wear on SiAlON ceramic tools in drilling of aerospace grade CFRP composites. Wear, 338-339: 11-21. doi: 10.1016/j.wear.2015.05. 009
- Che, D.; Saxena, I.; Han, P.; Guo, P.; Ehmann, K.F. (2014). Machining of carbon fiber reinforced plastics/polymers: A literature review. Journal of Manufacturing Science and Engineering, 136(3), 034001. doi: 10.1115/1.4026526.
- Chen, W.C. (1997). Some experimental investigations in the drilling of carbon fiber-reinforced plastic (CFRP) composite laminates. International Journal of Machine Tools and Manufacture, 37(8): 1097-1108. doi: 10.1016/S0890-6955(96)00095-8.
- Cheng, H.; Zhang, K.; Wang, N.; Luo, B.; Meng, Q. (2017). A novel six-state cutting force model for drilling-countersinking machining process of CFRP-Al stacks. International Journal of Advanced Manufacturing Technology, 89(5-8): 2063-2076. doi: 10.1007/s00170-016-9236-6.
- Colligan, K.; Ramulu, M. (1992). The effect of edge trimming on composite surface plies. Manufturing Review (Les Ulis), 5: 274-283.



- Cong, W.L.; Pei, Z.J.; Deines, T.W.; Liu, D.F.; Treadwell, C. (2013). Rotary ultrasonic machining of CFRP/Ti stacks using variable feedrate. Composites Part B: Engineering, 52: 303–310. doi: 10.1016/j.compositesb.2013.04.022
- Cong, W.L.; Zou, X.; Deines, T.W.; Wu, N.; Wang, X.; Pei, Z.J. (2012). Rotary ultrasonic machining of carbon fiber reinforced plastic composites: An experimental study on cutting temperature. Journal of Reinforced Plastics and Composites, 31(22): 1516-1525. doi: 10.1177/0731684412464913.
- Coromant, S. (2010). Users Guide Machining Carbon Fibre Materials. Sandvik Coromant, Malaysia.
- D'Orazio, A.; El Mehtedi, M.; Forcellese, A.; Nardinocchi, A.; Simoncini, M. (2017). Tool wear and hole quality in drilling of CFRP/AA7075 stacks with DLC and nanocomposite TiAlN coated tools. The Journal of Manufacturing Processes, 30: 582-592. doi: 10.1016/j. jmapro.2017.10.019.
- Dahnel, A.N.; Ascroft, H.; Barnes, S. (2016). The effect of varying cutting speeds on tool wear during conventional and Ultrasonic Assisted Drilling (UAD) of Carbon Fibre Composite (CFC) and titanium alloy stacks. Procedia CIRP, 46: 420-423. doi: 10.1016/j. procir.2016.04.044
- Dahnel, A.N.; Ascroft, H.; Barnes, S. (2020). An investigation of hole quality during drilling of carbon fibre reinforced plastic and titanium (Ti6Al4V) using tungsten carbide drills. Materials Today: Proceedings, 29: 161-167. doi: 10.1016/j.matpr.2020.05.640
- Dahnel, A.N.; Ascroft, H.; Barnes, S.; Gloger, M. (2015). Analysis of tool wear and hole quality during Ultrasonic Assisted Drilling (UAD) of Carbon Fibre Composite (CFC)/ titanium alloy (Ti6Al4V) stacks. Proceedings of the ASME 2015 International Mechanical Engineering Congress and Exposition, Houston, TX. doi: 10.1115/IMECE2015-50416
- Davim, J.P.; Reis, P. (2003a) Drilling carbon fiber reinforced plastics manufactured by autoclave-experimental and statistical study. Materials and Design, 24: 315-324.
- Davim, J.P.; Reis, P. (2003b) Study of delamination in drilling carbon fiber reinforced plastics (CFRP) using design experiments. Composite Structures, 59(4): 481-487. 10.1016/ S0263-8223(02)00257-X
- Denkena, B.; Boehnke, D.; Dege, J.H. (2008). Helical milling of CFRP-titanium layer compounds. CIRP Journal of Manufacturing Science and Technology, 1, 64-69.
- Dogrusadik, A.; Kentli, A. (2017). Comparative assessment of support plates' influences on delamination damage in micro-drilling of CFRP laminates. Composite Structures, 173: 156–167. doi: 10.1016/j.compstruct.2017.04.031
- Dornfeld, D.; Min, S. (2010). A Review of Burr Formation in Machining BT Burrs -Analysis, Control and Removal, J. C. Aurich and D. Dornfeld (Eds.), Springer Berlin Heidelberg, Berlin, Heidelberg, 3–11.
- Dornfeld, D.A.; Kim, J.S.; Dechow, H.; Hewson, J.; Chen, L.J. (1999). Drilling Burr formation in titanium alloy, Ti-6AI-4V. CIRP Annals, 48(1): 73-76. doi: 10.1016/S0007-8506(07)63134-5
- Durante, M.; Boccarusso, L.; De Fazio, D.; Langella, A. (2019). Circular cutting strategy for drilling of carbon fiber-reinforced plastics (CFRPs). Materials and Manufacturing Processes, 34(5): 554–566. doi: 10.1080/10426914.2019.1566615.
- El-Sonbaty, I.; Khashaba, U.A.; Machaly, T. (2004). Factors affecting the machinability of GFR/epoxy composites. Composite Structures, 63(3-4): 329-338. doi: 10.1016/S0263-8223(03)00181-8
- Eneyew, E.D.; Ramulu, M. (2014). Experimental study of surface quality and damage when drilling unidirectional CFRP composites. Journal of Materials Research and Technology, 3(4): 354–362. doi: 10.1016/j.jmrt.2014.10.003.



- Erik Oberg, A.H.H.R.; Jones, F.D.; Horton, H.L. (2004). Machinery's Handbook. 27th ed. Industrial Press, New York.
- ErmanAydın, M. (2020). CFRP/Al-7075 istifli delmede matkap uç açılarının delinebilirlik üzerine etkisi. GUMMFD, 35(2): 917–932.
- Erturk, A.T.; Vatansever, F.; Yarar, E.; Karabay, S. (2019). Machining behavior of multiple layer polymer composite bearing with using different drill bits. Composites Part B: Engineering, 176: 107318. doi: 10.1016/j.compositesb.2019.107318
- Ezugwu, E.O.; Wang, Z.M. (1997). Titanium alloys and their machinability—a review. Journal of Materials Processing Technology, 68(3): 262-274. doi: 10.1016/S0924-0136(96)00030-1
- Falconieri, D.; Franco, F. (2015). The effect of titanium insert repairs on the static strength of CFRP coupons and joints. Composite Structures, 134: 799-810. doi: 10.1016/j.compstruct.2015.08.042.
- Fan, L.; Wang, D. (2021). Study on delamination inhibition and chip breakage mechanism in drilling metal laminated materials with double cone drill. The Journal of Manufacturing Processes, 64: 81-94. doi: 10.1016/j.jmapro.2021.01.014
- Faraz, A.; Biermann, D.; Weinert, K. (2009). Cutting edge rounding: An innovative tool wear criterion in drilling CFRP composite laminates. International Journal of Machine Tools and Manufacture, 49(15): 1185-1196. doi: 10.1016/J.IJMACHTOOLS.2009.08.002.
- Feito, N.; Díaz-Álvarez, J.; López-Puente, J.; Miguelez, M.H. (2018). Experimental and numerical analysis of step drill bit performance when drilling woven CFRPs. Composite Structures, 184: 1147–1155. doi: 10.1016/j.compstruct.2017.10.061
- Feito, N.; López-Puente, J.; Santiuste, C.; Miguélez, M.H. (2014). Numerical prediction of delamination in CFRP drilling. Composite Structures, 108: 677-683. 10.1016/j.compstruct. 2013.10.014
- Fernández-Pérez, J.; Cantero, J.L.; Díaz-Álvarez, J.; Miguélez, M.H. (2019). Hybrid composite-metal stack drilling with different minimum quantity lubrication levels. Materials (Basel, Switzerland), 12(3): 448. doi: 10.3390/ma12030448.
- Fernandez-Vidal, S.R.; Fernandez-Vidal, S.; Batista, M.; Salguero, J. (2018). Tool wear mechanism in cutting of stack CFRP/UNS A97075. Materials (Basel, Switzerland), 11(8): 1276. doi: 10.3390/ma11081276.
- Ferreira, J.R.; Coppini, N.L.; Miranda, G.W.A. (1999). Machining optimisation in carbon fibre reinforced composite materials. Journal of Materials Processing Technology, 92-93: 135-140. doi: 10.1016/S0924-0136(99)00221-6
- Franke, V. (2018). Burr BT CIRP Encyclopedia of Production Engineering, Springer Berlin Heidelberg, Berlin, Heidelberg, 1-4. doi: 10.1007/978-3-642-35950-7_6393-4.
- Franz, G.; Vantomme, P.; Hafiz Hassan, M. (2022). A review on drilling of multilayer fiber-reinforced polymer composites and aluminum stacks: Optimization of strategies for improving the drilling performance of aerospace assemblies. Fibers 10: 78. doi: 10.3390/
- Fujiwara, J.; Nagaura, R.; Kuroda, K.; Tashiro, T. (2012). Drilling of CFRP/Ti6Al4V stack board. In ICMT 2012 - 16th International Conference on Mechatronics Technology, Department of Mechanical Engineering, Graduate School of Engineering, Osaka University, Osaka, Japan, 285-289.
- Gao, G.; Xia, Z.; Yuan, Z.; Xiang, D.; Zhao, B. (2021). Influence of longitudinal-torsional ultrasonic-assisted vibration on micro-hole drilling Ti-6Al-4V. Chinese Journal of Aeronautics, 34(9): 247–260. doi: 10.1016/j.cja.2020.06.012
- Gao, T.; Li, C.; Wang, Y.; Liu, X.; An, Q.; Li, H.N.; Zhang, Y.; Cao, H.; Liu, B.; Wang, D.; Said, Z.; Debnath, S.; Jamil, M.; Ali, H.M.; Sharma, S. (2022). Carbon fiber reinforced



- polymer in drilling: From damage mechanisms to suppression. Composite Structures, 286: 115232. doi: 10.1016/j.compstruct.2022.115232
- Garrick, R. (2007). Drilling of advanced aircraft structure with poly-crystalline diamond (PCD) drills. Aerospace Technology Conference and Exposition, Los Angels, CA. doi: 10. 4271/2007-01-3893.
- Gaugel, S.; Sripathy, P.; Haeger, A.; Meinhard, D.; Bernthaler, T.; Lissek, F.; Kaufeld, M.; Knoblauch, V.; Schneider, G. (2016). A comparative study on tool wear and laminate damage in drilling of carbon-fiber reinforced polymers (CFRP). Composite Structures, 155: 173-183. doi: 10.1016/j.compstruct.2016.08.004.
- Geier, N.; Davim, J.P.; Szalay, T. (2019). Advanced cutting tools and technologies for drilling carbon fibre reinforced polymer (CFRP) composites: A review. Composites Part A: Applied Science and Manufacturing, 125: 105552. doi: 10.1016/J.COMPOSITESA.2019. 105552.
- Geier, N.; Szalay, T. (2017). Optimisation of process parameters for the orbital and conventional drilling of uni-directional carbon fibre-reinforced polymers (UD-CFRP). Measurement, 110: 319-334. doi: 10.1016/j.measurement.2017.07.007
- Geier, N.; Szalay, T.; Takács, M. (2019). Analysis of thrust force and characteristics of uncut fibres at non-conventional oriented drilling of unidirectional carbon fibre-reinforced plastic (UD-CFRP) composite laminates. The International Journal of Advanced Manufacturing Technology, 100(9-12): 3139-3154. doi: 10.1007/s00170-018-2895-8.
- Geier, N.; Xu, J.; Pereszlai, C.; Poór, D.I.; Davim, J.P. (2021). Drilling of carbon fibre reinforced polymer (CFRP) composites: Difficulties, challenges and expectations. Procedia Manufacturing, 54: 284-289. doi: 10.1016/j.promfg.2021.07.045.
- Geng, D.; Liu, Y.; Shao, Z.; Lu, Z.; Cai, J.; Li, X.; Jiang, X.; Zhang, D. (2019). Delamination formation, evaluation and suppression during drilling of composite laminates: A review. Composite Structures, 216: 168-186. doi: 10.1016/J.COMPSTRUCT.2019.02.099.
- Geng, D.; Liu, Y.; Shao, Z.; Zhang, M.; Jiang, X.; Zhang, D. (2020). Delamination formation and suppression during rotary ultrasonic elliptical machining of CFRP. Composites Part B: Engineering, 183: 107698. doi: 10.1016/j.compositesb.2019.107698
- Ghassemieh, E. (2012). Performance and wear of coated carbide drill in machining of carbon fibre reinforced composite/titanium stack. International Journal of Materials and Product Technology, 43(1/2/3/4): 165-183. doi: 10.1504/12.47682. 10.1504/IJMPT.2012. 047682
- Giasin, K. (2016). Machining fibre metal laminates and Al2024-T3 aluminium alloy. PhD
- Giasin, K. (2018). The effect of drilling parameters, cooling technology, and fiber orientation on hole perpendicularity error in fiber metal laminates. The International Journal of Advanced Manufacturing Technology, 97(9-12): 4081-4099. doi: 10.1007/s00170-018-2241-1.
- Giasin, K.; Ayvar-Soberanis, S. (2016). Evaluation of workpiece temperature during drilling of GLARE fiber metal laminates using infrared techniques: Effect of cutting parameters, fiber orientation and spray mist application. Materials, 9(8): 622. doi: 10.3390/ ma9080622.
- Giasin, K.; Ayvar-Soberanis, S. (2017). An investigation of burrs, chip formation, hole size, circularity and delamination during drilling operation of GLARE using ANOVA. Composite Structures, 159: 745-760. doi: 10.1016/j.compstruct.2016.10.015.
- Giasin, K.; Ayvar-Soberanis, S. (2017). Microstructural investigation of drilling induced damage in fibre metal laminates constituents. Composites Part A: Applied Science and Manufacturing, 97: 166-178. doi: 10.1016/j.compositesa.2017.02.024.



- Giasin, K.; Ayvar-Soberanis, S.; French, T.; Phadnis, V. (2017). 3D finite element modelling of cutting forces in drilling fibre metal laminates and experimental hole quality analysis. Applied Composite Materials, 24(1): 113-137. doi: 10.1007/s10443-016-9517-0.
- Giasin, K.; Ayvar-Soberanis, S.; Hodzic, A. (2015). An experimental study on drilling of unidirectional GLARE fibre metal laminates. Composite Structures, 133(C): 794-808. doi: 10.1016/j.compstruct.2015.08.007.
- Giasin, K.; Hawxwell, J.; Sinke, J.; Dhakal, H.; Köklü, U.; Brousseau, E. (2020). The effect of cutting tool coating on the form and dimensional errors of machined holes in GLARE® fibre metal laminates. The International Journal of Advanced Manufacturing Technology, 107(5-6): 2817-2832. doi: 10.1007/s00170-020-05211-2.
- Giasin, K.; Hodzic, A.; Phadnis, V.; Ayvar-Soberanis, S. (2016). Assessment of cutting forces and hole quality in drilling Al2024 aluminium alloy: Experimental and finite element study. The International Journal of Advanced Manufacturing Technology, 87(5-8): 2041-2061. doi: 10.1007/s00170-016-8563-y.
- Gisip, J.; Gazo, R.; Stewart, H.A. (2009). Effects of cryogenic treatment and refrigerated air on tool wear when machining medium density fiberboard. Journal of Materials Processing Technology, 209(11): 5117-5122. doi: 10.1016/j.jmatprotec.2009.02.010.
- Gorynin, I.V. (1999). Titanium alloys for marine application. Materials Science and Engineering A, 263(2): 112–116. doi: 10.1016/S0921-5093(98)01180-0
- Haiyan, W.; Xuda, Q. (2016). A mechanistic model for cutting force in helical milling of carbon fiber-reinforced polymers. The International Journal of Advanced Manufacturing Technology, 82(9-12): 1485-1494. doi: 10.1007/s00170-015-7460-0.
- Hamran, N.N.N.; Ghani, J.A.; Ramli, R.; Haron, C.H.C. (2020). A review on recent development of minimum quantity lubrication for sustainable machining. Journal of Cleaner Production, 268: 122165. doi: 10.1016/j.jclepro.2020.122165.
- Hartung, P.D.; Kramer, B.M.; von Turkovich, B.F. (1982). Tool wear in titanium machining. CIRP Annals, 31(1): 75-80. doi: 10.1016/S0007-8506(07)63272-7
- Hassan, M. H. (2020). Optimization of customized twist drill geometry for single-shot drilling of composite-metal stack. PhD thesis, 1-191. Universiti Sains Malaysia.
- Hassan, M.H.; Abdullah, J.; Mahmud, A.S.; Supran, A. (2017). Burr height as quality indicator in single shot drilling of stacked CFRP/aluminium composite. Key Engineering Materials, 744: 327-331. 10.4028/www.scientific.net/KEM.744.327
- Hassan, M.H.; Jamaluddin, A.; Franz, G. (2022). Multi-objective optimization in single-shot drilling of CFRP/Al stacks using customized twist drill. Materials, 15(5): 1981. doi: 10. 3390/ma15051981.
- Hatamleh, M.M.; Wu, X.; Alnazzawi, A.; Watson, J.; Watts, D. (2018). Surface characteristics and biocompatibility of cranioplasty titanium implants following different surface treatments. Dental Materials: Official Publication of the Academy of Dental Materials, 34(4): 676-683. doi: 10.1016/j.dental.2018.01.016.
- Heath, P.J. (2001). Developments in applications of PCD tooling. Journal of Materials Processing Technology, 116(1): 31-38. doi: 10.1016/S0924-0136(01)00837-8
- Hocheng, H. (2012). Machining Technology for Composite Materials: Principles and Practice. Woodhead Publishing Limited, Cambridge.
- Hocheng, H.; Pwu, H.Y.; Yao, K.C. (1993). MACHINABILITY OF SOME FIBER-REINFORCED THERMOSET AND THERMOPLASTICS IN DRILLING. Materials and Manufacturing Processes, 8(6): 653-682. doi: 10.1080/10426919308934872.
- Hocheng, H.; Tsao, C.C. (2005). The path towards delamination-free drilling of composite materials. Journal of Materials Processing Technology, 167(2-3): 251-264. doi: 10.1016/J. JMATPROTEC.2005.06.039.



- Hocheng, H.; Tsao, C.C. (2006). Effects of special drill bits on drilling-induced delamination of composite materials. International Journal of Machine Tools and Manufacture, 46(12-13): 1403-1416. doi: 10.1016/j.ijmachtools.2005.10.004
- Hong, S.Y.; Markus, I.; Jeong, W. (2001). New cooling approach and tool life improvement in cryogenic machining of titanium alloy Ti-6Al-4V. International Journal of Machine Tools and Manufacture, 41(15): 2245-2260. doi: 10.1016/S0890-6955(01)00041-4
- Hussein, R.; Sadek, A.; Elbestawi, M.A.; Attia, M.H. (2018). Low-frequency vibrationassisted drilling of hybrid CFRP/Ti6Al4V stacked material. The International Journal of Advanced Manufacturing Technology, 98(9-12): 2801-2817. doi: 10.1007/s00170-018-2410-2.
- Hussein, R.; Sadek, A.; Elbestawi, M.A.; Attia, M.H. (2019). Elimination of delamination and burr formation using high-frequency vibration-assisted drilling of hybrid CFRP/ Ti6Al4V stacked material. The International Journal of Advanced Manufacturing Technology, 105(1-4): 859-873. doi: 10.1007/s00170-019-04248-2.
- Iliescu, D.; Gehin, D.; Iordanoff, I.; Girot, F.; Gutiérrez, M.E. (2010). A discrete element method for the simulation of CFRP cutting. Composites Science and Technology, 70(1): 73-80. doi: 10.1016/J.COMPSCITECH.2009.09.007.
- Impero, F.; Dix, M.; Squillace, A.; Prisco, U.; Palumbo, B.; Tagliaferri, F. (2018). A comparison between wet and cryogenic drilling of CFRP/Ti stacks. Materials and Manufacturing Processes, 33(12): 1354–1360. doi: 10.1080/10426914.2018.1453162.
- Isbilir, O.; Ghassemieh, E. (2013). COMPARATIVE STUDY OF TOOL LIFE AND HOLE QUALITY IN DRILLING OF CFRP/TITANIUM STACK USING COATED CARBIDE DRILL LIFE AND HOLE QUALITY IN DRILLING OF CFRP/TITANIUM STACK USING COATED CARBIDE. Machining Science and Technology, 17(3): 380-409. doi: 10. 1080/10910344.2013.806098.
- Isbilir, O.; Ghassemieh, E. May (2012). Delamination and wear in drilling of carbon-fiber reinforced plastic composites using multilayer TiAlN/TiN PVD-coated tungsten carbide tools. Journal of Reinforced Plastics and Composites, 31(10): 717-727. doi: 10.1177/ 0731684412444653.
- Iskandar, Y.; Damir, A.; Attia, M.H.; Hendrick, P. (2013). On the effect of MQL parameters on machining quality of CFRP. In ICCM International Conferences on Composite Materials, Mechanical Engineering Department, 3281-3290. Montreal, Canada: McGill University, International Committee on Composite Materials.
- Jayabal, S.; Natarajan, U. (2010). Optimization of thrust force, torque, and tool wear in drilling of coir fiber-reinforced composites using Nelder-Mead and genetic algorithm methods. The International Journal of Advanced Manufacturing Technology, 51(1-4): 371-381. doi: 10.1007/s00170-010-2605-7.
- Jebaratnam, J.M. (2025). Application of drill bit coatings for fiber/metal stack drilling in aircraft manufacturing: a comprehensive review. The International Journal of Advanced Manufacturing Technology, 136(7-8): 2987-3035. doi: 10.1007/s00170-024-14984-9.
- Jebaratnam, J.M.; Hassan, M.H. (2024). Process enhancement and performance evaluation of single-shot drilling of CFRP/aluminum stacks: a review. The International Journal of Advanced Manufacturing Technology, 135(7-8): 3015-3050. doi: 10.1007/s00170-024-14610-8.
- Jerold, B.D.; Kumar, M.P. (2013). The influence of cryogenic coolants in machining of Ti-6Al-4V. Journal of Manufacturing Science and Engineering, 135(3): 031005. doi: 10.1115/ 1.4024058.



- Ji, M.; Xu, J.; Chen, M.; Mansori, M.E.I. (2020). Effects of different cooling methods on the specific energy consumption when drilling CFRP/Ti6Al4V Manufacturing, 43: 95-102. doi: 10.1016/j.promfg.2020.02.118.
- Jia, Z.; Chen, C.; Wang, F.; Zhang, C.; Wang, Q.; Hao, J. (2020). Experimental study on drilling temperature and hole quality in drilling of carbon fiber reinforced plastic/titanium stacks. Proceedings of the Institution of Mechanical Engineers, Part C: Journal of Mechanical Engineering Science, 234(13): 2662–2672. doi: 10.1177/0954406220908617.
- Jia, Z.; Zhang, C.; Wang, F.; Fu, R. (2020). A mechanistic prediction model for thrust force and torque during drilling of CFRP/Ti stacks. The International Journal of Advanced Manufacturing Technology, 106(7-8): 3105-3115. doi: 10.1007/s00170-019-04861-1.
- Jiaying, G.; Ge, J.; Chen, G.; Su, Y.; Zou, Y.; Ren, C.; Qin, X.; Wang, G. (2022). Effect of cooling strategies on performance and mechanism of helical milling of CFRP/Ti-6Al-4 V stacks. Chinese Journal of Aeronautics, 35(2): 388-403. doi: 10.1016/j.cja.2020.12.003.
- Karpat, Y.; Bahtiyar, O. (2015). Comparative analysis of PCD drill designs during drilling of CFRP laminates. Procedia CIRP, 31: 316-321. doi: 10.1016/j.procir.2015.03.094
- Ke, F.; Ni, J.; Stephenson, D.A. (2005). Continuous chip formation in drilling. International Journal of Machine Tools and Manufacture, 45(15): 1652-1658. doi: 10.1016/j.ijmachtools.2005.03.011
- Kelly, J.F.; Cotterell, M.G. (2002). Minimal lubrication machining of aluminium alloys. Journal of Materials Processing Technology, 120(1-3): 327-334. 10.1016/S0924-0136(01)01126-8
- Kerrigan, K.; Scaife, R.J. (2018). Wet vs dry CFRP drilling: Influence of cutting fluid on tool performance. Procedia CIRP, 77(Hpc): 315-319. doi: 10.1016/j.procir.2018.09.024.
- Khanna, N.; Desai, K.; Sheth, A.; Øllgaard Larsen, J. (2019). CFRP machining on indigenously developing cryogenic machining facility: An initial study. Mater Today Proc, 18: 4598-4604. doi: 10.1016/j.matpr.2019.07.434
- Khashaba, U.A. (2013). Drilling of polymer matrix composites: A review. Journal of Composite Materials, 47(15): 1817-1832. doi: 10.1177/0021998312451609.
- Khashaba, U.A. (2018). Improvement of toughness and shear properties of multiwalled carbon nanotubes/epoxy composites. Polymer Composites, 39(3): 815-825. doi: 10.1002/pc. 24003
- Khashaba, U.A.; El-Keran, A.A. (2017). Drilling analysis of thin woven glass-fiber reinforced epoxy composites. Journal of Materials Processing Technology, 249: 415-425. doi: 10.1016/j.jmatprotec.2017.06.011.
- Khashaba, U.A.; El-Sonbaty, I.A.; Selmy, A.I.; Megahed, A.A. (2010). Machinability analysis in drilling woven GFR/epoxy composites: Part I - effect of machining parameters. Composites Part A: Applied Science and Manufacturing, 41(3): 391-400. doi: 10.1016/j. compositesa.2009.11.006
- Kim, D.; Beal, A.; Kang, K.; Kim, S.Y. (2017). Hole quality assessment of drilled CFRP and CFRP-TI stacks holes using polycrystalline diamond (PCD) tools. Carbon Letters, 23(3): 1-8. doi: 10.5714/CL.2017.23.001.
- Kim, D.; Beal, A.; Kwon, P. (2015). Effect of tool wear on hole quality in drilling of carbon fiber reinforced plastic-titanium alloy stacks using tungsten carbide and polycrystalline diamond tools. Journal of Manufacturing Science and Engineering, 138(3): 031006. doi: 10.1115/1.4031052.
- Kim, D.; Ramulu, M. (2004). Drilling process optimization for graphite/bismaleimide-titanium alloy stacks. Composite Structures, 63(1): 101-114. doi: 10.1016/S0263-8223(03)00137-5



- Kim, D.; Ramulu, M. (2007). Study on the drilling of titanium/graphite hybrid composites. Journal of Engineering Materials and Technology, 129(3): 390-396. doi: 10.1115/1. 2744397.
- Kim, D.; Ramulu, M.; Pedersen, W. (2005). Machinability of titanium/graphite hybrid composites in drilling. Transactions of the North American Manufacturing Research Institute of SME, 33: 445-452.
- Kim, D.; Sturtevant, C.; Ramulu, M. (2013). Usage of PCD tool in drilling of titanium/ graphite hybrid composite laminate. International Journal of Machining and Machinability of Materials, 13(2/3): 276-288. doi: 10.1504/IJMMM.2013.053228.
- Klocke, F.; Krieg, T. (1999). Coated tools for metal cutting features and applications. CIRP Annals, 48(2): 515-525. doi: 10.1016/S0007-8506(07)63231-4
- Klocke, F.; Sangermann, H.; Krämer, A.; Lung, D. (2011). Influence of a high-pressure lubricoolant supply on thermo-mechanical tool load and tool wear behaviour in the turning of aerospace materials. Proc Inst Mech Eng B J Eng Manuf, 225(1): 52-61. doi: 10.1177/09544054JEM2082.
- Ko, S.-L.; Chang, J.-E.; Yang, G.-E. (2003). Burr minimizing scheme in drilling. Journal of Materials Processing Technology, 140(1-3): 237-242. doi: 10.1016/S0924-0136(03)00719-2.
- Komanduri, R. (1997). Machining of fiber-reinforced composites. Machining Science and Technology, 1(1): 113-152. doi: 10.1080/10940349708945641.
- Komanduri, R.; Reed, W.R. (1983). Evaluation of carbide grades and a new cutting geometry for machining titanium alloys. Wear, 92(1): 113-123. doi: 10.1016/0043-1648(83)90011-X
- König, W.; Graß, P. (1989). Quality definition and assessment in drilling of fibre reinforced thermosets. CIRP Annals, 38(1): 119-124. doi: 10.1016/S0007-8506(07)62665-1
- Krishnaraj, V.; Prabukarthi, A.; Ramanathan, A.; Elanghovan, N.; Senthil Kumar, M.; Zitoune, R.; Davim, J.P. (2012). Optimization of machining parameters at high speed drilling of carbon fiber reinforced plastic (CFRP) laminates. Composites Part B: Engineering, 43(4): 1791-1799. doi: 10.1016/j.compositesb.2012.01.007
- Krishnaraj, V.; Vijayarangan, S.; Kumar, A.R. (2007). Effect of drilling parameters on mechanical strength in drilling glass fibre reinforced plastic. International Journal of Computer Applications in Technology, 28(1): 87-93. 10.1504/IJCAT.2007.012336
- Krolczyk, G.M.; Maruda, R.W.; Krolczyk, J.B.; Wojciechowski, S.; Mia, M.; Nieslony, P.; Budzik, G. (2019). Ecological trends in machining as a key factor in sustainable production – a review. J Clean Prod, 218: 601–615. doi: 10.1016/j.jclepro.2019.02.017
- Kumar, D.; Gururaja, S. (2018). Experimental investigation of CFRP/Ti stack drilling undercryogenic condition. International Conference on Composite Materials and structures - ICCMS. IIT Hyderabad.
- Kumar, D.; Gururaja, S. (2020). Machining damage and surface integrity evaluation during milling of UD-CFRP laminates: Dry vs. cryogenic. Composite Structures, 247(March): 112504. doi: 10.1016/j.compstruct.2020.112504.
- Kumar, D.; Gururaja, S.; Jawahir, I.S. (2020). Machinability and surface integrity of adhesively bonded Ti/CFRP/Ti hybrid composite laminates under dry and cryogenic conditions. J Manuf Process, 58: 1075–1087. doi: 10.1016/j.jmapro.2020.08.064.
- Kumar, M.S.; Prabukarthi, A.; Krishnaraj, V. (2013). Study on tool wear and chip formation during drilling carbon fiber reinforced polymer (CFRP)/titanium alloy (Ti6Al4V) stacks. Procedia Engineering, 64: 582-592. doi: 10.1016/j.proeng.2013.09.133.
- Kuo, C.L.; Soo, S.L.; Aspinwall, D.K.; Bradley, S.; Thomas, W.; M'Saoubi, R.; Pearson, D.; Leahy, W. (2014). Tool wear and hole quality when single-shot drilling of metallic-composite stacks with diamond-coated tools. Proceedings of the Institution of Mechanical



- Engineers, Part B: Journal of Engineering Manufacture, 228(10): 1314-1322. doi: 10.1177/ 0954405413517388.
- Kuo, C.L.; Soo, S.L.; Aspinwall, D.K.; Carr, C.; Bradley, S.; M'Saoubi, R.; Leahy, W. (2018). Development of single step drilling technology for multilayer metallic-composite stacks using uncoated and PVD coated carbide tools. J Manuf Process, 31: 286-300. doi: 10. 1016/j.jmapro.2017.11.026.
- Kuo, C.L.; Soo, S.L.; Aspinwall, D.K.; Thomas, W.; Bradley, S.; Pearson, D.; M'Saoubi, R.; Leahy, W. (2014). The effect of cutting speed and feed rate on hole surface integrity in single-shot drilling of metallic-composite stacks. Procedia CIRP, 13: 405-410. doi: 10. 1016/j.procir.2014.04.069
- Kurt, M.; Kaynak, Y.; Bagci, E. (2008). Evaluation of drilled hole quality in Al 2024 alloy. The International Journal of Advanced Manufacturing Technology, 37(11-12): 1051-1060. doi: 10.1007/s00170-007-1049-1.
- Lantrip, J. (2008). New tools needed. Cutting Tool Engineering, 60(8): 72-84.
- Lazar, M.-B.; Xirouchakis, P. (2011). Experimental analysis of drilling fiber reinforced composites. International Journal of Machine Tools and Manufacture, 51(12): 937-946. doi: 10.1016/j.ijmachtools.2011.08.009.
- Lee, E.; Cho, C.H.; Hwang, S.H.; Kim, M.-G.; Han, J.W.; Lee, H.; Lee, J.H. (2019). Improving the vertical thermal conductivity of carbon fiber-reinforced epoxy composites by forming layer-by-layer contact of inorganic crystals. Materials (Basel, Switzerland), 12(19): 3092. doi: 10.3390/ma12193092.
- Li, C.; Xu, J.; Chen, M.; An, Q.; El Mansori, M.; Ren, F. (2019). Tool wear processes in low frequency vibration assisted drilling of CFRP/Ti6Al4V stacks with forced air-cooling. Wear, 426-427: 1616-1623. doi: 10.1016/j.wear.2019.01.005
- Li, H.; Zhang, K.; Cheng, H.; Suo, H.; Cheng, Y.; Hu, J. (2019). Multi-stage mechanical behavior and failure mechanism analysis of CFRP/Al single-lap bolted joints with different seawater ageing conditions. Composite Structures, 208: 634-645. doi: 10.1016/J. COMPSTRUCT.2018.10.044.
- Li, M.; Huang, M.; Chen, Y.; Gong, P.; Yang, X. (2019). Effects of processing parameters on kerf characteristics and surface integrity following abrasive waterjet slotting of Ti6Al4V/CFRP stacks. J Manuf Process, 42: 82-95. doi: 10.1016/j.jmapro.2019.04.024
- Li, M.; Huang, M.; Jiang, X.; Kuo, C.; Yang, X. (2018). Study on burr occurrence and surface integrity during slot milling of multidirectional and plain woven CFRPs. The International Journal of Advanced Manufacturing Technology, 97(1-4): 163-173. doi: 10. 1007/s00170-018-1937-6.
- Li, M.; Soo, S.L.; Aspinwall, D.K.; Pearson, D.; Leahy, W. (2018). Study on tool wear and workpiece surface integrity following drilling of CFRP laminates with variable feed rate strategy. Procedia CIRP, 71: 407-412. doi: 10.1016/j.procir.2018.05.055
- Li, R.; Hegde, P.; Shih, A.J. (2007). High-throughput drilling of titanium alloys. International Journal of Machine Tools and Manufacture, 47(1): 63-74. doi: 10.1016/J. IJMACHTOOLS.2006.02.012.
- Li, R.; Shih, A.J. (2007). Spiral point drill temperature and stress in high-throughput drilling of titanium. International Journal of Machine Tools and Manufacture, 47(12-13): 2005-2017. doi: 10.1016/j.ijmachtools.2007.01.014
- Li, S.; Qin, X.; Jin, Y.; Sun, D.; Li, Y. (2018). A comparative study of hole-making performance by coated and uncoated WC/Co cutters in helical milling of Ti/CFRP stacks. The International Journal of Advanced Manufacturing Technology, 94(5-8): 2645-2658. doi: 10.1007/s00170-017-0842-8.



- Li, Y.X.; Jiao, F.; Zhang, Z.Q.; Bin Feng, Z.; Niu, Y. (2022). Research on entrance delamination characteristics and damage suppression strategy in drilling CFRP/Ti6Al4V stacks. The Journal of Manufacturing Processes, 76: 518-531. doi: 10.1016/j.jmapro.2022.02.018.
- Li, Z.; Zhang, D.; Jiang, X.; Qin, W.; Geng, D. (2017). Study on rotary ultrasonic-assisted drilling of titanium alloys (Ti6Al4V) using 8-facet drill under no cooling condition. The International Journal of Advanced Manufacturing Technology, 90(9-12): 3249-3264. doi: 10.1007/s00170-016-9593-1.
- Liang, L.; Liu, X.; Li, X.Q.; Li, Y.Y. (2015). Wear mechanisms of WC-10Ni3Al carbide tool in dry turning of Ti6Al4V. Int J Refract Metals Hard Mater, 48: 272-285. doi: 10.1016/j. ijrmhm.2014.09.019.
- Lin, S.C.; Chen, I.K. (1996). Drilling carbon fiber-reinforced composite material at high speed. Wear, 194(1-2): 156-162. doi: 10.1016/0043-1648(95)06831-7.
- Liu, D.F.; Tang, Y.J.; Cong, W.L. (2012). A review of mechanical drilling for composite laminates. Composite Structures, 94(4): 1265-1279. doi: 10.1016/J.COMPSTRUCT.2011. 11.024.
- Liu, H.; Xie, W.; Sun, Y.; Zhang, J.; Chen, N. (2018). Investigations on micro-cutting mechanism and surface quality of carbon fiber-reinforced plastic composites. The International Journal of Advanced Manufacturing Technology, 94(9-12): 3655-3664. doi: 10.1007/s00170-017-1110-7.
- Liu, J.; Chen, G.; Ji, C.; Qin, X.; Li, H.; Ren, C. (2014). An investigation of workpiece temperature variation of helical milling for carbon fiber reinforced plastics (CFRP). International Journal of Machine Tools and Manufacture, 86: 89-103. doi: 10.1016/j. ijmachtools.2014.06.008
- Liu, M.; Li, C.; Zhang, Y.; An, Q.; Yang, M.; Gao, T.; Mao, C.; Liu, B.; Cao, H.; Xu, X.; Said, Z.; Debnath, S.; Jamil, M.; Ali, H.M.; Sharma, S. (2021). Cryogenic minimum quantity lubrication machining: from mechanism to application. Frontiers of Mechanical Engineering, 16(4): 649-697. doi: 10.1007/s11465-021-0654-2.
- López De Lacalle, L.N.; Pérez, J.; Llorente, J.I.; Sánchez, J.A. (2000). Advanced cutting conditions for the milling of aeronautical alloys. Journal of Materials Processing Technology, 100(1-3): 1-11. doi: 10.1016/S0924-0136(99)00372-6.
- Luo, B.; Li, Y.; Zhang, K.; Cheng, H.; Liu, S. (2016). Effect of workpiece stiffness on thrust force and delamination in drilling thin composite laminates. Journal of Composite Materials, 50(5): 617-625. doi: 10.1177/0021998315580449.
- Luo, B.; Zhang, K.; Liu, S.; Cheng, H.; Wang, R. (2019). Investigation on the interface damage in drilling low-stiffness CFRP/Ti stacks. Chinese Journal of Aeronautics, 32(9): 2211-2221. doi: 10.1016/j.cja.2019.04.017
- M'Saoubi, R.; Axinte, D.; Soo, S.L.; Nobel, C.; Attia, H.; Kappmeyer, G.; Engin, S.; Sim, W.M. (2015). High performance cutting of advanced aerospace alloys and composite materials. CIRP Annals, 64(2): 557-580. doi: 10.1016/j.cirp.2015.05.002.
- Machado, A.R.; Wallbank, J. (1990). Machining of titanium and its alloys—a review. Proc Inst Mech Eng B J Eng Manuf, 204(1): 53-60. doi: 10.1243/PIME_PROC_1990_204_047_ 02.
- Madarkar, R.; Agarwal, S.; Attar, P.; Ghosh, S.; Rao, P.V. (2018). Application of ultrasonic vibration assisted MQL in grinding of Ti-6Al-4V. Materials and Manufacturing Processes, 33(13): 1445-1452. doi: 10.1080/10426914.2017.1415451.
- Mahdi, A.; Turki, Y.; Habak, M.; Salem, M.; Bouaziz, Z. (2020). Experimental study of thrust force and surface quality when drilling hybrid stacks. The International Journal of Advanced Manufacturing Technology, 107(9-10): 3981-3994. doi: 10.1007/s00170-020-05252-7.



- Masoudi, S.; Vafadar, A.; Hadad, M.; Jafarian, F. (2018). Experimental investigation into the effects of nozzle position, workpiece hardness, and tool type in MQL turning of AISI 1045 steel. Materials and Manufacturing Processes, 33(9): 1011-1019. doi: 10.1080/ 10426914.2017.1401716.
- Mathavan, J.J. (2023). Investigation of tool coated with tetrahedral amorphous carbon nanocomposite for single-shot drilling of CFRP/aluminium stack. MSc thesis, Universiti Sains
- Mathavan, J.J.; Patnaik, A. (2020). Development and characterization of polyamide fiber composite filled with fly ash for wind turbine blade. In Emerging Trends in Mechanical Engineering, L. Vijayaraghavan, K. H. Reddy, and S. M. Jameel Basha (Eds.), 131-139. Singapore: Springer Singapore.
- Matsumura, T.; Tamura, S. (2013). Cutting force model in drilling of multi-layered materials. Procedia CIRP, 8: 182-187. doi: 10.1016/j.procir.2013.06.086
- Mellinger, J.C.; Ozdoganlar, O.B.; DeVor, R.E.; Kapoor, S.G. (2002). Modeling chip-evacuation forces and prediction of chip-clogging in drilling. Journal of Manufacturing Science and Engineering, 124(3): 605-614. doi: 10.1115/1.1473146.
- Merino-Pérez, J.L.; Hodzic, A.; Merson, E.; Ayvar-Soberanis, S. (2015). On the temperatures developed in CFRP drilling using uncoated WC-Co tools Part II: Nanomechanical study of thermally aged CFRP composites. Composite Structures, 123: 30-34. doi: 10.1016/j. compstruct.2014.12.035
- Merino-Pérez, J.L.; Royer, R.; Ayvar-Soberanis, S.; Merson, E.; Hodzic, A. (2015). On the temperatures developed in CFRP drilling using uncoated WC-Co tools Part I: Workpiece constituents, cutting speed and heat dissipation. Composite Structures, 123: 161-168. doi: 10.1016/j.compstruct.2014.12.033
- Merino-Pérez, J.L.; Royer, R.; Merson, E.; Lockwood, A.; Ayvar-Soberanis, S.; Marshall, M.B. (2016). Influence of workpiece constituents and cutting speed on the cutting forces developed in the conventional drilling of CFRP composites. Composite Structures, 140: 621-629. doi: 10.1016/j.compstruct.2016.01.008
- Meshreki, M.; Damir, A.; Sadek, A.; Attia, M.H. (2016). Investigation of drilling of CFRPaluminum stacks under different cooling modes. Proceedings of the ASME 2016 International Mechanical Engineering Congress and Exposition. Volume 2: Advanced Manufacturing. Phoenix, Arizona, USA. doi: 10.1115/IMECE2016-67039.
- Min, S.; Kim, J.; Dornfeld, D.A. (2001). Development of a drilling burr control chart for low alloy steel, AISI 4118. Journal of Materials Processing Technology, 113(1-3): 4-9. doi: 10.1016/S0924-0136(01)00589-1
- Mkaddem, A.; Ben Soussia, A.; El Mansori, M. (2013). Wear resistance of CVD and PVD multilayer coatings when dry cutting fiber reinforced polymers (FRP). Wear, 302(1-2): 946-954. doi: 10.1016/j.wear.2013.03.017
- Montoya, M.; Calamaz, M.; Gehin, D.; Girot, F. (2013). Evaluation of the performance of coated and uncoated carbide tools in drilling thick CFRP/aluminium alloy stacks. The International Journal of Advanced Manufacturing Technology, 68(9-12): 2111-2120. doi: 10.1007/s00170-013-4817-0.
- Mori, M.; Fujishima, M.; Inamasu, Y.; Oda, Y. (2011). A study on energy efficiency improvement for machine tools. CIRP Ann Manuf Technol, 60(1): 145-148. doi: 10.1016/ j.cirp.2011.03.099.
- Mouleeswaran, S.; Karthi, P.; Vijayan, K.; Ramanathan, B.A.; Elangovan, N.; Zitoune, R. (2011). High speed drilling of CFRP-Ti stacks. Journal of Modern Manufacturing Technology, 3, p: 167-181.



- Mouritz, A.P. (2012). Introduction to Aerospace Materials. Woodhead Publishing Limited,
- Movahhedy, M.R.; Gadala, M.S.; Altintas, Y. (2000). Simulation of chip formation in orthogonal metal cutting process: An ALE finite element approach. Machining Science and Technology, 4(1): 15-42. doi: 10.1080/10940340008945698.
- Nam, J.; Lee, S.W. (2018). Machinability of titanium alloy (Ti-6Al-4V) in environmentally-friendly micro-drilling process with nanofluid minimum quantity lubrication using nanodiamond particles. International Journal of Precision Engineering and Manufacturing-Green Technology, 5(1): 29-35. doi: 10.1007/s40684-018-0003-z.
- Narutaki, N.; Murakoshi, A.; Motonishi, S.; Takeyama, H. (1983). Study on machining of titanium alloys. CIRP Annals, 32(1): 65-69. doi: 10.1016/S0007-8506(07)63362-9
- Nouari, M.; Ginting, A. (2006). Wear characteristics and performance of multi-layer CVDcoated alloyed carbide tool in dry end milling of titanium alloy. Surface and Coatings Technology, 200 (18-19), 5663-5676.
- Onawumi, P.Y.; Roy, A.; Silberschmidt, V.V.; Merson, E. (2018). Ultrasonically assisted drilling of aerospace CFRP/Ti stacks. Procedia CIRP, 77: 383-386. doi: 10.1016/j.procir. 2018.09.041
- Pan, W.; Ding, S.; Mo, J. (2014). Thermal characteristics in milling Ti6Al4V with polycrystalline diamond tools. The International Journal of Advanced Manufacturing Technology, 75(5-8): 1077-1087. doi: 10.1007/s00170-014-6094-y.
- Panchagnula, K.K.; Palaniyandi, K. (2018). Drilling on fiber reinforced polymer/nanopolymer composite laminates: A review. Journal of Materials Research and Technology, 7(2): 180-189. doi: 10.1016/j.jmrt.2017.06.003
- Park, K.-H.; Beal, A.; (Dae-Wook) Kim, D.; Kwon, P.; Lantrip, J. (2014). A comparative study of carbide tools in drilling of CFRP and CFRP-Ti stacks. Journal of Manufacturing Science and Engineering, 136(1): 14501. doi: 10.1115/1.4025008.
- Park, K.-H.; Beal, A.; Dae, D.; Kim, W.; Kwon, P.; Lantrip, J. (2011). Tool wear in drilling of composite/titanium stacks using carbide and polycrystalline diamond tools. Wear, 271(11–12): 2826–2835. doi: 10.1016/j.wear.2011.05.038.
- Park, K.-H.; Kwon, P.; Dae, D.; Kim, W. (2012). Wear characteristic on BAM coated carbide tool in drilling of composite/titanium stack. International Journal of Precision Engineering and Manufacturing, 13(7): 1073-1076. doi: 10.1007/s12541-012-0140-1.
- Park, S.Y.; Choi, W.J.; Choi, C.H.; Choi, H.S. (2018). Effect of drilling parameters on hole quality and delamination of hybrid GLARE laminate. Composite Structures, 185: 684-698. doi: 10.1016/j.compstruct.2017.11.073.
- Pawar, O.A.; Gaikhe, Y.S.; Tewari, A.; Sundaram, R.; Joshi, S.S. (2015). Analysis of hole quality in drilling GLARE fiber metal laminates. Composite Structures, 123: 350-365. doi: 10.1016/J.COMPSTRUCT.2014.12.056.
- Pecat, O.; Brinksmeier, E. (2014). Low damage drilling of CFRP/titanium compound materials for fastening. Procedia CIRP, 13: 1-7. doi: 10.1016/j.procir.2014.04.001.
- Pecat, O.; Brinksmeier, E. (2014). Tool wear analyses in low frequency vibration assisted drilling of CFRP/Ti6Al4V stack material. Procedia CIRP, 14: 142-147. doi: 10.1016/j.procir.2014.03.050.
- Perçin, M.; Aslantas, K.; Ucun, İ.; Kaynak, Y.; Çicek, A. (2016). Micro-drilling of Ti-6Al-4V alloy: The effects of cooling/lubricating. Precision Engineering, 45: 450-462.
- Pereira, R.B.D.; Brandão, L.C.; de Paiva, A.P.; Ferreira, J.R.; Davim, J.P. (2017). A review of helical milling process. International Journal of Machine Tools and Manufacture, 120: 27-48. doi: 10.1016/j.ijmachtools.2017.05.002



- Pereszlai, C.; Geier, N. (2020). Comparative analysis of wobble milling, helical milling and conventional drilling of CFRPs. The International Journal of Advanced Manufacturing Technology, 106(9-10): 3913-3930. doi: 10.1007/s00170-019-04842-4.
- Pereszlai, C.; Geier, N.; Poór, D.I.; Balázs, B.Z.; Póka, G. (2021). Drilling fibre reinforced polymer composites (CFRP and GFRP): An analysis of the cutting force of the tilted helical milling process. Composite Structures, 262: 113646. doi: 10.1016/j.compstruct.2021.
- Poutord, A.; Rossi, F.; Poulachon, G.; M'Saoubi, R.; Abrivard, G. (2013). Local approach of wear in drilling Ti6Al4V/CFRP for stack modelling. Procedia CIRP, 8: 316-321. doi: 10. 1016/j.procir.2013.06.109
- Prabukarthi, A.; Krishnaraj, V.; Senthil Kumar, M. (2013). Multi-objective optimization on drilling of titanium alloy (Ti6Al4V). Materials Science Forum, 763: 29-49. doi: 10.4028/ www.scientific.net/MSF.763.29.
- Pradeep Kumar, M.; Shakeel Ahmed, L. (2017). Drilling of AISI 304 stainless steel under liquid nitrogen cooling: A comparison with flood cooling. Materials Today: Proceedings, 4(2): 1518-1524. doi: 10.1016/j.matpr.2017.01.174
- Prajapati, J.P.; Bhatt, P.M.; Patel, N.S. (2015). Force and wear analysis of PVD coated cutting tool - a review. International Journal of Advance Research and Innovative Ideas in Education (1): 9-16.
- Pramanik, A.; Littlefair, G. (2014). Developments in machining of stacked materials made of CFRP and titanium/aluminum alloys. Machining Science and Technology, 18(4): 485-508. doi: 10.1080/10910344.2014.955718.
- Prisco, U.; Impero, F.; Rubino, F. (2019). Peck drilling of CFRP/titanium stacks: Effect of tool wear on hole dimensional and geometrical accuracy. Production Engineering, 13(5): 529-538. doi: 10.1007/s11740-019-00915-1.
- Prisco, U. (2019). Drilling of CFRP/Ti stacks in wet and cryogenic condition. Journal of Modern Mechanical Engineering and Technology, 6: 31-39. doi: 10.31875/2409-9848.2019. 06.5.
- Pu, F.; Stoi, A.; Kopa, J. (2009). The role of cryogenics in machining processes. Technical Gazette, 4: 3-9.
- Pusavec, F.; Krajnik, P.; Kopac, J. (2010). Transitioning to sustainable production Part I: application on machining technologies. Journal of Cleaner Production, 18(2): 174-184. doi: 10.1016/j.jclepro.2009.08.010.
- Qi, Z.; Zhang, K.; Cheng, H.; Wang, D.; Meng, Q. (2015). Microscopic mechanism based force prediction in orthogonal cutting of unidirectional CFRP. The International Journal of Advanced Manufacturing Technology, 79(5-8): 1209-1219. doi: 10.1007/s00170-015-6895-7.
- Qi, Z.; Zhang, K.; Li, Y.; Liu, S.; Cheng, H. (2014). Critical thrust force predicting modeling for delamination-free drilling of metal-FRP stacks. Composite Structures, 107: 604-609. doi: 10.1016/j.compstruct.2013.07.036.
- Qiu, X.; Li, P.; Li, C.; Niu, Q.; Chen, A.; Ouyang, P.; Ko, T.J. (2018). Study on chisel edge drilling behavior and step drill structure on delamination in drilling CFRP. Composite Structures, 203: 404-413. no september 2017 doi: 10.1016/j.compstruct.2018.07.007.
- Qiu, X.-Y.; Yu, Z.; Li, C-p.; Niu, Q.-L.; Li, S.-J.; Li, P.-N.; Ko, T.J. (2021). Influence of main cutting edge structure on hole defects in CFRP/titanium alloy stacks drilling. Journal of Manufacturing Processes, 69: 503-513. doi: 10.1016/j.jmapro.2021.07.061.
- Reddy, R.H.N.; Alphonse, M.; Bupesh Raja, V.K.; Palanikumar, K.V.; Sai Krishna Sanjay, D.R.; Madhu Sudhan, S.K. (2021). Evaluating the wear studies and tool characteristics of



- coated and uncoated HSS drill bit a review. Materials Today: Proceedings, 46: 3779-3785. doi: 10.1016/j.matpr.2021.02.022.
- Rahim, E.A.; Sasahara, H. (2010). Effect of machining parameters and MQL liquids on surface integrity of high speed drilling Ti-6Al-4V, in Advances in Precision. Key Engineering Materials, 447-448: 816-820. 10.4028/www.scientific.net/KEM.447-448.816.
- Rahim, E.A.; Sharif, S. (2007). Tool failure modes and wear mechanism of coated carbide tools when drilling Ti-6Al-4V. International Journal of Precision Technology, 1(1): 30-39. doi: 10.1504/IJPTECH.2007.015342.
- Raj, D.S.; Karunamoorthy, L. (2016). Study of the effect of tool wear on hole quality in drilling CFRP to select a suitable drill for multi-criteria hole quality. Materials and Manufacturing Processes, 31(5): 587-592. doi: 10.1080/10426914.2015.1004713.
- Ramulu, M.; Branson, T.; Kim, D. (2001). A study on the drilling of composite and titanium stacks. Composite Structures, 54(1): 67-77. doi: 10.1016/S0263-8223(01)00071-X.
- Rawat, S.; Attia, H. (2009). Characterization of the dry high speed drilling process of woven composites using machinability maps approach. CIRP Annals, 58(1): 105-108. doi: 10. 1016/j.cirp.2009.03.100
- Rawat, S.; Attia, H. (2009). Wear mechanisms and tool life management of WC-Co drills during dry high speed drilling of woven carbon fibre composites. Wear, 267(5-8): 1022-1030. doi: 10.1016/j.wear.2009.01.031.
- Rodríguez, A.; Calleja, A.; de Lacalle, L.N.L.; Pereira, O.; Rubio-Mateos, A.; Rodríguez, G. (2021). Drilling of CFRP-Ti6Al4V stacks using CO₂-cryogenic cooling. J Manuf Process, 64: 58-66. doi: 10.1016/j.jmapro.2021.01.018.
- Rodriguez, I.; Arrazola, P.J.; Cuesta, M.; Sterle, L.; Pušavec, F. (2023). Improving surface integrity when drilling CFRPs and Ti-6Al-4V using sustainable lubricated liquid carbon dioxide. Chinese Journal of Aeronautics, 36(7): 129-146. doi: 10.1016/j.cja.2022.09.004.
- Saracoglu, G.; Yapici, A. (2020). The effects of interface and matrix reinforcements on fracture toughness of E-Glass/epoxy laminate. Materials Research Express, 7(6): 065305. doi: 10.1088/2053-1591/ab98ce.
- Sato, H.; Tanaka, H.; Yamamoto, K. (2016). Temperature variations in drilling of CFRP/ aluminum and CFRP/titanium stacks. International Journal of Automation Technology 10(3):348–355. doi: 10.20965/ijat.2016.p0348.
- Seeholzer, L.; Voss, R.; Marchetti, L.; Wegener, K. (2019). Experimental study: comparison of conventional and low-frequency vibration-assisted drilling (LF-VAD) of CFRP/aluminium stacks. The International Journal of Advanced Manufacturing Technology, 104(1-4): 433-449. 10.1007/s00170-019-03837-5
- Senthilkumar, M.; Prabukarthi, A.; Krishnaraj, V. (2018). Machining of CFRP/Ti6Al4V stacks under minimal quantity lubricating condition. Journal of Mechanical Science and Technology, 32(8): 3787-3796. doi: 10.1007/s12206-018-0731-6.
- Seo, J.; Kim, D.Y.; Kim, D.C.; Park, H.W. (2021). Recent developments and challenges on machining of carbon fiber reinforced polymer composite laminates. International Journal of Precision Engineering and Manufacturing, 22(12): 2027-2044. doi: 10.1007/s12541-021-00596-w.
- Shao, Z.; Jiang, X.; Geng, D.; Liu, Y.; Zhou, Z.; Li, S.; Zhang, D.; Zheng, W. (2021). The interface temperature and its influence on surface integrity in ultrasonic-assisted drilling of CFRP/Ti stacks. Composite Structures, 266(January): 113803. doi: 10.1016/j.compstruct.2021.113803.
- Shao, Z.; Jiang, X.; Li, Z.; Geng, D.; Li, S.; Zhang, D. (2019). Feasibility study on ultrasonicassisted drilling of CFRP/Ti stacks by single-shot under dry condition. The International



- Journal of Advanced Manufacturing Technology, 105(1-4): 1259-1273. doi: 10.1007/ s00170-019-04329-2.
- Sharif, S.; Rahim, E.A. (2007). Performance of coated- and uncoated-carbide tools when drilling titanium alloy-Ti-6Al4V. Journal of Materials Processing Technology, 185(1-3): 72-76. doi: 10.1016/j.jmatprotec.2006.03.142.
- Sheikh-Ahmad, J.Y. (2015). Machining of Polymer Composites. Springer-Verlag, AbuDhabi, UAE. doi 10.1007/978-0-387-68619-6.
- Shu, L.; Li, S.; Fang, Z.; Kizaki, T.; Kimura, K.; Arai, G.; Arai, K.; Sugita, N. (2021). Study on dedicated drill bit design for carbon fiber reinforced polymer drilling with improved cutting mechanism. Composites, 142: 106259-102021. doi: 10.1016/j.compositesa.2020. 106259.
- Shyha, I.; Soo Leung, S.; Aspinwall, D.K.; Bradley, S.; Dawson, S.; Pretorius, C.J. (2010). Drilling of titanium/CFRP/aluminium stacks. Key Engineering Materials, 447-448(448): 624-633. doi: 10.4028/www.scientific.net/KEM.447-448.624.
- Shyha, I.S.; Aspinwall, D.K.; Soo, S.L.; Bradley, S. (2009). Drill geometry and operating effects when cutting small diameter holes in CFRP. International Journal of Machine Tools and Manufacture, 49(12-13): 1008-1014. doi: 10.1016/j.ijmachtools.2009.05.009
- Shyha, I.S.; Soo, S.L.; Aspinwall, D.K.; Bradley, S.; Perry, R.; Harden, P.; Dawson, S. (2011). Hole quality assessment following drilling of metallic-composite stacks. International Journal of Machine Tools and Manufacture, 51(7-8): 569-578. doi: 10.1016/j.ijmachtools. 2011.04.007.
- Singh, A.P.; Sharma, M.; Singh, I. (2013). A review of modeling and control during drilling of fiber reinforced plastic composites. Composites Part B Engineering, 47: 118-125. doi: 10.1016/j.compositesb.2012.10.038.
- Sinmazçelik, T.; Avcu, E.; Bora, M.O.; Çoban, O. (2011). A review: Fibre metal laminates, background, bonding types and applied test methods. Materials and Design, 32(7): 3671-3685. doi: 10.1016/j.matdes.2011.03.011
- Soo, S.L.; Abdelhafeez, A.M.; Li, M.; Hood, R.; Lim, C.M. (2019). The drilling of carbon fibre composite-aluminium stacks and its effect on hole quality and integrity. Proc Inst Mech Eng B J Eng Manuf, 233(4): 1323-1331. doi: 10.1177/0954405417728312.
- Sorrentino, L.; Turchetta, S.; Bellini, C. (2018). A new method to reduce delaminations during drilling of FRP laminates by feed rate control. Composite Structures, 186: 154-164. doi: 10.1016/j.compstruct.2017.12.005
- Stocchi, C.; Robinson, P.; Pinho, S.T. (2013). A detailed finite element investigation of composite bolted joints with countersunk fasteners. Composites Part A: Applied Science and Manufacturing, 52: 143-150. doi: 10.1016/j.compositesa.2012.09.013.
- Sui, S.; Song, G.; Sun, C.; Zhu, Z.; Guo, K.; Sun, J. (2020). Experimental investigation on the performance of novel double cone integrated tool in one-shot drilling of metal stacks. The International Journal of Advanced Manufacturing Technology, 109(1-2): 523-534. doi: 10.1007/s00170-020-05474-9.
- Sun, L.; Gao, H.; Wang, B.; Bao, Y.; Wang, M.; Ma, S. (2020). Mechanism of reduction of damage during helical milling of titanium/CFRP/aluminium stacks. The International Journal of Advanced Manufacturing Technology, 107(11-12): 4741-4753. doi: 10.1007/ s00170-020-05177-1.
- Sushinder, K.; Shivaram, P.R.; Nivedh Kannaa, S.B.; Gupta, N.; Sekar, K.S.V. (2015). Investigation of thrust forces, torque and chip microstructure during drilling of Ti-6Al-4V titanium alloy. Applied Mechanics and Materials, 787: 431-436. doi: 10.4028/www.scientific.net/AMM.787.431.



- Tashiro, T.; Fujiwara, J.; Inada, K. (2011). Drilling of CFRP/Ti-6Al-4V stacks. Advanced Materials Research, 325: 369-374. doi: 10.4028/www.scientific.net/AMR.325.369.
- Trent, E.M.; Wright, P.K. (2000). No title. Metal Cutting, 157–159: 195–199.
- Tsao, C.C. (2008). The geometrical effect between stages in step drilling of composite materials. International Journal of Materials and Product Technology, 32(2/3): 202-212. doi: 10.1504/IJMPT.2008.018981.
- Tsao, C.C.; Hocheng, H. (2007). Parametric study on thrust force of core drill. Journal of Materials Processing Technology, 192-193: 37-40. doi: 10.1016/j.jmatprotec.2007.04.062
- Turner, J.; Scaife, R.J.; El-Dessouky, H.M. (2015). Effect of machining coolant on integrity of CFRP composites. Advanced Manufacturing: Polymer and Composites Science, 1(1): 54-60. doi: 10.1179/2055035914Y.0000000008.
- Tyczyński, P.; Lemańczyk, J.; Ostrowski, R.; Ewa S'liwa, R. (2014). Drilling of CFRP, GFRP, glare type composites. Aircraft Engineering and Aerospace Technology, 86(4): 312-322. doi: 10.1108/AEAT-10-2012-0196.
- Uhlmann, E.; Mullany, B.; Biermann, D.; Rajurkar, K.P.; Hausotte, T.; Brinksmeier, E. (2016). Process chains for high-precision components with micro-scale features. CIRP Annals, 65(2): 549-572. doi: 10.1016/j.cirp.2016.05.001
- Unai, A.; Madalina, C.; Girot, F.; Edurne, I. (2019). Influence of flute number and stepped bit geometry when drilling CFRP/Ti6Al4V stacks. The Journal of Manufacturing Processes, 39: 356-370. doi: 10.1016/j.jmapro.2019.02.006
- Vijayan, K.; Zitoune, R.; Collombet, F. (2010). Comprehensive review on drilling of multimaterials stacks. Journal of Machining and Forming Technologies, 2(3/4): 171-200.
- Vlot, A.; Gunnink, J.W. (Ed.). (2001). Fibre Metal Laminates: An Introduction. 1st ed. Springer, Dordrecht. doi: 10.1007/978-94-010-0995-9.
- Wang, B.; Wang, Y.; Zhao, H.; Sun, L.; Wang, M.; Kong, X. (2020). Effect of a Ti alloy layer on CFRP hole quality during helical milling of CFRP/Ti laminate. Composite Structures, 252: 112670. doi: 10.1016/j.compstruct.2020.112670
- Wang, B.; Yin, W.; Wang, M.; Zheng, Y.; Li, X.; Ma, Z. (2017). Edge chipping mechanism and failure time prediction on carbide cemented tool during drilling of CFRP/Ti stack. The International Journal of Advanced Manufacturing Technology, 91(9-12): 3015-3024. doi: 10.1007/s00170-017-0017-7.
- Wang, B.; Zhao, H.; Zhang, F.; Wang, M.; Zheng, Y. (2021). Comparison of the geometric accuracy of holes made in CFRP/Ti laminate by drilling and helical milling. The International Journal of Advanced Manufacturing Technology, 112(11-12): 3343-3350. doi: 10.1007/s00170-021-06594-6.
- Wang, C.-Y.; Chen, Y.-H.; An, Q.-L.; Cai, X.-J.; Ming, W.-W.; Chen, M. (2015). Drilling temperature and hole quality in drilling of CFRP/aluminum stacks using diamond coated drill. International Journal of Precision Engineering and Manufacturing, 16(8): 1689–1697. doi: 10.1007/s12541-015-0222-y.
- Wang, D.H.; Ramulu, M.; Arola, D. (1995). Orthogonal cutting mechanisms of graphite/ epoxy composite. Part I: unidirectional laminate. International Journal of Machine Tools and Manufacture, 35(12): 1623-1638. doi: 10.1016/0890-6955(95)00014-O.
- Wang, F.J.; Zhao, M.; Fu, R.; Yan, J.B.; Qiu, S.; Hao, J.X. (2021). Novel chip-breaking structure of step drill for drilling damage reduction on CFRP/Al stack. Journal of Materials Processing Technology, 291(December 2020): 117033. doi: 10.1016/j.jmatprotec.2020. 117033.
- Wang, F.; Yin, J.; Ma, J.; Jia, Z.; Yang, F.; Niu, B. (2017). Effects of cutting edge radius and fiber cutting angle on the cutting-induced surface damage in machining of unidirectional



- CFRP composite laminates. The International Journal of Advanced Manufacturing Technology, 91(9–12): 3107–3120. doi: 10.1007/s00170-017-0023-9.
- Wang, J.; Feng, P.; Zhang, J.; Shen, H. (2017). Experimental investigation on the effects of thermomechanical loading on the vibrational stability during rotary ultrasonic machining. Machining Science and Technology, 21(2): 239-256. doi: 10.1080/10910344.2017. 1283962.
- Wang, J.; Ge, J.; Chen, G.; Liu, J.; Wang, Z.; Ren, C. (2023). Sustainable cooling/lubrication induced thermo-mechanical effects on ultrasonic vibration helical milling of CFRP/Ti-6Al-4V stacks. International Journal of Lightweight Materials and Manufacture, 6(3): 311-328. doi: 10.1016/j.ijlmm.2023.02.002
- Wang, J.; Zhang, J.; Feng, P.; Guo, P.; Zhang, Q. (2018). Feasibility study of longitudinaltorsional-coupled rotary ultrasonic machining of brittle material. Journal of Manufacturing Science and Engineering, 140(5) Mar doi: 10.1115/1.4038728.
- Wang, X.; Kwon, P.Y.; Sturtevant, C.; Dae, D.; Kim, W.; Lantrip, J. (2013). Tool wear of coated drills in drilling CFRP. The Journal of Manufacturing Processes, 15(1): 127-135. doi: 10.1016/j.jmapro.2012.09.019
- Wang, X.; Kwon, P.Y.; Sturtevant, C.; Kim, D.D.W.; Lantrip, J. (2014). Comparative tool wear study based on drilling experiments on CFRp/Ti stack and its individual layers. Wear, 317(1-2): 265-276. doi: 10.1016/j.wear.2014.05.007.
- Wang, X.; Li, C.; Zhang, Y.; Ali, H.M.; Sharma, S.; Li, R.; Yang, M.; Said, Z.; Liu, X. (2022). Tribology of enhanced turning using biolubricants: A comparative assessment. Tribology International, 174: 107766. doi: 10.1016/j.triboint.2022.107766
- Wei, Y.; An, Q.; Ming, W.; Chen, M. (2016). Effect of drilling parameters and tool geometry on drilling performance in drilling carbon fiber-reinforced plastic/titanium alloy stacks. Advances in Mechanical Engineering, 8(9): 1687814016670281. doi: 10.1177/ 1687814016670281.
- Wika, K.K.; Sharman, A.R.C.; Goulbourne, D.; Ridgway, K. (2011). Impact of number of flutes and helix angle on tool performance and hole quality in drilling composite/titanium stacks, SAE International, United States. doi: 10.4271/2011-01-2744
- Won, M.S.; Dharan, C.K.H. (2002). Chisel Edge and Pilot Hole effects in drilling composite laminates. Journal of Manufacturing Science and Engineering, 124(2): 242–247. doi: 10. 1115/1.1448317.
- Xia, R.S.; Mahdavian, S.M. (2005). Experimental studies of step drills and establishment of empirical equations for the drilling process. International Journal of Machine Tools and Manufacture, 45(2): 235-240. doi: 10.1016/j.ijmachtools.2004.07.002
- Xia, T.; Kaynak, Y.; Arvin, C.; Jawahir, I.S. (2016). Cryogenic cooling-induced process performance and surface integrity in drilling CFRP composite material. The International Journal of Advanced Manufacturing Technology, 82(1-4): 605-616. doi: 10.1007/s00170-015-7284-y.
- Xu, J. (2016). Numerical and experimental study of machining titanium-composite stacks. Mechanics of materials [physics.class-ph]. PhD Thesis, Ecole nationale supérieure d'arts et métiers - ENSAM, 2016. English.
- Xu, J.; An, Q.; Chen, M. (2014). A comparative evaluation of polycrystalline diamond drills in drilling high-strength T800S/250F CFRP. Composite Structures, 117(1): 71-82. doi: 10. 1016/j.compstruct.2014.06.034.
- Xu, J.; El Mansori, M. (2016). Experimental study on drilling mechanisms and strategies of hybrid CFRP/Ti stacks. Composite Structures, 157: 461-482. doi: 10.1016/j.compstruct. 2016.07.025.



- Xu, J.; El Mansori, M.; Chen, M.; Ren, F. (2019). Orthogonal cutting mechanisms of CFRP/ Ti6Al4V stacks. The International Journal of Advanced Manufacturing Technology, 103(9-12): 3831-3851. doi: 10.1007/s00170-019-03734-x.
- Xu, J.; El Mansori, M.; Voisin, J.; Chen, M.; Ren, F. (2019). On the interpretation of drilling CFRP/Ti6Al4V stacks using the orthogonal cutting method: Chip removal mode and subsurface damage formation. The Journal of Manufacturing Processes, 44: 435-447. doi: 10.1016/j.jmapro.2019.05.052.
- Xu, J.; et al. (2022). A critical review addressing the drilling-induced damage issues for CFRP composites. Composite Structures, 294(April): 115594. doi: 10.1016/j.compstruct. 2022.115594.
- Xu, J.; Ji, M.; Chen, M.; El Mansori, M. (2020). Experimental investigation on drilling machinability and hole quality of CFRP/Ti6Al4V stacks under different cooling conditions. The International Journal of Advanced Manufacturing Technology, 109(5-6): 1527-1539. doi: 10.1007/s00170-020-05742-8.
- Xu, J.; Ji, M.; Chen, M.; Ren, F. (2019). Investigation of minimum quantity lubrication effects in drilling CFRP/Ti6Al4V stacks. Materials and Manufacturing Processes, 34(12): 1401-1410. doi: 10.1080/10426914.2019.1661431.
- Xu, J.; Ji, M.; Davim, J.P.; Chen, M.; El Mansori, M.; Krishnaraj, V. (2020). Comparative study of minimum quantity lubrication and dry drilling of CFRP/titanium stacks using TiAlN and diamond coated drills. Composite Structures, 234: 111727. doi: 10.1016/j. compstruct.2019.111727.
- Xu, J.; Li, C.; Chen, M.; El Mansori, M.; Davim, J.P. (2020). On the analysis of temperatures, surface morphologies and tool wear in drilling CFRP/Ti6Al4V stacks under different cutting sequence strategies. Composite Structures, 234: 111708. 10.1016/j.compstruct. 2019.111708
- Xu, J.; Li, C.; Chen, M.; Ren, F. (2019). A comparison between vibration assisted and conventional drilling of CFRP/Ti6Al4V stacks. Materials and Manufacturing Processes, 34(10): 1182-1193. doi: 10.1080/10426914.2019.1615085.
- Xu, J.; Mkaddem, A.; El Mansori, M. (2016). Recent advances in drilling hybrid FRP/Ti Composite: A State-of-the-Art review. Composite Structures, 135(C): 316-338. doi: 10. 1016/j.compstruct.2015.09.028.
- Xu, J.; Zhou, L.; Chen, M.; Ren, F. (2019). Experimental study on mechanical drilling of carbon/epoxy composite-Ti6Al4V stacks. Materials and Manufacturing Processes, 34(7): 715-725. doi: 10.1080/10426914.2019.1594275.
- Xu, W.; Zhang, L. (2018). Tool wear and its effect on the surface integrity in the machining of fibre-reinforced polymer composites. Composite Structures, 188: 257-265. doi: 10. 1016/J.COMPSTRUCT.2018.01.018.
- Yan, M.; Shao, H. (2011). Analysis of temperature and wear of tool of ultrasonic vibration drilling Ti alloys. Tool Engineering, 45(8): 26-30.
- Yang, H.; Chen, Y.; Xu, J.; Ladonne, M.; Lonfier, J.; Ding, W. (2020). Chip control analysis in low-frequency vibration-assisted drilling of Ti-6Al-4V titanium alloys. International Journal of Precision Engineering and Manufacturing, 21(4): 565-584. doi: 10.1007/s12541-019-00286-8.
- Yang, H.; Chen, Y.; Xu, J.; Ladonne, M.; Lonfier, J.; Fu, Y. (2019). Tool wear mechanism in low-frequency vibration-assisted drilling of CFRP/Ti stacks and its individual layer. The International Journal of Advanced Manufacturing Technology, 104(5-8): 2539-2551. doi: 10.1007/s00170-019-03910-z.
- Yang, X.; Richard Liu, C. (1999). MACHINING TITANIUM AND ITS ALLOYS. Machining Science and Technology, 3(1): 107-139. doi: 10.1080/10940349908945686.



- Yang, Z.; Zhu, L.; Zhang, G.; Ni, C.; Lin, B. (2020). Review of ultrasonic vibration-assisted machining in advanced materials. International Journal of Machine Tools and Manufacture, 156: 103594. doi: 10.1016/j.ijmachtools.2020.103594
- Yaşar, N.; Korkmaz, M.E.; Gupta, M.K.; Boy, M.; Günay, M. (2021). A novel method for improving drilling performance of CFRP/Ti6AL4V stacked materials. The International Journal of Advanced Manufacturing Technology, 117(1-2): 653-673. doi: 10.1007/s00170-021-07758-0.
- Yildiz, Y.; Nalbant, M. (2008). A review of cryogenic cooling in machining processes. International Journal of Machine Tools and Manufacture, 48(9): 947-964. doi: 10.1016/j. ijmachtools.2008.01.008
- Yuan Jia, Z.; Zhang, C.; Wang, F. j.; Fu, R.; Chen, C. (2020). An investigation of the effects of step drill geometry on drilling induced delamination and burr of Ti/CFRP stacks. Composite Structures, 235: 111786. doi: 10.1016/j.compstruct.2019.111786.
- Yuan Jia, Z.; Zhang, C.; Wang, F. j.; Fu, R.; Chen, C. (2020). Multi-margin drill structure for improving hole quality and dimensional consistency in drilling Ti/CFRP stacks. Journal of Materials Processing Technology, 276(September 2019): 116405. doi: 10.1016/j. jmatprotec.2019.116405.
- Zenia, S.; Ben Ayed, L.; Nouari, M.; Delamézière, A. (2015). Numerical analysis of the interaction between the cutting forces, induced cutting damage, and machining parameters of CFRP composites. The International Journal of Advanced Manufacturing Technology, 78(1-4): 465-480. doi: 10.1007/s00170-014-6600-2.
- Zhang, L.; Liu, Z.; Tian, W.; Liao, W. (2015). Experimental studies on the performance of different structure tools in drilling CFRP/Al alloy stacks. The International Journal of Advanced Manufacturing Technology, 81(1-4): 241-251. doi: 10.1007/s00170-015-6955-z.
- Zhang, L.-B.; Wang, L.-J.; Liu, X.-Y. (2001). A mechanical model for predicting critical thrust forces in drilling composite laminates. Proceedings of the Institution of Mechanical Engineers, Part B: Journal of Engineering Manufacture, 215(2): 135-146. doi: 10.1243/ 0954405011515235.
- Zhang, P.F.; Churi, N.J.; Pei, Z.J.; Treadwell, C. (2008). Mechanical drilling processes for titanium alloys: A literature review. Machining Science and Technology, 12(4): 417-444. doi: 10.1080/10910340802519379.
- Zhou, L.; Ke, Y.; Dong, H.; Chen, Z.; Gao, K. (2016). Hole diameter variation and roundness in dry orbital drilling of CFRP/Ti stacks. The International Journal of Advanced Manufacturing Technology, 87(1-4): 811-824. doi: 10.1007/s00170-016-8528-1.
- Zhu, Z.; Guo, K.; Sun, J.; Li, J.; Liu, Y.; Chen, L.; Zheng, Y. (2018). Evolution of 3D chip morphology and phase transformation in dry drilling Ti6Al4V alloys. The Journal of Manufacturing Processes, 34: 531-539. doi: 10.1016/j.jmapro.2018.07.001
- Zitoune, R.; Collombet, F. (2007). Numerical prediction of the thrust force responsible of delamination during the drilling of the long-fibre composite structures. Composites Part A: Applied Science and Manufacturing, 38(3): 858-866. doi: 10.1016/j.compositesa.2006.07.009.
- Zitoune, R.; Krishnaraj, V.; Collombet, F. (2010). Study of drilling of composite material and aluminium stack. Composite Structures, 92(5): 1246-1255. doi: 10.1016/J. COMPSTRUCT.2009.10.010.
- Zitoune, R.; Krishnaraj, V.; Collombet, F.; Le Roux, S. (2016). Experimental and numerical analysis on drilling of carbon fibre reinforced plastic and aluminium stacks. Composite Structures, 146: 148-158. 10.1016/j.compstruct.2016.02.084
- Zitoune, R.; Krishnaraj, V.; Sofiane Almabouacif, F.; Collombet, B.; Sima, M.; Jolin, A. (2012). Influence of machining parameters and new nano-coated tool on drilling performance of CFRP/Aluminium sandwich. Composites Part B: Engineering, 43(3): 1480-1488. doi: 10.1016/j.compositesb.2011.08.054.